National Library
of Canada

Bibliothèque nationale
du Canada

Canadian Theses Service

Service des thèses canadiennes

Ottawa, Canada
K1A 0N4

NOTICE

The quality of this microform is heavily dependent upon the quality of the original thesis submitted for microfilming. Every effort has been made to ensure the highest quality of reproduction possible.

If pages are missing, contact the university which granted the degree.

Some pages may have indistinct print especially if the original pages were typed with a poor typewriter ribbon or if the university sent us an inferior photocopy.

Reproduction in full or in part of this microform is governed by the Canadian Copyright Act, R.S.C. 1970, c. C-30, and subsequent amendments.

AVIS

La qualité de cette microforme dépend grandement de la qualité de la thèse soumise au microfilmage. Nous avons tout fait pour assurer une qualité supérieure de reproduction.

S'il manque des pages, veuillez communiquer avec l'université qui a conféré le grade.

La qualité d'impression de certaines pages peut laisser à désirer, surtout si les pages originales ont été dactylographiées à l'aide d'un ruban usé ou si l'université nous a fait parvenir une photocopie de qualité inférieure.

La reproduction, même partielle, de cette microforme est soumise à la Loi canadienne sur le droit d'auteur, SRC 1970, c. C-30, et ses amendements subséquents.

NL-339 (r. 88/04) c

Canada

UNIVERSITY OF ALBERTA

A Light Stable Isotope and Fluid Inclusion Study of the Sheep Creek Gold Camp, Salmo, British Columbia

by
Robert V. Hardy

A THESIS
Submitted to the Faculty of Graduate Studies and Research
In Partial Fulfilment of the Requirements For The Degree Of

MASTER OF SCIENCE

Department of GEOLOGY

EDMONTON, ALBERTA
Spring 1992

National Library of Canada
Canadian Theses Service
Ottawa, Canada
K1A 0N4

Bibliothèque nationale du Canada
Service des thèses canadiennes

The author has granted an irrevocable non-exclusive licence allowing the National Library of Canada to reproduce, loan, distribute or sell copies of his/her thesis by any means and in any form or format, making this thesis available to interested persons.

The author retains ownership of the copyright in his/her thesis. Neither the thesis nor substantial extracts from it may be printed or otherwise reproduced without his/her permission.

L'auteur a accordé une licence irrévocable et non exclusive permettant à la Bibliothèque nationale du Canada de reproduire, prêter, distribuer ou vendre des copies de sa thèse de quelque manière et sous quelque forme que ce soit pour mettre des exemplaires de cette thèse à la disposition des personnes intéressées.

L'auteur conserve la propriété du droit d'auteur qui protège sa thèse. Ni la thèse ni des extraits substantiels de celle-ci ne doivent être imprimés ou autrement reproduits sans son autorisation.

ISBN 0-315-73152-4

Canada

UNIVERSITY OF ALBERTA

RELEASE FORM

NAME OF AUTHOR: Robert Verne Hardy

TITLE OF THESIS: **A Light Stable Isotope and Fluid Inclusion Study of the Sheep Creek Gold Camp, Salmo, British Columbia.**

DEGREE: Master of Science

YEAR THIS DEGREE GRANTED: Spring 1992

Permission is hereby granted to the University of Alberta Library to reproduce single copies of this thesis and to lend or sell such copies for private scholarly or scientific purposes only.

The author reserves other publication rights, and neither the thesis nor extensive extracts from it may be printed or otherwise reproduced without the author's written permission.

Robert V. Hardy

Permanent Address:
P.O. Box 24
Viking, Alberta
Canada
TOB 4NO

Dated 21 april 1992

UNIVERSITY OF ALBERTA

FACULTY OF GRADUATE STUDIES AND RESEARCH

The Undersigned certify that they have read, and recommend to the Faculty of Graduate Studies and Research for acceptance, a thesis entitled: **A Light Stable Isotope and Fluid Inclusion Study of the Sheep Creek Gold Camp, Salmo, British Columbia** submitted by **Robert V. Hardy** in partial fulfillment of the requirements for the Degree of **MASTER OF SCIENCE.**

Dr. Bruce Nesbitt, Supervisor

Dr. Karlis Muehlenbachs

Tom Chacko

Dr. Tom Chacko

Dr. Jerry Whiting

Dated 13 April 1992

DEDICATIONS
to

Arinna

Mother Earth: may she continue to bear this great burden,

Humanity,

and continue to do so with all her Power, Grace and Beauty.

Mom and Dad

ABSTRACT

The Sheep Creek Gold Camp is located within an Upper Proterozoic-Cambrian miogeoclinal succession that straddles the eastern edge of the Kootenay Arc, an east facing terrane boundary that has been identified as a segment of the western margin of the ancient North America craton. The camp produced in excess of 750,000 oz. gold and half as much silver from 1.7 million tons of ore between 1900 to 1951. Recent exploration in the camp has delineated new ore reserves.

Most production has come from high angle, northeasterly trending vertically and laterally extensive massive and laminated quartz± pyrite veins which transect regional structures and all penetrative deformation. The major structures are doubly-plunging, north-trending, overturned tight to isoclinal anticlines composed predominantly of upper greenschist facies quartzites, phyllites, micaceous schists and argillaceous quartzites.

A light stable isotope (O, H, C) and fluid inclusion research project was undertaken to investigate the geochemical nature of the gold mineralization, resulting in an understanding of the P-V-T-X parameters of the vein forming fluids.

Fluid inclusion research indicates that these veins formed from H_2O-CO_2 ($\pm CH_4$)-rich, low to moderately saline fluids at temperatures of 300±50°C under conditions of variable pressures between 1-2 kbars. Phase separation is indicated by the presence of consanguineous high X_{H_2O}-low X_{CO_2} and high X_{CO_2}-low X_{H_2O} primary fluid inclusions. A west to east regional depletion of methane in fluid inclusions has been documented.

$\delta^{18}O_{Quartz}$ values average 14.4±3 ‰ and calculated $\delta^{18}O_{Fluid}$ values average 7.3±1.5‰. An east to west increase in $\delta^{18}O_{Quartz}$ values of three to four per mil has been observed and indicates either a local thermal gradient with higher temperatures towards the east at the time of mineralization or that lithological heterogeneities resulted in the moderate variations in fluid isotopic evolution.

δD values from vein quartz hosted inclusion waters range from -90 to-170 ‰, averaging -129±21 ‰ indicating a meteoric water origin for the bulk of the vein forming fluids. $\delta^{13}C$ values for vein calcites average -2.5±1.3 ‰ and $\delta^{13}C$ values for limestones and calcareous argillites average -1.9±2.4 ‰. Decarbonization reactions of the local calcareous lithologies is the indicated source of carbon in the vein carbonates.

ACKNOWLEDGEMENTS

I would like to thank Bruce Nesbitt and Karlis Muehlenbachs for having given me the opportunity to continue my studies and for the multitude of 'things' both concrete and abstract that are associated with the process of starting and completing a research project.

The luxury of having so many fine geologists in such a confined place has allowed for the many opportunities to talk with these men and women about the issues of science and the intrigue of academic politics. Thank you; Bud, Tom C., Henry, Brian, Philip, Richard, Bob, Hans, Roger, Tom M., George, Nat, Dorain, Ron, Jack, Charlie, Pat, Rob,K., Reidar, and Walter.

A special thank you to all of the non-academic staff members that have not only giving me assistance with all the complexities of survival at grad school but have allowed me to maintain a special sense of perspective when those times of academic drowning seemed eminent. Thank you; Louise, Isabell, Yves, Nicolette, Sherry, Alex, Ron, Diane, Paul, and Frank. Special thanks to Don R. for all the conversation we shared while logging the hours in the thin section room and to Irene as she made the evening rounds picking up after the bunch of us.

Isotopic analyses were performed in Karlis's lab and I would like to thank James S., Rob K, Olga, Cam, Bjarni and Karlis for all the numbers, and all the thoughts on isotopes and rocks, analytical machines. A special thank you to Ralph R.for the FIInc, all the business and those times; hark, a call for beer, study a little phase-separation.

Without the financial assistance of the British Columbia Department of Energy, Mines and Petroleum resources the opportunity to do this project would probably not have arisen. Additional financial support was provided for by the Geology department in the form of Graduate Teaching Assistantship, to which I would care to add that the T.A. positions were welcomed from more than the financial perspective as they allowed for a certain and necessary break from the 'joys' of research. To this list of financial support I would like to thank Trigg, Woollett, Olson Consulting Ltd., Stratabound Minerals Corp. Faculty of Extension, Steve Prevec and Andrew Locock who gave me the opportunity to work on various geological projects over the period of this work.

To all of you who have helped to make my life at the University of Alberta an enjoyable and enlivening experience I thank from the depths of my soul, and to all of you who have contributed to my 'greater' education, I thank you for having brought out the best and the worst in me and I trust that yes, I have grown much from all of that. Thank you for the good times eh, Al and Al; Rob and Rob and Bob, Steve and Steve, Andrew, Peter, Dan, Cam and Kun, Jackie, Jim and James, Dave. I would also like to extend my thanks to all of those fine people on the 'outside', who have been 'there' when it was so important that they were 'there'. Thank you Rus, Gertjan, Dave and Gail, Ken, Gerry, Janice, Charrer; Daryl, Sarah, Craig and Stephen. Thank you Jeanette G. for all the patience and all your power. Oh ya, a very big thank you to the University of Alberta squad of parking police, who are still; "...doing their jobs".

TABLE OF CONTENTS

Page #

CHAPTER I The Sheep Creek Camp

Introduction 1
Objective of Study 2

CHAPTER II Geology

Introduction 6
Tectonic Setting and Terrane Evolution 7
Lithologies 10
    Toby Formation 11
    Irene Volcanics
    Monk Formatio
    Three Sisters Formation
PreCambrian-Cambrian Boundary 12
    Quartzite Range Formation 13
        Mother Lode Member
        Nugget Member
        Navada Member
    Reno Formation 14
    Laib Formation 15
    Nelway Formation 16
    Active Formation
Intrusive Rocks 16
Jurassic Intrusives 17
    Silver King Suite
    "Tail" of the Nelson Batholith
Cretaceous Intrusives 18
    Salmo Stock
    The Lost Creek Stock
    The Sheep Creek Stock

TABLE OF CONTENTS (continued)

Eocene Intrusives 20

Aplitic Sills and Dikes 20

Lamprophyre Dikes 21

Metamorphism 22

Structural Geology 23

- Primary Sedimentary Features 24
- Folds 24
- Folds to the East and Folds to the West
- Faults 26
- Faults and Joints in the Sheep Creek Camp
- Vein Fractures 27
- Northwesterly Trending Faults
- Northerly Trending Normal Faults
- Flat Lying Faults

Ore Petrology, Quartz Veins and Mineralization 29

- Quartz and Quartz Veins
- Veins, Controls on Widths
- Mineralization 31
  - Gold
  - Silver

Wall Rock Alteration 33

CHAPTER III Fluid Inclusion Research

Introduction 40

Analytical Techniques 42

Phase Transitions 42

COOLING 43

HEATING 46

Results of the Fluid Inclusion Research 47

- Inclusion Classification

Locale Observations 48

- Reno Peripheral and Vsc#205
- Hidden Creek Ridge
- Reno East, Donny Brook

TABLE OF CONTENTS (continued)

Panther Lake, Far East 52
Gold Belt Yell Mom
Stag Leap+; The Salmo-Creston Transect
Billings Creek, Mnt. Waldie, Active #265
GEOBAROMETRY and GEOTHERMOMETRY;
INTERPRETATIONS and INTERDEPENDENCIES 56
Composition of the Inclusions
Bulk Densities 57
Experimental and Theoretical P-V-T-X Data
Independent 'Tt' and 'Pt' 58
Discussion 59

CHAPTER IV Stable Isotope Research
Introduction 87
Summary of Isotope Data
Analytical Technique and Methodology 88
Results of Isotope Analyses 89
Quartz Oxygen 90
$\delta^{18}O_{Fluid}$ Isotopic Composition of Fluids:
$\delta^{18}O_{Quartz}$ Trend 91
Hydrogen Isotopes; Veins Rocks and Minerals
Quartz-Muscovite Geothermometry 95
CARBONATES: $\delta^{13}C$ and $\delta^{18}O$ 96

CHAPTER V Comparisons and Discussion
Comparisons of Parameters 112
The Sheep Creek Camp and The Pamour #1 Mine 120
Genetic Hypotheses 122
REFERENCES 126

LIST OF TABLES

		Page #
Table 1.1	Production summary for the Sheep Creek Camp; 1900-1951.	5
Table 3.1	Fluid inclusion data summary for all locales: Averages	72-73
Table 3.2	Fluid inclusion data summary for specific locales	74-86
Table 4.1	Oxygen, deuterium and carbon isotope data summary	108-111

LIST OF FIGURES

Page #

Figure 1.1 Cordilleran physiographic terranes and general location of the research area 4

Figure 2.1 Tectonic assemblage map of southeastern British Columbia with location of Sheep Creek Camp 34

Figure 2.2 Simplified geological map of the Sheep Creek Camp and immediate district 37

Figure 2.3 Mine locations and vein orientations 38

Figure 2.4 Paragenetic sequence for the Sheep Creek Gold Camp 39

Figure 3.1 Fluid inclusion classification scheme 62

Figure 3.2 Inclusion localities map and inclusion compositions 63

Figure 3.3 Temperature of carbonic phase homogenization 64

Figure 3.4 Temperture of carbonic phase melting vs. carbonic phase homogenization temperture (Tm_{carb} vs.Th_{carb}) 65

Figure 3.5 Fluid inclusion salinity estimates 66

Figure 3.6 Total homogenization and decrepitation temperatures (Figure 3.6a, and Figure 3.6b) 67

Figure 3.7 Isochores and miscibility gap diagrams 69

Figure 3.8 Temperatures vs X_{CO_2} for 6 eq.wt.% NaCl, miscibility diagram at 1.2 kbars 70

Figure 3.9 CO_2 isochores (in gms/cc) in pressure-temperature space 71

Figure 3.10 H_2O ±NaCl isochores (in gms/cc) in P-T space 71

Figure 4.1a $\delta^{18}O_{Quartz}$ value histogram 100

Figure 4.1b $\delta^{18}O_{Fluid}$ value histogram 100

Figure 4.2 $\delta^{18}O_{Quartz}$ locations map and $\delta^{18}O_{Quartz}$ projected section line 101

Figure 4.3 $\delta^{18}O$ projected section showing east-west trend in values 102

LIST OF FIGURES (continued)

		Page #
Figure 4.4	δD values from decrepitation of quartz vein hosted inclusions and quartzites	103
Figure 4.5	δD vs. $\delta^{18}O$ fluids plot, including magmatic, metamorphic and evolved meteoric water regions	104
Figure 4.6	Latitudinal variations of δD and $\delta^{18}O$ values	105
Figure 4.7	$\delta^{18}O$ vs. $\delta^{13}C$ values and statistics from carbonates; vein calcites and calcareous host rocks	106
Figure 4.8	Isotope exchange equilibrium diagram for quartz-calcite and quartz-muscovite pairs	107
Figure 5.1	Summation diagram of vertical transitions in mineralogy and geochemistry	125

CHAPTER I

INTRODUCTION and RESEARCH OBJECTIVE

INTRODUCTION

The Sheep Creek Gold Camp is centred upon 117° 09' W longitude, 49° 08'N latitude within the Nelson Range of the Selkirk Mountains in southeastern British Columbia. The overall region, within which the Kootenay Arc (to be described) and the Sheep Creek Camp are located, is depicted in the physiographics terranes diagram (Figure 1.1.) from Monger et al (1982). The Kootenay Arc is located to the west of the Purcell Anticlinorium (Figure 2.1) which defines the eastern margin of the Omineca Crystalline Belt

The Kootenay Arc is host to a large number of past and present producing mines with five mining regions being of particular importance. These are: (1) the Rossland camp located in the south western region of the the Canadian portion of the Kootenay Arc. The first claim in the camp was the Lily May (1887) and in the summer of 1890 the main ore bodies, the LeRoi, Centre Star and War Eagle were claimed. Although copper and gold were the major metals produced from the camp, silver, zinc, lead and cadmium were also recovered; (2) The Slocan camp, located approximatly 100 kms NNE of Rossland, is similarly famous for its early beginnings with the discovery of the Payne vein in 1891 resulting in a rush of stakings and an extended history of Ag, Pb, Zn, and minor Au and cadmium production; (3) The BlueBell mine, located within the Badshot marbles of the Riondel Peninsula was first staked in 1882 by R.E. Sproule and produced about 5 million tons of ore averaging approximately 5-8 % zinc, 5 % lead, 1-2 oz/ton silver, 0.1% copper and cadmium (Höy, 1980). (4) The Salmo; lead-zinc, mine-Belt (Fyles and Hewlett, 1959), located just west of the Sheep Creek Camp is of particular interest in that it is within this belt of replacement and skarn deposits that the Emerald, Feeney, and Dodger tungsten mines are located which were major producers of tungsten in British Columbia (80%) until the early 1960s. The H.B. mine, located just north of Emerald mine (Figure 2.2) is defined as a zinc-lead-silver replacement deposit. (5) Sheep Creek mesothermal lode gold deposits.

Detailed descriptions of more than 300 mineral properties in the region are given in the works of Little (1960), Fyles and Hewlett (1959), Fyles (1970), Ohmoto and Rye (1970), Reesor (1973), Höy (1980). These are only a few of the many geologists who have worked in the region. Interestingly enough, exploration and research in the Kootenay Arc is continuing today at a level typically found for newly discovered regions, newly discovered ideas. The group of geoscientists who have worked in and published from Kootenay Arc research is impressive and they have made this task of the Arc an enjoyable one. A few of these works are cited within the body of this paper.

THE SHEEP CREEK CAMP

Interest in the lode gold deposits in the Sheep Creek area was aroused as early as 1885 when the Hall brothers staked claims near the headwaters of Ymir Creek. The Yellowstone and Queen veins of the Sheep Creek Camp, located about 18 kms south of Ymir Creek were staked in 1896 and since that time the camp has produce approximately 28.9 million grams (32 tons) of gold, 15.5 million grams (17 tons) of silver and modest amounts of lead and zinc (Schroeter et al., 1986; Mathews, 1953). Production to the end of 1951 from the Sheep Creek, as delineated by Mathews (1953), is listed in Table 1.1. In 1986 the camp was ranked seventh of British Columbia's gold camps in terms of total historic production. Mining activity was intense from the turn of the century until the outbreak of World War I, began again in 1928 and reached its peak in 1937. There was little activity in the camp from about 1942 onwards. Most of the camp region is however held by active claims and is, even amidst these times of economic recession, continuing to be explored.

OBJECTIVE OF THIS STUDY

As a portion of a much larger scale crustal fluids research project being conducted by Bruce Nesbitt and Karlis Muehlenbachs, the Sheep Creek Camp was chosen for a fluid inclusion and light stable isotope study. One of the main objectives of the study was to investigate the relationship between the geology of the vein system(s) and the light stable isotopic (carbon, oxygen and hydrogen) signatures of the veins and the host rocks. In conjunction with this investigation, a fluid inclusion study of both mineralized and unmineralized quartz veins was undertaken with the purpose defining, as much as possible, the nature of the vein-forming fluids. The inclusion study resulted in a better understanding of the pressure-temperature regime of vein formation as well as a good understanding of the compositions of the vein-forming fluids and possible mechanisms for gangue and metal precipitation. The isotopic study reveals and further supports the notion that this piece of the Canadian Cordillera has experienced a protracted tectono-thermal history and this has resulted in a complex of isotopic signatures, some of which can be interpreted directly while others have indicated scenarios of isotopic (and/or mineralogical) disequilibrium, and periods of thermal (hydrothermal) overprinting.

An attempt was made to sample not only the region of the gold mineraliztion but to extend the research outward into the surrounding geology. The reason for the expanded sampling was to investigate any possible lateral variations in the geochemistry of the veins Interestingly enough, trends in both fluid composition and isotopic signature were identified. In addition, because of the nature of some of the fluids in the quartz veins (they carry a significant methane component) it was possible to initiate an isotopic investigation of the carbon and deuterium ratios in the vein methane. Although the result from this portion of the study are inconclusive, the research has opened another avenue for investigating crustal fluid-rock interactions.

The paper is organized into five chapters. Chapter II is a summary of the geology of the camp and the region that surrounds it. An attempt was made to consider some of the salient regional features. As will become obvious to the reader or is already known to anyone who has worked in the Kootenay Arc, a thorough investigation into the salient features would be another book in itself. Lithologies, structures and metamorphism within the region is presented and to this, a summary of the mineralogical-hydrothermal characteristics of the Sheep Creek Gold Camp is added. Chapter III is a detailed account of the fluid inclusion study. Chapter IV is a detailed account of the isotope study and Chapter V is a comparison of the Sheep Creek vein system with the well documented characteristics of known mesothermal gold systems (Nesbitt,1991; Kerrich,1991) and a comparison with the Pamour #1 mine of the Porcupine Camp, Ontario, Canada. A short discussion regarding genetic models is also included in Chapter V.

So where's the gold ? The possibility that there is still a significant quantity of ore grade mineralization in the Sheep Creek camp is presently being investigated by Yellowjack resources through a shallow drill program in the south sector of the camp. The geological information that is available regarding this particular gold camp is relatively thorough. Additional, well constrained geological, geochemical and geophysical research (exploration) is however needed to further assess the mineral potential of the region. The term region is used here to suggest that it is probable that high grade mineralization is to be found in similar strucural features as those that carry the bulk of the Sheep Creek gold. These structures are discussed in the body of this work, Mathews (1953) and Fyles and Hewlett (1959).

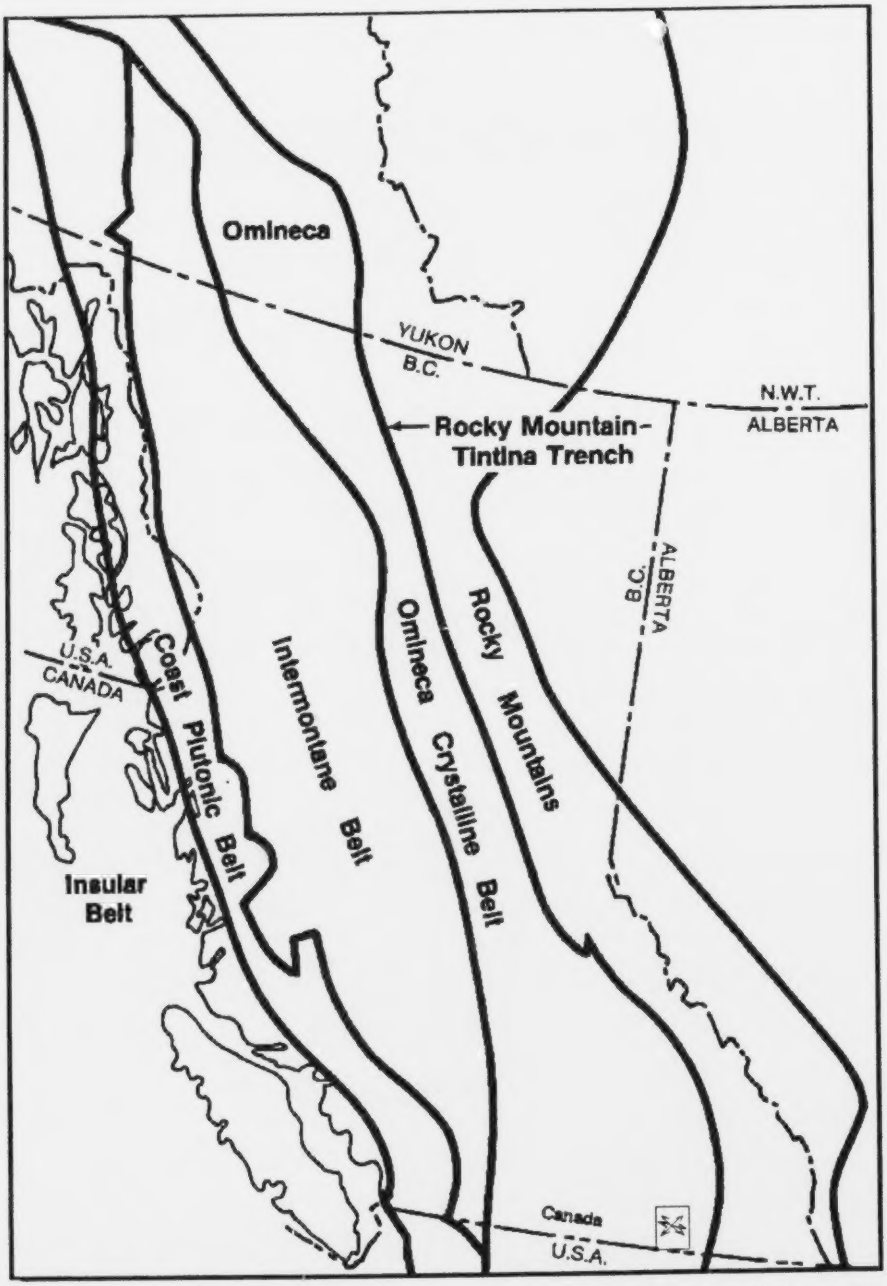
Omineca
YUKON
B.C.
N.W.T.
ALBERTA
Rocky Mountain-Tintina Trench
B.C.
ALBERTA
Rocky Mountains
Omineca Crystalline Belt
Intermontane Belt
Coast Plutonic Belt
U.S.A.
CANADA
Insular Belt
Canada
U.S.A.

Figure 1.1 Cordilleran physiographic terranes map and general location of the study area. Modified from Monger et al., 1982

TABLE 1.1.
SUMMARY OF TOTAL RECORDED PRODUCTION (1900-1951)
SHEEP CREEK GOLD CAMP

	ORE TONS	GOLD OZ.	SILVER OZ.	LEAD LBS.	ZINC LBS.
COLUMBIA 1932, 1933	42	31	46		
FAWN 1915, 1935	74	131	13		
GOLD BELT	257,338	79,984	32,761		
KOOTENAY BELLE	292,893	109,937	37,153		
MOTHER LODE, NUGGET 1906-1922	429,667	231,932	184,502		
RENO, BLUESTONE 1928-1938 (LEAD AND ZINC) →	155,625			143,033	92,625
ORE HILL 1906-1940	3,669	2,849	5,415	186,940	166,784
SUMIT 1906-1938	1,205	870	1,218	30,264	28,634
QUEEN 1900-1938	358,524	162,719	100,182 Queen & Sheep Creek Mines		
SHEEP CREEK (GOLD MINES LTD.) 1938-1951	360,796	140,992			
VANCOUVER 1909-1933	383	964	421		
YELLOWSTONE 1900-1902	16,989	5,606	3,091		
TOTALS	1,721,580	736,015	364,793	377,568	312,633

CHAPTER II.

GEOLOGY

INTRODUCTION:

Massive or laminated (in some cases brecciated) quartz veins, occupying east-trending high-angle dextral, strike-slip fault zones are the dominate source of gold mineralization in the Sheep Creek Camp (Mathews, 1953; Robinson, 1949).

The camp, located in the Eastern Belt of the Salmo lead-zinc map-area, as defined by Fyles and Hewlett (1959), is structurally dominated by the Sheep Creek Anticline. This anticline is a major, overturned-isoclinal structure composing the medial portion of the southern end of the Kootenay Arc. This, and associate structures, extend beyond the camp to the north and south for more than fifty kilometers forming one of the more prominent features of the Kootenay Arc, the Nelson Range, formerly named the "Quartzite Range" of the Selkirk Mountains (Little, 1960).

Hedley (1955), introduced the name Kootenay Arc, a misnomer with respect to present plate tectonic theory and nomenclature (Lambert,1989), the name does however aptly describes this northerly trending, convex to the east, arcuate belt of polydeformed and metamorphosed, thrust-imbricated Proterozoic to early Mesozoic, autochthonous and allocthonous composite terrane (Figure 2.1, from Parrish et al.,1988). The Kootenay Arc extends from near Clearwater Lake at approximately 120°W, 52°N to the Columbia River near 118°W, 48°N (Lambert,1989) and separates the Purcell Anticlinorium in the east from the Mesozoic island arcs of Quesnellia in the west. It has undergone a protracted tectonic history including plutonic activity beginning possibly as early as the late Triassic (Höy, per.comm.) and continuing into the mid-Jurassic (≈165 Ma.), the mid-Cretaceous (≈100 Ma.) and the mid-Eocene (≈ 50 Ma.) (Archibald et al., 1983, 1984; Little,1960; Armstrong, 1988).

Prominent geological structures within or bounding the Kootenay Arc include the Valhalla high-grade metamorphic complex, which is separated from the Nelson plutonic complex, immediately to the east of the Valhalla complex, by the Slocan Lake Fault in the north and the Champion Lake Fault, the southern extension of the Slocan Lake Fault . These faults are early-Tertiary, north trending shallow to steeply east dipping (30-40°; 40-85° respectively) brittle-ductile zones of normal faulting (Parrish,1984; Parrish et al., 1988; Corbett and Simony, 1984). Other regional scale normal faults are found to the east of the camp, two of which are the Blazed Creek Fault and centered upon the Kootenay Lake, the Purcell Trench fault (Figure 2.1)

A well documented north trending, 10-15 km wide zone of high grade metamorphism (sillimanite, K-feldspar) diminishing to greenschist to upper-greenschist facies metamorphism is found straddling the Kootenay Lake. Potassium-argon dating of rocks in this region show that there was a protracted cooling history as has been interpreted by the strong correspondence and parallelism of the Cretaceous to Eocene trend in isochrons with the increasing grades of metamorphism (Archibald et al., 1984).

The miogeoclinal Proterozoic to Lower Paleozoic metasedimentary sequence that constitutes the Salmo-lead zinc map-area and the Windermere Supergroup rocks located to the east of this belt, are separated from the early-Jurassic eugeoclinal rocks of the Rossland Group by a composite region of thrust (± strike-slip) faults including the Waneta, Tillicum (Einarson,1991), Argillite and Black Bluff faults which approximately parallel the local stratigraphic trend of the Kootenay Arc (Höy et al.,1990; Andrew and Höy,1990; Fyles and Hewlett,1959). The regional north-east trending fold structure, the shearing and penetrative foliation and these faults are considered to be manifestations of "... two periods of pre-middle to late-Jurassic compressional deformation" (Höy et al.,1990).

TECTONIC SETTING and TERRANE EVOLUTION:

A century of mineral exploration and geological research has resulted in a good interpretation of the stratigraphic successions and their regional correlations as well as a moderate understanding of the geological evolution of the region. Recent deep crustal structural research from Lithoprobe (Cook et al., 1988) and COCORP studies (Potter et al., 1986) have shown that a number of Tertiary extensional structures extend to depths of around 10 kilometers. Other deep crustal structures are being investigated further. Lambert (1989) summarizes three of the present existing theories of the tectonic origins of the Arc and discussed the relative merits and shortcomings of each of these theories. The interpretive complexities inherent in delineating an all inclusive tectonic theory for the Arc is far beyond the scope of this research. The following summary of the tectono-thermal evolution of the Arc draws heavily upon the work of Archibald et al. (1983; 1984) and does not directly address tectonic theory, but does consider the evolution of thought regarding the Canadian Cordillera and a tectono-thermal history for the Kootenay Arc.

The Canadian Cordillera is essentially composed of a collage of what Coney et al., (1980) first termed suspect terranes,"...characterized by internal homogeneity and continuity of stratigraphy, tectonic style and history", with terrane boundaries that are fundamental stratigraphic discontinuities that separate distinct temporal or physical geological sequences (Coney et al., 1980). Much of the Canadian Cordillera is composed of a collage of allocthonous terranes, tectonically welded to a "...compressed, parautochthonous continental margin terrace wedge consisting mainly of sediments eroded from the North American craton and deposited along its rifted western (paleo) margin" (Archibald et al.,1983). Monger et al.(1982) expanded upon the earlier work of Coney et al.(1980) and divided the Cordillera into five physiographically distinct belts based upon the distinct geology and geomorphology of the belts. Monger et al (1982) subsequently groups the allochthonous belts into two large, composite, allochthonous terranes as a function of the belt's relationships with two major regional tectonic 'welts', the Coast Plutonic Complex and the Omineca Crystalline Belt. It has been observed that "...the Rocky Mountain, Intermontane and the Insular belts are suprastructures composed of unmetamorphosed and low-grade metamorphic rocks, (which contrast with) the Omineca Crystalline Belt and the Coast Plutonic Complex, in which the metamorphic and plutonic infrastructure of the Cordillera is exposed and which became differentiated between Jurassic and mid-Tertiary time when deformation, metamorphism, granitic magmatism and uplift were concentrated in them."

It is within the Omineca Crystalline Belt, which Monger et al. (1982) originally described as "...Mid-Proterozoic to mid-Paleozoic miogeoclinal rock, Paleozoic and lower Mesozoic volcanogenic and pelitic rock, local Precambrian crystalline basement, highly deformed and variably metamorphosed up to high-grades in mid-Mesozoic to early Tertiary time and intruded by Jurassic and Cretaceous plutons" that the Kootenay Arc is located. Archibald et al. (1983) summarizes the Kootenay Arc as "... a west facing monocline along which the displaced continental margin terrace wedge is draped over the rifted Proterozoic margin of the craton, and across which there is a change in structural level involving an aggregate of about 20 km of mid-Proterozoic to Middle Jurassic strata (Price,1981)". This monocline is characterized by intense penetrative foliation, coaxially refolded, early-west verging faults and folds and regions of amphibolite-facies metamorphism as well as numerous synkinematic and post-kinematic (Middle to Late Jurassic and Middle Cretaceous) granitoid plutons.

Archibald et al., (1983; 1984) have developed an evolutionary profile of deformation, metamorphism and plutonism from the early -Jurassic to Eocene periods for the Southern Kootenay Arc. The Sheep Creek Camp is located within their study area and it is therefore believed that the tectonic evolution summarized below applies in part if not wholly to the geological evolution of the Sheep Creek Camp.

Prior to the protracted compressional, transpressional and extensional tectonics that is suggested by the following, it is believed that the autochthonous North America off-shelf facies that compose much of the Kootenay Arc was subject to repeated rifting events (Nelson, 1991; Thompson et al., 1987; Devlin, 1989). Höy (1982) has suggested that the complex carbonate hosted Pb-Zn deposits (Kootenay Arc-Type deposits, including H.B., Feeney, Jackot, etc.; see figure 2.2) found straddling the western edge of the miogeocline are fundamentally syngenetic stratabound-strataform, proximal-distal sedimentary exhalative deposits which moderately resemble the MacMillan Pass area in the Selwyn Basin (Nelson,1991).These deposits are hosted by the Reeves-Badshot limestone-dolomite unit which is a significant marker horizon that extends along the greater portion of the Kootenay Arc. As a result of there location in the Kootenay Arc, these deposits have been subsequently deformed and altered. These deposits, located in Fyles and Hewlett's "Mine Belt" are presented here in an attempt to broaden the reader's understanding of the regional ore mineralogy, which will not be dealt with in any detail in this study.

In mid-Jurassic time, Quesnellia, a composite allochthonous terrane (Tipper,1984) was accreted to and overlapped the western margin of ancient North America between 166 and 156 Ma. The Proterozoic Windermere Supergroup (southern Kootenay Arc) and the early Paleozoic Lardeau Group (central Kootenay Arc) were carried rapidly to depths of more than 20 km. resulting in synkinematic regional metamorphism (Archibald,et al., 1983). Syn- to post-kinematic granitic rocks intruded both the descending miogeoclinal rocks and Quesnellia during this time. These deformed and metamorphosed miogeoclinal rocks were then uplifted by more than 7 km and subsequently thrust over and into the composite accreted terrane "... prior to being intruded by post-kinematic granitic rocks, many of which belong to the two mica suite of mid-Cretaceous ages". Archibald et al.(1983) further suggest that by mid-Cretaceous time the area "...had evolved into a tectonically active metamorphic infrastucture and a tectonically dormant suprastructure" and that this major period of magmatism may have been a result of Cretaceous compression affecting the rocks of the Purcell Anticlinorium " prior to emplacement of the post-kinematic, mid-Cretaceous plutons into a then tectonically dormant suprastructure between 115 and 90 Ma. They further suggest that following the mid-Cretaceous thermal culmination, protracted cooling and slow uplift occurred until late-Cretaceous time and that this preceded Paleocene to Eocene "... rapid cooling of the still hot mid-Cretaceous infrastucture due to uplift and erosion (0.4 - 0.6 km./Ma.) accompanying thrusting of the miogeoclinal strata over a steplike ramp in the basement during formation and final stages of development of the Purcell Anticlinorium (Price,1981) between 65 and 55 Ma." (Archibald et al.,1984). Differential uplift and/or tectonic denudation of the infrastructure occurred in Eocene time.

K-Ar geochronology of biotites in the Salmo and Summit areas of the Arc suggest that post kinematic plutons were emplaced in mid-Cretaceous (≈ 100 Ma.) time and that these dates provide a minimum estimate of the "true" cooling date (biotite K-Ar cooled below its closure temperature of approximately 280-320° C; Berger and York, 1979) and a maximum estimate of the period of tectonic or hydrothermal overprinting. The younger mica date recorded for the Sheep Creek stock is interpreted as a result of hydrothermal alteration associated with the mineralization found there (≈ 98.3±1.1 Ma.) and the concordant mica date of 102 Ma. for the Lost Creek and Summit stocks are considered to be the age of these plutons (Archibald et al., 1983).

LITHOLOGIES:

The essentially conformable sequence of metasedimentary , Upper Proterozoic to Ordovician, North American miogeoclinal rocks that host the Sheep Creek vein system is diverse in composition but contains units of remarkable homogeneity. The following is a brief description of these lithologies and begins with those rocks of the Hadrynian Windermere Supergroup found east of the camp.

TOBY FORMATION:

Daly (1912) originally placed this thick (2.5 km) "roundstone" conglomerate unit with the Irene Formation and termed it the Irene conglomerates. Little (1960) chose to apply the name 'Toby' to it to avoid any confusion with the overlying Irene Volcanic Formation which is, in the lower portion of the section, interbedded with and transitional to the conglomerate. The unit is well exposed from south of the border along a strike of ≈5°N to its contact with the Bayonne batholith nearly 50 kms to the north.

Well rounded, coarse sand-size grains through to half metre boulders of micaceous quartzite, white sucrosic quartz and subordinate amounts of grey or white dolomitic marble are cemented together by a rather uniform greenish grey and grey muscovite, biotite, chlorite schist. The unit is characteristically crushed and sheared and the majority of the pebbles are deformed into strike parallel obloids and lenses. Daly (1912), was probably the first to suggest that because of the similarities in cobble color, composition and 'general field habit', the source of this material was from the unconformably-underlying, Helikian-Purcell Supergroup (Daly's Priest River Terrane) to the east and suggests further that these systems may have experienced penecontemporaneous deformation. No confirmation or direct rejection of such an hypothesis has yet to be established, though Wheeler (1966) has suggested "...that during the Windermere time, sediments deposited in the eastern belt were derived from the east. The source was partly from the edge of the continental interior, portions of which apparently exposed areas of crystalline basement, and partly from the actively eroded highlands of the ancestral Purcell Mountains uplifted during the preceding orogeny". The relationship between the Purcell and Windermere Supergroups is quite important to the issue of mineralization within the Kootenay Arc but is not considered further in this study.

IRENE VOLCANICS:

Conformably overlying and intercalated with the top of the Toby conglomerate is this northerly trending (7°-30°N), steeply dipping (70°E-70°W) highly altered andesitic volcanic unit with a 10 m. interbed of fine grained black limestone and lenticular intercalations of dolomite and phyllite. The "greenstone" (the Irene Volcanics) is predominantly schistose and is composed of actinolite, saussuritized plagioclase, quartz, calcite, epidote, sericite and minor amounts of magnetite, pyrite and ilmenite (Little, 1960; Daly, 1912). Daly (1912) reports that much of the greenstone contains schistosity parallel lenses of calcite (± quartz) amygdules. Although the precise origin of this unit has been debated, Rice (1941), Park and Cannon, (1943), and Little (1950) have confirmed the original extrusive origin that Daly had reported.

MONK FORMATION:

The Monk Formation (Unit 0, Figure 2.2) is characterized by the parallelism of its penetrative foliation (strike N10°E, dipping 79°W-55°E) with the regional fabric; including schistosity, bedding and axial planes and possibly some of the major thrust faults. The original sedimentary structures in this formation have been effectively obliterated by regional deformation though Daly (1912) has established bedding attitude (N10°E and 75-90°W) from the contacts between grit and conglomerate units and the schists. The unit is exposed as the core of a southerly plunging anticline overlain by the Three Sisters Formation. The unit is composed of a 1.3 km section of phyllitic slates, phyllites, schistose conglomerates, sheared quartzites and quartz grits as well as kyanite bearing sericite-quartz schists . Walker (1934), states that "...the scarcity of outcrops, coupled with the knowledge that the formation is highly folded upon itself, renders it impossible to describe it fully or to estimate its thickness". The significance of the unit with respect to this study is the parallelism of structure and foliation and the presence of kyanite.

THREE SISTERS FORMATION:

The top of the "...Monk Formation is conformably overlain by a mass of very heavily bedded sandstones, grits and fine grained conglomerates, which in all respects are identical in character with the coarser-grained phases of the Monk Formation" (Daly,1912).

Daly (1912) originally subdivided this massive, greenish-grey grit and fine conglomerate unit into the Wolf Formation and the overlying Dewdney Formation which as Daly stated;"...By insensible gradations the Wolf Formation passes into the conformably overlying Dewdney Formation. The plane separating them is thus an arbitrary one", suggests that no significant breaks in deposition occurred within this unit. Walker (1934) attributed the name Three Sisters Formation to this uniform (in thickness and composition) unit after the Three Sisters Peaks located east of the headwaters of the Sheep Creek, where it is well exposed and forms the highest peaks in the area. The formation is the most massive of any of the units in the area and generally exhibits little evidence of bedding. The rock fractures across the schistose cement and quartz grains to produce huge angular blocks in the talus and scree slopes. Interbedded with the massive quartzite however are minor units of alternating beds of grey grits and white quartzites and an interlying set of argillaceous units which Daly (1912) describes as "...felted aggregates of quartz, feldspar, biotite sericite and iron oxides". It is also clear from the bedding parallel schistosity, which does not flow around the clastic grains and is cut off sharply by the grains, that the "...schistosity produced by the common orientation of the micas is not due either to shearing of the rock or to the rotation of pre-existing sericite and biotite, but is due to the crystallization of the minerals with their cleavages lying perpendicular to the direction of a compressive force" (Daly,1912).

This formation occupies the core of the Sheep Creek Anticline, the core of the Baldy Anticline (conceivably the northern extension of the Sheep Creek Anticline) and a wide northerly trending belt in the east of the map area (Figure 2.2).

PRECAMBRIAN - CAMBRIAN BOUNDARY:

The delineation of the boundary between the Precambrian Windermere Supergroup lithologies and the conformably overlying Paleozoic rocks of the Quartzite Range Formation has proven to be difficult. Ultimately, after a number of attempts to chronologically locate these rocks (Daly,1912; Walker,1934; Rice, 1941; Park and Cannon, 1943), Little, (1960) chose to place this boundary at the base of the Quartzite Range Formation. This decision was based upon the presence of a few Cambrian trilobite fragments (found south of the border in the "Gypsy Quartzite", the Quartzite Range Formation correlative in the Metaline quadrangle in Washington) as well as abundant Lower Cambrian archaeocyathids hosted by the basal limestone of the Laib Group, which conformably overlies the Reno Formation, which similarly overlies the Quartzite Range Formation.

QUARTZITE RANGE FORMATION:

The Quartzite Range Formation is the most significant lithological unit of the Sheep Creek Gold Camp. It is within this unit that the majority of the gold mineralization has been obtained. Mathews (1953), subdivided the Quartzite Range Formation into three major divisions; the Motherlode, the Nugget and the Navada Members and further subdivided the Motherlode and Nugget Members into the Lower, Middle and Upper units and the Navada into the Lower Navada and the Upper Navada.

These predominantly massive, white-quartzites with minor intercalated argillaceous quartzites retain much of their primary sedimentary structure including multiple beds of well-preserved ripple marks and extensive crossbedded lithologies. This formation is best exposed in the limbs of the Sheep Creek and the Baldy anticlines and has been traced for nearly 240 kms northwards along the trend of the Kootenay Arc.

MOTHERLODE MEMBER:

This 335 metre thick unit of competent massive white-quartzite is so homogeneous that stratification is barely discernable although the Middle Motherlode is slightly more argillaceous and contains a minor green-schist phase. The Motherlode occurs as a single broad zone straddling the axis of the Sheep Creek Anticline in the southeast near Mount Waldie and is separated north of there, where the Three Sisters Formation core the anticline at surface. It is also found to the east of the Sheep Creek Anticline as a broad northerly trending unit between the Laib Syncline and the Three Sisters Formation

NUGGET MEMBER:

The Nugget Member consists of 165-275 metres of argillaceous quartzites, minor argillites overlain by mixed argillaceous quartzites and massive quartzites which are in turn overlain by massive white-quartzites. The Upper Nugget is the most competent structural unit in the camp and the vein fissures (normal fault structures to be discussed) crossing these quartzites are very clean and display minimal drag or shearing. The significance of this ≈80 metre thick succession of strata is that nearly all of the productive veins in the camp (excluding the Reno and Bluestone veins) "...have yielded ore from the Upper Nugget beds, and it is estimated that fully half the production of the camp has come from veins" in this unit (Mathew,1953). This portion of the Quartzite Range Formation is found in both limbs of the Sheep Creek Anticline and in the core of the Western Anticline near the confluence of Waldie and Sheep Creek where much of the vein system was highly mineralized.

The Middle Nugget beds are a distinctively less competent assemblage of quartzites, dark argillaceous quartzites and stratified argillites. These beds display minor variations in thickness and where they are intersected by quartz veining contain (ed) some significant ore shoots however, most of the "...vein fractures cutting the Middle Nugget beds contain either no quartz or quartz with subcommercial gold values" (Mathews,1953).

The top of the Lower Nugget is essentially the lowest portion of the succession that has produced any gold and has been thus described as the bottom of the critical quartzite beds. This notably incompetent, ≈50 metre thick succession of argillites interbedded with argillaceous quartzites does not, interestingly enough, display the complexities of variable thicknesses and complex folding as are observed in the incompetent Reno Formation overlying the Quartzite Range Formation and is essentially unmineralized.

NAVADA MEMBER:

This somewhat thinner member of the Quartzite Range Formation is, from the Lower Navada upwards, a relatively competent succession of dark, thin-bedded quartzites and argillaceous quartzites extending into the massive white quartzites of the the Upper Navada. The member does however display some close folding and variable thickness and has been host to oreshoots in a number of the mines including the Gold Belt; Kootenay Belle A; the Bluestone; the Reno mine and the Queen vein.

RENO FORMATION:

Conformably overlying and locally transitional into the Upper Navada quartzites is this complex succession of micaceous quartzites and phyllites, which have been severely folded into a package of lithologies of variable thicknesses. (Mathews termed these rocks argillites and argillaceous quartzites but Little (1960) believes these to be less descriptive terms. In the following discussion both terms will be used interchangeably as I cannot qualify the situation directly.) As is the case with all the other lithological units in this district, the actual definitions of the formations have varied and evolved. Mathews (1953) has adequately defined this formation as occurring between the Upper Navada member, located east of the summit, and the base of the infolded Laib formation, an easily recognized white, massive limestone which weather buff-honey comb. The greater proportion of the Reno Formation (estimated to be approximately 200 metres thick though varying from as little as 15m. to as much as 275m, as observed on the eastern limb of the Western Anticline) is comprised of phyllitic quartzites, phyllites and light brown micaceous schists. North of the Reno mine, Mathews (1953) was able to subdivide the formation into the lower phyllitic and micaceous quartzites and the upper impure greenish-grey quartzites members. He did not attempt this subdivision elsewhere. The formation has been severely folded with numerous and complex dragfolds (parasitic folds) that range in amplitude from a few inches to tens of feet (how do you convert imperial approximations ?). The beds thicken and thin as a result of this folding and Mathews suggests that abnormally thick sections of this incompetent formation is a function of duplication by tight and small scale folding. In the type locality near Reno Mountain, contact metamorphism has increased the competency of the formation and as a result of this, the vein fracturing in the Reno mine has allowed for the extensive ore bodies which contrasts with elsewhere, where the fractures in the Reno formation tend to either die out or diminish in displacement with significant changes in attitude as the faults pass from the Navada Quartzites into the incompetent Reno beds. Other than the Reno mine and two veins in the upper portions of the Gold Belt mine, veins in the Reno Formation have been non-productive.

LAIB FORMATION:

Further up this conformable succession of formations is the Laib Formation which has been defined as a thick assemblage of phyllites, micaceous quartzites and limestones (Fyles and Hewlett, 1959). The sequence, described originally as the lower part of Walkers' and Dalys' Pend d'Oreille series (including parts of Dalys' Beehive and the entire Lonestar Formations) is best exposed on the upper slopes of Reno Mountain and the ridge northwest of the Reno mine (termed Hidden Creek ridge in this report). The formation also occupies the trough of the Laib syncline and the basal limestone is reported to extend along the core of the isoclinal syncline, located between the Sheep Creek Anticline and the Western Anticline, from Reno Mountain southwards beyond Mnt. Waldie to just above Lost Creek. These rocks have been mapped as an extensive portion of Fyles and Hewlett's(1959) "Mine Belt", which extends southward across the U.S. border and northwards, (where it is correlated with the Badshot marbles and the overlying Lardeau Formation) along the Kootenay Arc as far north as the Goldstream district.

The importance of this succession of limestones (marbles) and dolomitic limestones, phyllites and schists lies in its potential for hosting Pb-Zn (± Ag,Au,W,Cd) deposits as well as being a possible source for some of the constituents found in the vein systems of the Sheep Creek Camp, (eg. carbonates). Mathews (1953) subdivided the formation, within the Sheep Creek Camp, into six members of which the first, third and fifth are distinctly calcareous and the intervening members are exclusively argillaceous. The 'argillaceous' beds are locally metamorphosed to biotite and amphibolite schists and this entire package is similarly complicated by numerous folds and much faulting though detailed mapping in the camp is limited.

Although this formation comprises a relatively significant portion of the lithological package comprising the Sheep Creek Camp, the mineralization hosted by these units is essentially restricted to the calcareous beds and is base metal enriched and carries a higher percentage of silver. The total amount of ore from the Sumit and Ore Hill mines is comparatively small relative to the production for the camp with widths of high-grade mineralization being "...measurable in inches rather than feet" (Mathews,1953).

NELWAY FORMATION:

These Middle Cambrian, predominantly black-dark grey, limestones, phyllites and calcareous schists, occur in a number of areas within the district (Little,1960) but only outcrop as a fault bound inlier found east of the camp near the core of the Laib syncline. Where the formation can be observed without fault relationships, it grades conformably into the underlying Laib Formation and has been paleontologically dated (using trilobite and brachiopod faunas by association with its correlative unit, the 'Metaline' limestones south of the U.S. border), as mid-Middle Cambrian.

ACTIVE FORMATION:

As a direct result of the "...fortuitous discovery of Ordovician fossils in" this formation, Little (1960) was able to separate this discontinuous belt of dominantly black argillites with minor slates, phyllites, argillaceous limestones and dolomites of this disconformably fault bound unit from the Laib Formation. Fyles and Hewlett (1959) have essentially defined their Black Argillite Belt as a function of this succession bound on the east by the Black Bluff Fault and on the west by the Argillite Fault. These rocks, as occur in the Sheep Creek region, comprise a more or less monotonous succession of well cleaved argillites and rare calcareous intercalations; all of which appear to be intensely silicified. As Little (1960) points out "... The structure of the Active Formation in the type area (northwest of the Sheep Creek Camp) is baffling and only by very detailed mapping might the solution of the problem be obtained. The formation appears to be completely 'wrapped around' the large granite stock on Porcupine Creek". In the region depicted in Figure 2.2, the strata strike roughly parallel with the thrust faults, having extremely variable dips and as Fyles and Hewlett suggest, the Black Bluff Fault is folded in the valley of Hidden Creek which may account for the presently unexplained seemingly conformable relationship of this formation with Lower Cambrian rocks found in the Hidden Creek valley (Little, 1960).

INTRUSIVE ROCKS:

A remarkable complex of intrusive bodies has literally saturated the supracrustal rocks detailed above. Throughout the Kootenay Arc are granitic through to syenitic bodies that span an intrusive history of at least 130 million years. In an attempt to establish a framework from which a discussion of heat sources or volatile and/or fluid sources may be based, a few of the local intrusive rocks will be considered.

JURASSIC INTRUSIVE:

Silver King Suite;

The oldest intrusive rocks within the immediate district (within approximately 40 kms radius from the Sheep Creek Camp) is a suite of essentially granodioritic-dioritic albite porphyry rocks called the Silver King suite. Originally, these rocks were considered as a proximal satellite suite of the Nelson Batholith. Recent work has shown that these rocks are separate from the Nelson Batholith and have been dated as being approximately 10 Ma older, as syntectonic bodies of 178-182 Ma age (Höy, pers.comm.). This suite of small, semi-concordant plutons are hosted by the Elise and Hall formations of the Rossland Group and are located approximately 20 kilometers N-NW of the Sheep Creek Camp. (Höy, and Andrew, 1988).

"Tail" of the Nelson Batholith;

Recent work on the 'tail' of the Nelson Batholith done by Vogl and Simony (1992) has shown that this portion of the much larger intrusive body to the north and west, "...consists of three subvertical, subparallel, compositionally distinct sheets: a western quartz diorite, a central leuco-quartz monzonite and an eastern quartz monzonite".

This complex intrusive body has been dated by Duncan and Parrish (1979), (Rb-Sr, whole rock) at 150 ±9 Ma which is somewhat younger than the dates listed for the various phases of the main Nelson body which span the period of 160-172 Ma (see Brown and Logan, 1988 for references and dates).

As is the case with many of the plutonic bodies in the region, xenolithic masses, roof pendants and screens of local supracrustal rocks are found within the 'tail'. Two of these bodies which are of particular interest are found near Kutetl Creek (approximately 24 kms north of the Sheep Creek Camp). Recent work by Jon Einarson identifies the fault that juxtaposes Ymir Group (late Triassic-early Jurassic) allochthonous rocks from rocks that resemble the Upper Mississippian to late Triassic Slocan/Milford (pericratonic) rocks, as a northern extension of the Waneta Fault. Further detailed study of the deformation and strain within the screens and pendants and the granitic rock itself "...suggests that deformation within the 'tail' took place during or shortly after emplacement with the heat from emplacement providing a thermal softening and giving rise to wide homogeneous shear zones" (Vogl and Simony, 1992).

Other mid-late Jurassic, granitoid intrusive bodies that occur closer to the Sheep Creek Camp include the Mine Stock, dated at 171 Ma (U-Pb by Calderwood et al., 1990) which also has a K-Ar muscovite date of 166 Ma and a K-Ar biotite date of 165 Ma (Archibald et al., 1983). The Wall Stock, located just north of the Mine Stock, has a K-Ar biotite date of 147 Ma and a K-Ar muscovite date of 156 Ma, whereas the Porcupine Creek Stock, located north of the camp has been dated by Wanless et al. (1968) at 157 Ma from hornblende K-Ar and 107 Ma from biotite. Archibald et al. (1983) suggests that the anomalous biotite date is a result of K-Ar resetting by the influence of the nearby Cretaceous plutons and stocks.

CRETACEOUS INTRUSIVES:

Salmo Stock;

The Sheep Creek Camp is essentially surrounded by and in parts underlain by granitoid bodies of mid-Cretaceous age. These bodies include the relatively large Salmo Stock to the north-northwest of the camp. This body, as described by Fyles and Hewlett (1959) and observed by the author, is composed of variable medium grained rocks ranging from quartz-rich biotite granite to diorite phases and has an extremely complex marginal transition into the surrounding supracrustal rocks including xenolithic fragments, granitization (*) of the country rock and complex biotite-granodiorite migmatites. ((*) Granitization, as defined by Mason (1978); is a process whereby rocks are progressively transformed in the solid state, below their melting points into granite, a special case of regional metasomatism. What geological phenomena Fyles and Hewlett are actually referring to is difficult to surmise though metasomatic alteration of the metasediments is locally abundant.) This marginal zone of granitized and brecciated metasediments is cut by massive dikes of granite containing inclusions of rock that resembles more pristine granite which suggests "...that granitization of the sedimentary rocks was followed by intrusion of large parts of the stock and or peripheral dikes" (Fyles and Hewlett, 1959). This body has been dated at 115 Ma (Rb-Sr; Einarson 1991).

The Lost Creek Stock;

The Lost Creek Stock is exposed in the Lost Creek valley over an area of about 40 km^2 and through a vertical range of about 1.2 km. Mathews (1953) has described this 102

Ma intrusive body (Archibald et al.,1983) as a quartz monzonite which consists of microcline-microperthite, abundant albite, strained quartz and muscovite with minor garnet. This stock transgresses the deformed metasediments in the region but has not disrupted the pre-existing structure.

North of the northern apophysis of the Lost Creek Stock, in the valley of the Sheep Creek, it is believed that this same body was intersected at the bottom of the Queen shaft and in a hole drilled towards the west from the #12 level of the Queen vein. Mathews (1953) interprets the mineralogical and structural similarities of this buried granitic mass to more closely resemble the Lost Creek Stock than the Sheep Creek Stock which is located a mere 800 (±) metres to the west-northwest.

The Sheep Creek Stock;

The Sheep Creek Stock is mapped as a microcline-microperthite, quartz, oligoclase biotite, muscovite-bearing granite. The quartz is relatively unstrained though the biotite is commonly replaced by chlorite and garnet; sphene(titanite), zircon and apatite are locally present. The stock is certainly not an homogeneous body and as reported by Walker (1934), on the northwest side of the stock, the porphyritic granite is intruded by a fine grained granite which in turn is intruded by a hornblende granodiorite (Mathews,1953). An approximately 40 m section of this body near Fawn Creek contains from east to west, a friable section of biotite-muscovite granite, discordantly intersected by a 30 cm aplitic dike. Underlying the two mica granite is a 2 metre thick microcline-porphyry lamprophyre which is overlying a complex mylonitic cataclastic zone containing coarse two-mica granite and quartz vein breccia blocks and semi-obloid serpentinized lamprophyre clasts in a matrix of saussuritized plagioclase, talc and serpentinite. This fault zone is transgressed by an extremely lustrous, almost opalescent 5cm white quartz vein. The rest of the section (about 15 metres) is composed of a fine grained granodiorite-quartz monzonite which ultimately disappears to the west under overburden. North of this outcrop the Sheep Creek Stock contains an inlier mafic (hornblende-augite 'diorite') phase or this coarse grained basic rock is a xenolith from some unknown source.

The walls of this stock are reported to be nearly vertical and by observations of its contacts with the country rock, Mathews believes that the stock does not widen with depth. Unlike the Lost Creek Stock, the Sheep Creek Stock has thrusted into and deformed the structure of the surrounding metasediments (Active and Laib Formations) producing a bowing of the folded beds around the stock. As has been stated previously, the stock is tentatively classified as a mid-Cretaceous body though it is obvious from this discussion that a detailed petrologic, structural, radiogenic and stable isotopic study would reveal a plethora of interesting data regarding the origin of this 'granitic' stock.

The 98.3±1.1 Ma, K-Ar biotite date for this rock is possibly not only a result of hydrothermal alteration but conceivably only one of many radiogenic isotopic data that could be obtained from the 'suite' of rocks that compose this stock.

EOCENE INTRUSIVES:

Coryell augite-biotite monzonite plugs have not been observed in the Sheep Creek Camp, but they do occur less than seven kilometers to the southwest in both the Active Formation on the north west face of Iron Mountain and in the Laib Formation immediately east of the Emerald skarn deposit. One other Eocene plug occurs approximately 23 kilometer north-northeast of the camp essentially on strike with the Laib syncline. Fyles and Hewlett (1959) describe the bodies to the southwest as uniform, coarse-grained, equigranular, augite-biotite, orthoclase, oligoclase-labradorite bearing rocks with the plugs having steeply dipping cylindrical surface configurations. The contacts with the country rock are moderately sharp and do not noticeably deform the surrounding suggesting that they were "...emplaced by a passive process involving stoping and assimilation" (Fyles and Hewlett,1959).

APLITIC SILLS AND DIKES:

Quartz porphyries, quartz-feldspar porphyries or more typically, 'aplites' occur as a major sill swarm and as isolated sills and dikes in the Sheep Creek Camp and throughout the greater part of the district (Mathews, 1953). In most instances these bodies, which range from less than a metre to more than thirty metres thick, parallel the strike of the foliation of the enclosing rock but will not necessarily be found parallel to its dip (Fyles and Hewlett, 1959). Some of the sills have been mapped along strike for distances in excess of 8.5 kilometers as is exemplified by the sill swarm which extends along the east limb of the intervening syncline. This sill exits in places as two or three en échelon sills separated by metasediment (ie. multiple sills), and will converge into a complex sill consisting of one or more phases and in other places exists as a single massive phase.

In the Sheep Creek Camp, the aplite is typically a light grey to green-brown-grey, dense composite of scattered phenocrysts of quartz and/or microcline-microperthite in a fine groundmass of feldspar, quartz and muscovite. The groundmass, as described by Mathews (1953), can range texturally from micrographic, to microspherulitic to an irregular mass. The interesting aspect of these bodies is that they weather in such a fashion as to be practically indistinguishable from the white quartzites.

Although no radiogenic dates exist for these sills and dikes, structural relationships show that the sill swarm clearly post-dates folding, regional metamorphism and probably all of the aplites post-date the dextral displacement along the northeasterly-trending vein fractures. Vein quartz is truncated by the sills but as minor pyrite veinlets sometimes transgress the sills in the vicinity of the major vein fractures, it is difficult to establish the timing of certain portions of the vein paragenesis with that of the aplitic intrusions. Also worth considering is the observation in the Clyde No.3 adit where aplite terminates against the vein fracture and "...at one place a projection of quartz porphyry extends across the fault and has been faulted to the left about 10 inches. It is apparent that this sill has been affected only by very late movement along the Clyde vein fracture which was in the opposite direction and of much smaller magnitude than that of the main period of faulting" (Mathews,1953).

LAMPROPHYRE DIKES:

The Salmo area is also characterized by a wide variety of both pre-mineralization and post-mineralization lamprophyre dikes which exhibit a broad range of texture and mineralogical compositions. These bodies are generally dark colored with aphanitic, porphyritic and medium grained textures and have well defined country rock contacts and chill margins. Compositions range from grey, biotite-talc-serpentinized olivine rich rocks to light grey-green chloritic rich dikes, all of which are further characterized by the presence of both angular and well rounded inclusions of the host rock metasediments, granitoids and vein quartz (Little, 1960).

In the Sheep Creek Camp, Mathews (1953) has identified pre-vein and post-vein lamprophyres. The pre-vein dikes are generally parallel with the regional foliation and fold axes and dip both conformably and disconcordantly with the surrounding metasediments. They have been observed in a number of the underground workings to be clearly offset by the northeasterly trending vein fractures and are cut by vein quartz. These lamprophyres display metamorphic textures and along with the biotite, epidote, clinozoisite and amphibole alteration, commonly carry pyrite, some of which is auriferous, although far below mining grade.

The post-vein dikes range in width from a few centimetres to more than a metre. Although expressing many of the same alteration characteristics and attitudes as the pre-vein dikes (they parallel regional strike and are locally enclosed by the metasediments, conforming to bedding as concordant sheets) they generally transgress bedding and relate much more closely to pre-existing faults.

Preliminary lead isotope data obtained from a number of the lamprophyres from both in and near the camp (Al Smith, pers comm.) plot within a crustal contamination (±

source) region, which neither supports nor contradicts either a mantle or crustal origin but is ultimately regarded as the most probable Pb-Pb compositions, considering the amount of upper crustal material included within these bodies (Al Smith and Al Brandon, pers. comm.).

The abundance of olivine and biotite with ultrabasic alteration products such as antigorite, serpentinite, carbonate and talc, suggest these rocks to be of mica-olivinite of kimberlitic affinity; however chemical analyses indicate that they are significantly more siliceous and, except for the difficulties inherent in classifying these altered minettes, kersantites and/or absorkites, these classifications would be more appropriate (Mathews,1953). The term, lamprophyres, is therefore most commonly used.

METAMORPHISM:

Regional and contact metamorphism has affected most if not all of the rock in this region. On a regional basis, the summary work of Archibald et al. (1983,1984 and references cited) have identified a consistent pattern of high grade (sillimanite, K-feldspar) metamorphism diminishing to greenschist (biotite, chlorite) phase metamorphism which straddles the Kootenay Lake in the central Kootenay Bay region and essentially parallels the structural trend of the region. Archibald et al. (1983) expands upon these observations and attempts to a apply the bathozonal scheme of Carmichael (1978) to the region "...in an attempt to estimate the amount of post-metamophic uplift and erosion" as well as to further qualify the metamorphic complexities of the region. Sillimanite-K-feldspar regional metamorphic assemblages are indicative of pressures in the range of 5 to 6 kbars and because of the presence of muscovite (muscovite in the presence of quartz, will breakdown between 650 and 700°C (Hyndman,1981)) the inferred temperature maximum is $< 650°C$

Closer to the Sheep Creek Camp, Glover (1978, from Archibald et al.,1983) "...reported that andalusite in the contact aureole of the Summit Stock overgrew the pre-existing foliation as well as synkinematic staurolite porphyroblasts in the aureole of the Mine Stock" and Archibald et al. (1983) have inferred that the complex contact metamorphism in the aureole of the Summit Stock is characteristic of bathozones 1 to bathozones 2 (pressure = ($> 2.0 < 3.5$ kbars)) and that regional metamorphism in this area occurred at deeper crustal levels in the realm of bathozones 3 to 5; (pressure = (> 3.5 to $\approx$ 7.0 kbars)).

The Sheep Creek Camp has been described by Mathews (1953) as having been affected by relatively low-grade regional metamorphism, and he argues this point on the grounds that there is a general lack of characteristic metamorphic minerals. He continues though with a description of the spotted (dark-grey spots consisting of lens shaped segregations of quartz-biotite and muscovite) phyllites and the lustrous white and grey andalusite schists which occur near the Columbia adit and southeast of the Reno mine. Also worth noting is the amphibolite developed from the schists of the Motherlode and Three Sisters Formations located on the east ridge of Reno Mountain.

Contact metamorphism affects much of the geology in the region. The most important of which is probably the biotite rich hornfels that occur in the Reno mine and the lower western workings of the Sheep Creek mine. Garnet is locally present in the metasediments north of the Reno mine. In a number of the quartz-calcite veins studied for fluid inclusion work; tremolite, clinozoisite, epidote and chlorite have been observed.

Sorting through this array of metamorphic assemblages and overprinting phenomenon and establishing a conclusion on the relative grade of the metamorphism for the Sheep Creek Camp is at this time not possible, though an estimate of upper greenschist to amphibolite grade metamorphism may be sufficient for further considerations regarding metallogenesis.

STRUCTURAL GEOLOGY:

The Kootenay Arc is unique in that unlike the northwestern regional trend for the greater portion of the Canadian Cordillera, the trend of the 'Arc' essentially outlines the trend of the high grade metamorphic complexes to the west (ie. Monashee, Frenchman Cap, Thor Odin, Valhalla, and Kettle-Grand Forks) and the eastern edge of the Nelson and Kuskanex batholiths (Little,1960). Parallelism of foliations, fold axes, and many of the regional fault structures is of particular interest as the regional trend swings from essentially east in the southern region, through north-northeast in the region of the Sheep Creek Camp, to north along the Kootenay Lake and northwest and west at points beyond. The similarities of the detailed structure throughout the Arc are remarkable. This system of complex polydeformation includes: three phases of folding (Crosby, 1968; Hoy,1980) and many fault structures including; thrusts, oblique thrusts, strike-slip faults, en échelon sets of normal and oblique normal faults, vertical faults through to horizontal faults.

Mineralization within the Kootenay Arc and the Sheep Creek Camp has been shown to be intimately related to structural controls (Hedley,1955; Walker,1934; Mathews, 1953; Fyles and Hewlett,1959; Fyles, 1967; Ohmoto and Rye,1971) and although the structures of the region are extremely complex, a good understanding of these systems has evolved over the past century.

The following is a summary of the structure of the Sheep Creek Camp proper with an inclusion of a few of the regional structural entities believed to be of significance to the mineralizing event(s) in the camp. Structures include; primary sedimentary features, folds, joints, faults, radial tension cracks, cleavage and crenulations.

PRIMARY SEDIMENTARY FEATURES:

Bedding, cross bedding and graded bedding have in many instances, survived the intense deformation that has affected all of the sedimentary rocks of the camp. None of the rather spectacular ripple structures observed in the Quartzite Formation southwest and northwest of the camp have however been observed. The significance of the primary features is that they have been of considerable value in defining the multiplicity of primary and secondary structural features.

FOLDS:

A complex of north-northwest trending, tight to isoclinal overturned to vertical synclines and anticlines characterize the Sheep Creek Camp and the district to the east and the district to the west. The Sheep Creek Anticline ('Eastern' Anticline) is characterized by a somewhat serpentine axial plane which fluctuates in strike from N15°E in the south, to about N20°E in the central region, to N10°E near Reno Mnt., where the fold is believed to be truncated by the geological complexities of the Hidden Creek Valley (an east-west extension of the Black Bluff fault (?))(Little, 1960). From limb attitudes, the overturned structures axial plane dips from 75°E in the south to about 65°E near Yellowstone Peak, and farther north on the east ridge of Reno Mountain the axial plane is generally 10° of vertical. Mathews (1953) also states that structural observations in the underground workings in the Kootenay Belle mine have shown a flattening of nearly 20° from the upper levels to the lower levels (75°E to 55°E).

The anticline is further characterized by late cross folding which has resulted in a sinuous axes that plunges south from Reno Mountain, north on the south side of Sheep Creek and then reverses again to plunge (up to 30°S) in the region of the South Salmo River (Highway #3a). The anticline opens considerably from the north to the south and south of the Ripple Creek fault, the structure is neither isoclinal or overturned (Little,1960).

The complexities of the Western Anticline have been unravelled to a greater degree as a result of the observations in the extensive mine workings. The Western Anticline is similarly overturned and tight with the western limb dipping steeply east and the eastern limb dipping from 25-60° eastward. The fold parallels the Eastern Anticline and the intervening synclinal structure and plunges similarly. The Western Anticline has not however been observed south of the Lost Creek Stock (though many fold structures are recorded in the area, (Fyles and Hewlett,1959; Little,1960) or north of Hidden Creek Ridge. Any simplistic notions about these structures are further undermined by the detailed studies which show that infolded subsidiary structures and large to mesoscopic dragfolds (parasitic) are common features, particularly in the less competent lithologies and that all of these structures are faulted by transverse, vertical and dipping strike-parallel and horizontal faults.

FOLDS TO THE EAST and FOLDS TO THE WEST:

Structures to the east of the 'Unnamed fold' (cored by the Monk Formation, lithology (0) on Figure 2.2) have been described by Daly (1912), Walker (1934), and Little (1960) as homoclinal: however, several small folds have been observed south-southeast of Bridal Lake. Glover (1978) reports that the region surrounding the Summit Creek Stock is much more complex than suggested by earlier works. The structures involve the superposition of small scale northerly plunging Z-shaped folds which are overprinted by the Summit Creek Anticline, "... a steep to moderate northwesterly plunging fold" which probably developed in response to differential movement along the Blazed Creek Fault to the east of the fold and the emplacement of the Mine Stock.

The regionally extensive Laib syncline has been described as overturned, with a steep easterly dipping axial plane. The structure has been traced from south of the Ripple Creek fault, where it is complicated by faulting, through the region depicted in Figure 2.2, and north of the Hidden Creek Fault for more than 20 kms where it is ultimately truncated by the Seeman Creek Fault. Little (1960) describes this fault as a zone, defined by small fault scarps which juxtaposes the Quartzite Range and Three Sisters Formations in the south block (no attitude on the fault is available) against younger (?) Paleozoic rocks (Vogl and Simony's (1992) 'Distal North American Miogeoclinal rocks').

Folding to the west of the Western Anticline (west of the intervening Active Formation where the structure has not been detailed) has been well documented by Fyles and Hewlett (1959) and similar to those folds discussed above, is representative of a period of overturned, tight to isoclinal folding followed by secondary folding, which is essentially coaxial. The secondary folding probably occurred late within the primary tectonic compressive regime.

Folding of a similar nature has also been identified in the Rossland Group rocks located across the Paleozoic (miogeoclinal)-Mesozoic (eugeoclinal) zone of unconformity. The only recorded folds are the 20°S plunging Mnt. Kelly Syncline, an unnamed faulted syncline to the east and an intervening antiformal structure described by Little (1960). Recent research by Höy and Andrew (1990) has suggested that the antiform can be attributed to complex faulting in the region and is not, therefore mapped as an anticline.

FAULTS:

The Sheep Creek Camp and surrounding region has undergone an extended period of faulting including thrust faulting, normal faulting, strike-slip faulting and combinations of these. The most significant regional structures were originally defined by Fyles and Hewlett (1959) as regional thrust faults and these faults were used to delineate the four areas or belts. The Mesozoic volcanic area (Rossland Group) is separated to the east from the lead-zinc Mine Belt by the Waneta Fault and the Mine Belt is separated from the Argillite Belt by the Argillite Fault. Farther to the east the Argillite Belt is separated from the Eastern Belt ,where the Sheep Creek Camp is located, by the Black Bluff Fault. In addition to these three major faults, a fourth regionally extensive structure, named the Tillicum Creek Fault (Einarson,1991), exhibits similar characteristics and is located between the Argillite Fault and the Waneta "thrust". The quotation marks are placed upon the word "thrusts" to introduce the fact that although these structures were defined as thrust faults, limited field data did not at the time allow for estimates of movement and the structures were therefore regarded as thrusts by their steep easterly dips and their relationships to the primary folds (Fyles and Hewlett,1959). In addition, early movement differed from late movement; the movement in the northern portions of these faults differed from that in the south and recent work by Einarson (1991) suggests that these structures (the Waneta and Tillicum Faults) may be overturned.

The Waneta fault predates the Wallack Creek Pluton (115 - pre-108 Ma, Einarson,1991) though post-intrusive movement is indicated by shears and fault parallel mylonitic zones developed within the intrusive body (Höy and Andrew,1990). Farther north, in the region of the metasedimentary pendants within the tail of the Nelson Batholith, Vogl and Simony (1992) have suggested that trace parallel mylonitic zones within the central phase of the batholith indicate that there was possibly synchronous emplacement and fault shear. If these two temporal constraints (the Wallack Creek Pluton (108 Ma) and the Nelson Batholith tail (150 Ma)) are considered, the Waneta fault is an expression of either protracted movement or periodic reactivation spanning a period of at least 42 million years.

The Black Bluff Fault straddles the eastern boundary of the Active Formation and brings it into contact with rocks of the Laib or Nelway Formations. The fault has been observed to acutely cross strata of the Reeves Member, the dolomitic member of the Nelway Formation and, although not intimately known, crosses stratigraphic units of the Active Formation. The Black Bluff Fault has been traced from northwest of the Reno mine along the western contact of the Reeves limestone, southwards essentially parallel to regional trend of the Arc, to the Pend dé Oreille river about half a kilometer south of the

Remac mine. Variations in the the character of the shear zone depends upon the lithologies that the fault transgresses. Highly fractured and crushed dolomite, crushed and sheared lamprophyre and polished, graphitic fault-planes in the Active Formation define the fault zone. Details of the fault show that it is highly irregular along strike and fluctuates from nearly vertical to gently east-southeast dips. Surface expression of the fault is rare in the region north of the Lost Creek Pluton and it has been defined more as a function of the offsetting of the lithologies than as a zone of movement. Strike parallel, north-trending normal faults, (discussed below) may possibly be correlatives of the Black Bluff Fault, though neither Fyles and Hewlett nor Mathews have presented such a relationship.

FAULTS AND JOINTS IN THE SHEEP CREEK CAMP:

The rocks of the Sheep Creek Camp have been faulted, jointed and cleaved along essentially every possible attitude. The five best defined sets of faults are: (1) "vein fractures", which are northeasterly trending, dextral, oblique-normal faults characterized by steep (often listric) shear planes that may or may not contain quartz veins with or without gold and associate mineralization. (2) Northwesterly trending, sinistral faults which are generally not gold bearing but are possibly coeval with the vein fractures. (3) Northerly trending, dextral-normal faults which clearly post-date the transverse faults. (4) Horizontal or near horizontal faults with hanging wall displacement towards the west. These faults are also late relative to the transverse faults. (5) Mathews (1953) includes these bedding plane faults in his discussion of joints. The spatial significance and relative movement along these structures suggest that they should be considered under the heading faults.

VEIN FRACTURES;

The term "vein fracture" has been applied to this set of east, northeast trending (N50°E-90°E) faults, which transgress all folding and foliation throughout the entire length of the camp. It is this en échelon system of faults and veins that host all of the known production in the camp.

It has been shown that along these faults the north wall has been displaced eastward, from more than 60 metres to less than a metre, and in most cases the south wall has been displaced down dip generally less than half of the horizontal displacement. In contrast to this, late left-hand displacement has been observed in some of the fractures notably the Clyde, Queen, 75 and 2590 vein fractures. Vein fractures exist as single fractures, metre wide zones of closely spaced fractures, branching vein fractures or en échelon fracture sets distributed over a width of as much as 60 metres. These fractures are also observed to deviate along strike as a function of the host rock competency, the general rule being that the strike will swing to the left as the fracture progresses from competent lithologies to less competent rock. Vein fractures are generally steep south dipping but range from 45°S as in the Kootenay Belle A mine to 80°N as is exposed in portions of the Reno veins. Eighty five degrees, south is the average dip of these fractures in the camp, though it has been observed in many of the mines that the vein fractures flatten somewhat with depth. The reverse of the last observation is also recorded for a number of the veins.

Vein fractures generally have lateral extents in excess of 350 metres and have been traced for distances exceeding a kilometer. None of the mine workings have bottomed out and therefore no lower limit of vertical extent has been established; however, " the vertical range through which vein fractures are known to occur exceeds (1500 m) between the lowest level of the Queen vein in the central part of the camp and the highest exposures of the Reno vein on the north and of an unnamed vein fracture 250m south of Mount Waldie" (Mathews,1953). Several of the individual fractures have been traced through vertical extents of 500 metres and the Reno vein system has been followed continuously for nearly 600 metres. Single veins have as a rule a tendency to widen at depth and total thicknesses in excess of five metres (Queen vein) have been observed (Mathews, 1953).

NORTHWESTERLY-TRENDING FAULTS:

These nearly vertical WNW (45°W on average) striking faults have been observed to be sinistral, essentially strike-slip with displacements of not more than 10 metres. One of these faults, intersected in the 1880 drift of the Gold Belt mine does carry sulfide bearing quartz though assay values across the vein did not exceed 0.10 oz./ton gold (Mathews,1953). One interesting observation regarding these faults is that the number of these northwesterly trending fault is remarkably small compared to those that are recorded from the Rossland Group rocks and the northern portions of the Salmo-lead zinc belt, where northwest trending faults are downthrown to the north (Fyles and Hewlett, 1959).

NORTHERLY-TRENDING NORMAL FAULTS:

Three of the five known northerly trending normal faults, the Queen, the Thompson and the Hangingwall faults, are exposed in the underground workings of the Sheep Creek mine, where they acutely transect and/or follow the axis of the Western Anticline. The Queen fault strikes between N5°E and N10°W, dips about 45°E and has hangingwall displacement of about 15 metres left strike-slip and about one hundred metres of dip slip. The Queen fault consists generally as a single, one (±) metre gouge zone but has also been recognized to branch into several faults.

The Thompson fault essentially parallels the Queen fault in strike but dips much more steeply east (50° to nearly vertical). Dip-slip is recorded as fluctuating between 15 and 9 metres and strike-slip displacement, because of the faults parallel orientation with respect to the axial plane of the Western Anticline,has not been measured accurately though both left lateral movement from less than a metre to 15 metres and minor right lateral movement has been observed. The Hangingwall Fault, exposed east of the Thompson Fault, strikes approximately 30° west and dips steeply south, southwest with apparently normal movement of a few metres. Little data is available regarding the Cayote adit normal fault which transgresses the Western Anticline about two and a half kilometers north of the Queen, Thompson and Hanging faults. The dip on this fault varies from 45 to 70° east with a dip-slip of (estimated) 15 metres.

The Weasel Creek Fault, the largest normal fault known in the camp, trends nearly parallel to the beds throughout the entire extend of the camp from north of Reno Mountain, across the east face of Yellowstone Peak and south past King Lake along the Lost Creek-Waldie Creek divide. The fault is poorly defined, consisting of a zone of shattered rock that at one point is so obscure that dip cannot be determined. The orientation and repetition of stratigraphy suggest however that the rocks have been displaced no less than 300 metres along a moderate to steep westerly dipping fault zone.

FLAT-LYING FAULTS:

Many horizontal, hanging wall to the west faults, have been observed offsetting rock in the order of less than a metre to ten metres or less. These faults are observed to be post-vein fracture and are observed to be both younger (Gold Belt mine) and older than (Reno mine) lamprophyre dikes. (Mathews, 1953).

ORE PETROLOGY: QUARTZ VEINS and MINERALIZATION:

An excellent review of the quartz vein characteristics, gold and sulphide mineralogy as well as a paragenetic sequence is given by Mathews' (1953), "Geology of the Sheep Creek Camp". Sources for Mathews' work were primarily from mine records of vein grades and widths and the extensive study done by Robinson (1949) on the geology and mineralization of the camp. Petrological work done throughout the course of this study has, in most instances, concurred with the findings of Mathews and Robinson.

Gold mineralization is intimately associated with massive or laminated quartz veins that are confined, in this particular setting, to the easterly trending fault structures previously described as vein fractures. The following is a short description of the quartz mineralization, the general vein structure, the sulphide and associated gold mineralization as well as a statement on wall rock alteration.

Quartz and Quartz Veins:

Milky-white, massive quartz and/or laminated quartz with sulphide mineralization is the principal constituent of these veins. The quartz is typically an aggregate of small (<4mm to tenths of a millimetre) quartz grains that are generally anhedral and equidimensional to slightly elongate. Only rarely do elongate crystals develop and for the most part, no preferred orientation of grains is observed and only rarely is there any indication of open space filling. As Mathews (1953) suggests, less than a few per cent of the quartz has grown in open spaces. Vug and comb structures have been observed in some of the rare small (<3mm) branching veinlets. In the massive quartz veins, crystals of quartz are typically interlocking and in many instances the grain boundary suturing is very complex, "...like those of some particularly intricate jig-saw puzzle" (Mathews,1953). In much of the vein quartz there is a complex of: (1) larger quartz grains that exhibit incipient recrystallization and/or complex strain characteristics, (2) relatively homogenous masses of equidimensional quartz and (3) complexes of (1and2) with zones of unstrained slightly coarser simply sutured quartz crystals.

Two generations of quartz mineralization have been documented. The first generation produced the bulk of the vein material, followed by complex fracturing and the second generation of quartz, which also included sulphides infilling the fractures and shears. Much fracturing and shearing of the vein quartz occurs, with simple shearing being roughly parallel to the vein walls and complex, intersecting braided-shearing being relatively restricted to internal portions of the vein. Cross fracturing has been documented to occur near the margins of the veins (Robinson,1949).

Veins, Controls on Widths;

The width of the quartz veining within the vein fractures is apparently related to five physical (chemical) factors:

(1) Greater vein widths are observed to occur where the vein fracture is within the more competent quartzites or argillaceous quartzites. It has been also been noted that the massive veining will pinch out as the vein fracture enters incompetent rock (argillites, phyllites) and then returns to massive veining as the fracture passes back into competent stratigaphic units.

(2) As is the case with the orientation of the vein fractures, (they tend to swing easterly as they pass from incompetent to competent rock) vein widths increase substantially as the vein trends more easterly.

(3) Where veins intersect (branch) vein widths tend to be greater.

(4) Those vein fractures that have undergone the greatest right lateral displacement are most often thicker than those that exhibit only minimal displacement.

(5) In all veins, the tendency to increase in width with depth has been observed. Pinching and swelling throughout the extent of the vein is also commonly observed, though veins have only been observed to pinch out with elevation and none at depth.

The actual geometry of these veins is extremely complex with variations in both thicknesses and attitudes throughout their extents.

MINERALIZATION:

Ore mineralization within the vein structures occurs as ore shoots and these shoots are irregular to vertically elongate and occur for the most part, randomly throughout the vein and the vein system. One of the most significant constraints upon the localization of the ore is the relationship of mineralized veins to either the Nugget or Navada Members of the Quartzite Range Formation. Nearly all of the gold production has been from those parts of the vein where one or both walls consist of quartzite. The one exception to this observation being the Reno mine where it has been observed that contact metamorphism has altered much of the less competent rock to a hornfels, which is characteristically more competent and behaves, structurally, more like that of the underlying quartzites (Mathews,1953).

Some changes with depth in the mineralization and textural characteristics have been observed. Reports indicate that some of the veins at depth contain various aluminum silicates as well as chlorite. A decrease in the proportion of galena and sphalerite to that of quartz has been observed in the Reno and Kootenay Belle veins and the general observation of lower grades of ore at increasing depths has been considered an important parameter for exploration; however, no actual confirmation on this possibility has occurred.

The mineralogy of the ore shoots is simple, basically pyrite and quartz with minor amounts of sphalerite and less amounts of galena. Other minerals of less abundance are; calcite, siderite, muscovite, sericite, pyrrhotite, chalcopyrite, scheelite, (wolframite ?), arsenopyrite, marcasite, tetrahedrite, pyrargyrite or proustite, and gold. Supergene minerals that have been observed in the camp include; limonite, malachite, anglesite, smithsonite and (tungstite).

A paragenetic sequence for these veins has been worked out by Robinson (1949) and is presented in Figure 2.4 and summarized by Mathews (1953).

(a) Introduction of quartz and scheelite

(b) Shearing and fracturing of early vein filling

(c) Introduction of sulphides, late quartz and calcite

with the vein minerals introduced, essentially sequentially, with minor overlap in the following order;

(1) Quartz, pyrite and (?Arsenopyrite)
(2) Pyrrhotite, sphalerite and chalcopyrite
(3) Galena, tetrahedrite and ruby silver minerals
(4) Gold

Many of these mineral are rare to the point of exclusion, and therefore it would be possible to constrict the paragenetic sequence for a greater portion of the overall camp to:

(a) Introduction of quartz
(b) Shearing and fracturing of early vein filling
(c) Introduction of pyrite
(d) Deposition of gold.

Sulphides occur as: (1) long vein parallel laminations often of considerable width, interlayered with the quartz, (2) in oblique fractures in the vein quartz, (3) as small (>5mm) irregular masses or as, (4) disseminated crystal.

Pyrite is most commonly found as single grains or laminations or disseminated, anhedral to euhedral masses. Pyrite is observed to traverse fractured quartz grains, but more commonly fractures in pyrite grains or masses are infilled with quartz.

Sphalerite and galena occur occasionally within the quartzite bearing gold veins but are more commonly encountered in either the Reno mine or the limestone hosted veins of the Ore Hill and Sumit mines. Sphalerite, the second most common sulphide, is often accompanied by galena, pyrrhotite and periodically chalcopyrite. It occurs as irregular masses and/or veinlets that cut through and/or embay pyrite.

Gold

Gold is found "..as minute, isolated particles in quartz or as small grains adjacent to, or in grains of suphide minerals" (Robinson,1949). The majority of the gold has been observed to occur with pyrite and sphalerite at the contacts between the sulphides and the quartz grains. Gold grains have also occasionally been observed within the sulphides as isolated particles and/or fracture infillings. Particles of gold more typically occur at contacts between quartz and pyrite, quartz and sphalerite and less commonly between sulphide grains.

About a third of the gold observed by Robinson (1949) occurs in quartz as small (≈30 microns, though grains of 200 microns are indicated) isolated, rounded to irregular particles. March larger grains (≈2mm) irregular and rounded particles of gold, enclosed by quartz, were observed through the course of this study, though most of the polished section work on sulphide bearing ore, confirmed the observations of Robinson.

Silver

The Sheep Creek Camp has produced 364,793 ounces of silver . The Au:Ag ratio (Table 1.1) is noticeably reversed in a number of the mines and this reflects the fact that these ore bodies (Ore Hill, Sumit, Columbia, and portions of the Reno) carry significantly more base metal sulphides. Much of the silver is intimately associated with the base metals as either proustite-pyrargyrite (Ag_3AsS_3-Ag_3SbS_3), tetrahedrite 'blebs' in and about the galena and sphalerite rich vein material, or as elemental replacements in galena. Some of the silver is undoubtedly associated with the gold as a number of the 'gold only' veins have produced silver. Robinson (1949) reports that the Au:Ag ratios in these veins are quite variable and no geological association has been identified for these variabilities.

WALL ROCK ALTERATION:

Hydrothermal alteration of the country rock hosting the auriferous quartz veins, excluding those veins that are hosted by limestones, is minimal and is described as minor amounts of host rock invading veinlets of quartz, with or without calcite. Calcite is observed as a late alteration mineral and may exist as veining or local carbonate floodings. Sericite and muscovite have been observed to overprint metamorphic biotite in some of the more schistose host rocks and pale green sericite has been observed to fill short fractures within the quartzites at distances generally no more than a half metre from veins. Pyrite has been observed in Reno Formation quartzites at a distance of two and a half metres from the nearest known vein, though this mineral is more often observed as minor disseminations closer to those veins that actually produced some degree of alteration in their host rocks.

Much of the quartz that is located in veins is considered as being altered, bleached and silicified quartzites. This concept is argued for in many of the discussions presented by Mathews (1953) and observations in the field seem to confirm this interpretation of some of the less understood veins.

Figure 2.1. Location of the Sheep Creek Camp (identified by the star) within the generalized tectonic assemblage map of southeastern British Columbia and northern Washington, Idaho and Montana (modified from Parrish et al., 1988). Faults and metamorphic complexes are designated as follows: BF, Blazed Creek fault; CC, Clachnacudainn complex; CRF, Columbia River fault; ERF, Eagle River fault; GF, Granby fault; GWF, Greenwood fault system; HLF, Hall Lake Fault; JJF, Jumpoff Joe fault; KC Kettle-Grand Forks complex; MC, Monashee complex; MY, Moyie fault; NF, Newport fault; PRC, Priest River complex; PTF, Purcell Trench fault; SLF, Slocan Lake fault; SMF, St. Mary fault; TO, Thor Odin area; VC, Valhalla complex; VSZ, Valkyr Shear zone; WF, Waneta fault.

LEGEND

Stratified Rocks

5	Miocene-Pliocene basalt
▦	Middle Eocene volcanic, sedimentary rocks
4	Late Paleozoic-Early Mesozoic allochthonous terrane
●	Paleozoic allochthonous ultramafic rocks
3	Paleozoic rocks of North American affinity
2	Windermere Supergroup
1	Purcell-Belt Supergroup
a	Metamorphosed inferred equivalent of above units

Metamorphic Core Complexes

☐	Late Cretaceous to Early Eocene metaplutonic rocks
☐	Paragneiss, minor orthgneiss: age uncertain
▨	Proterozoic crystalline basement complex

Granitic Plutonic Rocks

▦	Middle Eocene syenite, granite
░	Early-Middle Eocene Ladybird granite suite
░	Mid-Late Cretaceous granitic rocks
▨	Middle Jurassic granitic rocks
▦	Paleozoic granitic rocks

Structural Symbols

Eocene regional normal faults of moderate dip

Eocene high angle normal fault

Middle Jurassic to Paleocene thrust fault

Geological contact

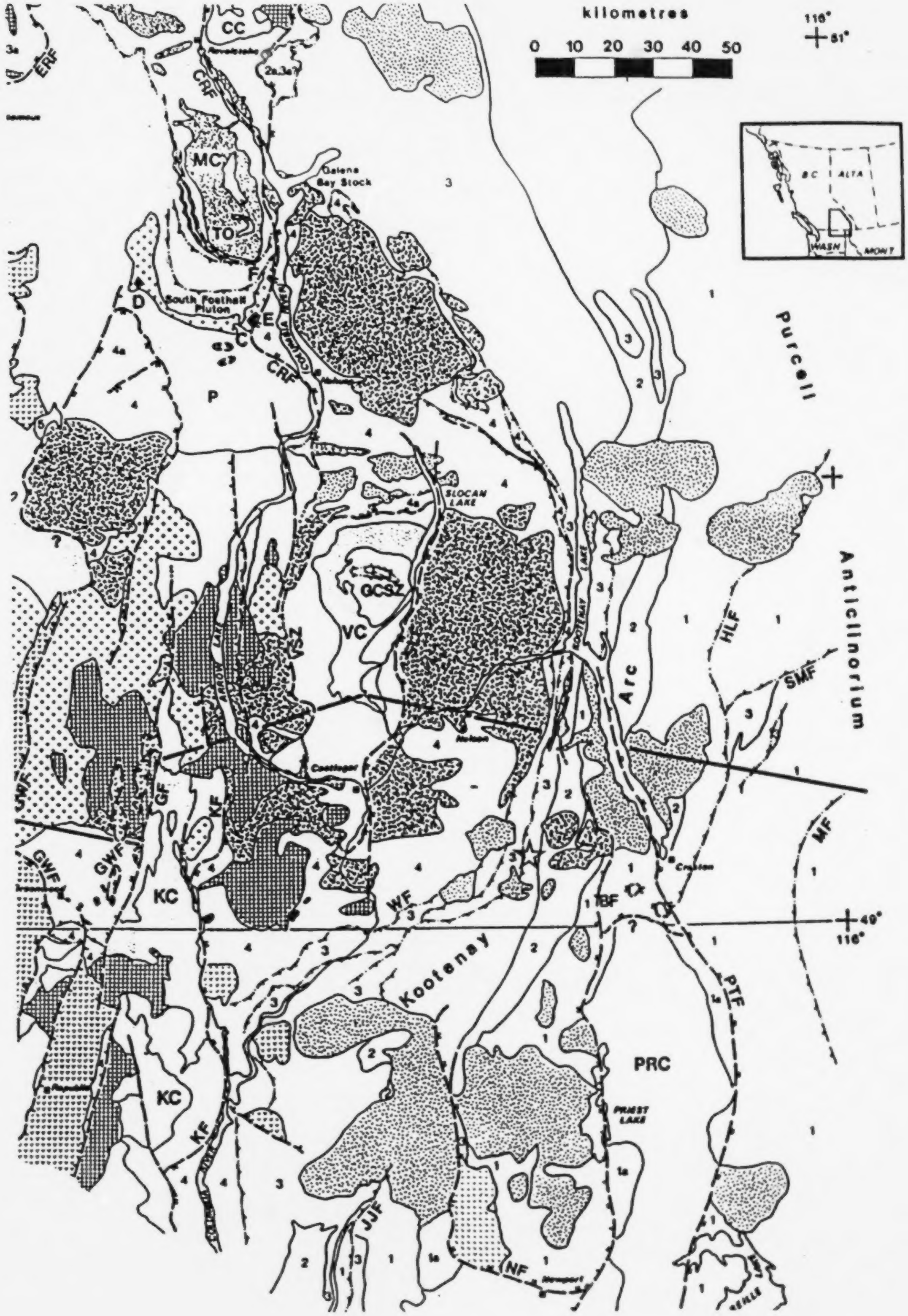
kilometres
0 10 20 30 40 50
118°
51°
BC
ALTA
WASH
MONT
CC
Revelstoke
ERF
CRF
MC
TO
Galena Bay Stock
South Foothill Pluton
D
E
C
P
Slocan Lake
GCS
VC
VSZ
Purcell
Anticlinorium
Arc
HLF
SMF
MF
Nelson
Castlegar
GF
KF
GWF
KC
WF
TBF
Creston
Kootenay
PTF
49°
116°
PRC
Priest Lake
JJF
NF
Newport
1
2
3
4

Legend for Sheep Creek Geology

▲ Thrust Faults, ± oblique displacement

┅ Normal or oblique-normal faults

⇇ Overturned Anticline

⇇ Overturned Syncline

⬡ B **MINES**

A: Queen
B: Reno
C: Jackpot
D: Aspen
E: H.B.
F: Feeney
G: Emerald
H: Jersey
I: Tungsten King
J: Truman
K: Ore Hill

Eo	Eocene CORYELL PLUTONICS: Augite-biotite monzonite
Kr	Mid-Cretaceous PLUTONICS: Granitic rocks
Ju	Mid-Jurassic NELSON PLUTONICS: Granitic rocks, porphyritic, granodioritic, quartz monzonites
6	Active Formation: black argillite and slate, grey limestone and argillaceous limestone, dolomite, dolomite breccia.
5	Nelway Formation: grey dolomite, limestones and argillite
4	Laib Formation: phyllite, argillite, schist, micaceous quartzite and limestone 4a, Reeves Member; grey limestone (dolomite) 4b, Upper Laib Formation; phyllite, schist, micaceous quartzite, minor limestone
3	Reno Formation: argillites, argillaceous quartzite; including minor phyllite and calcareous argillite.
2	Quartzite Range Formation: Motherlode, Nugget and Nevada Members; white, green and pinkish quartzites, minor intercalated argillites.

Windemere Supergroup

1	Three Sisters Formation: Quartzites, metaconglomerate, micaceous - chloritic schists
0	Monk Formation : Metaconglomerate, micaceous - chloritic schists quartzites, limestones, grits

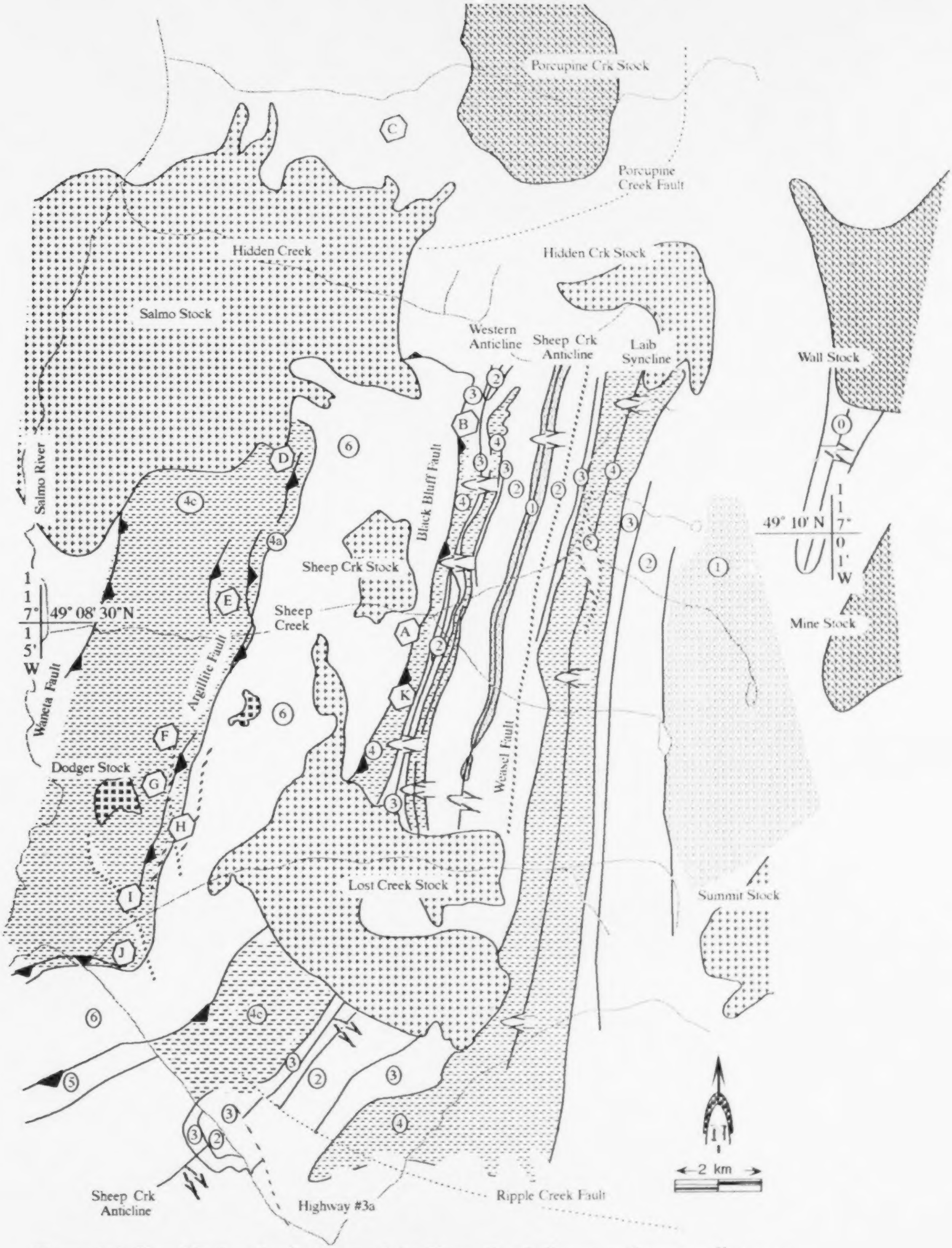
Porcupine Crk Stock
C
Porcupine Creek Fault
Hidden Creek
Hidden Crk Stock
Salmo Stock
Western Anticline
Sheep Crk Anticline
Laib Syncline
Wall Stock
0
Salmo River
B
D
6
4c
4a
Black Bluff Fault
Sheep Crk Stock
E
Sheep Creek
A
K
49° 10' N
117° 01' W
1
2
3
4
49° 08' 30"N
117° 15' W
Mine Stock
Waneta Fault
Argillite Fault
Weasel Fault
F
G
H
I
J
Dodger Stock
Lost Creek Stock
Summit Stock
5
Sheep Crk Anticline
Highway #3a
Ripple Creek Fault
2 km

Figure 2.2. Simplified geological map of the Sheep Creek Camp and surrounding area. Modified from Little (1960).

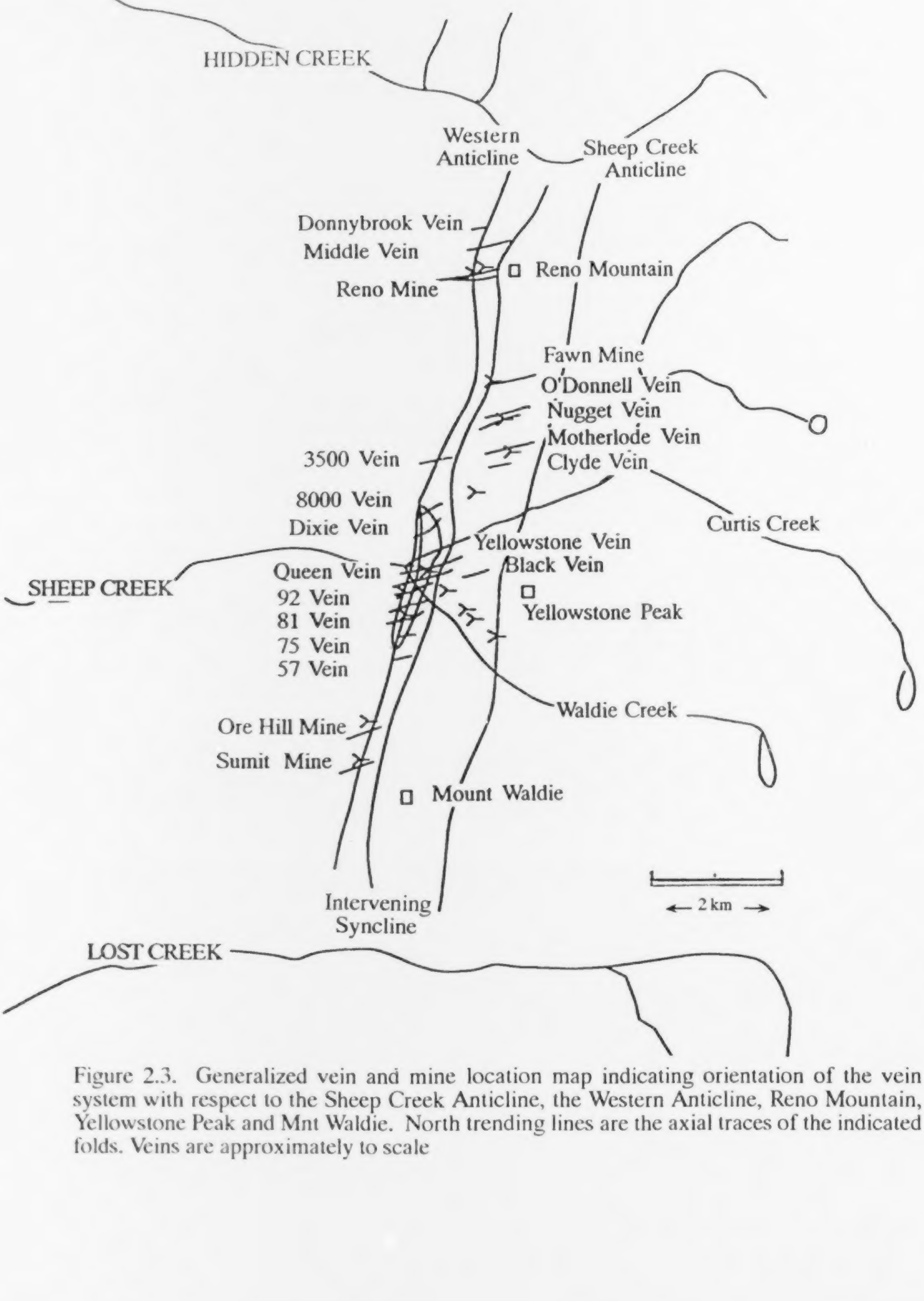
HIDDEN CREEK
Western Anticline
Sheep Creek Anticline
Donnybrook Vein
Middle Vein
Reno Mine
Reno Mountain
Fawn Mine
O'Donnell Vein
Nugget Vein
Motherlode Vein
Clyde Vein
3500 Vein
8000 Vein
Dixie Vein
Curtis Creek
Yellowstone Vein
Black Vein
SHEEP CREEK
Queen Vein
92 Vein
81 Vein
75 Vein
57 Vein
Yellowstone Peak
Waldie Creek
Ore Hill Mine
Sumit Mine
Mount Waldie
2 km
Intervening Syncline
LOST CREEK

Figure 2.3. Generalized vein and mine location map indicating orientation of the vein system with respect to the Sheep Creek Anticline, the Western Anticline, Reno Mountain, Yellowstone Peak and Mnt Waldie. North trending lines are the axial traces of the indicated folds. Veins are approximately to scale

PARAGENETIC SEQUENCE
SHEEP CREEK VEINS

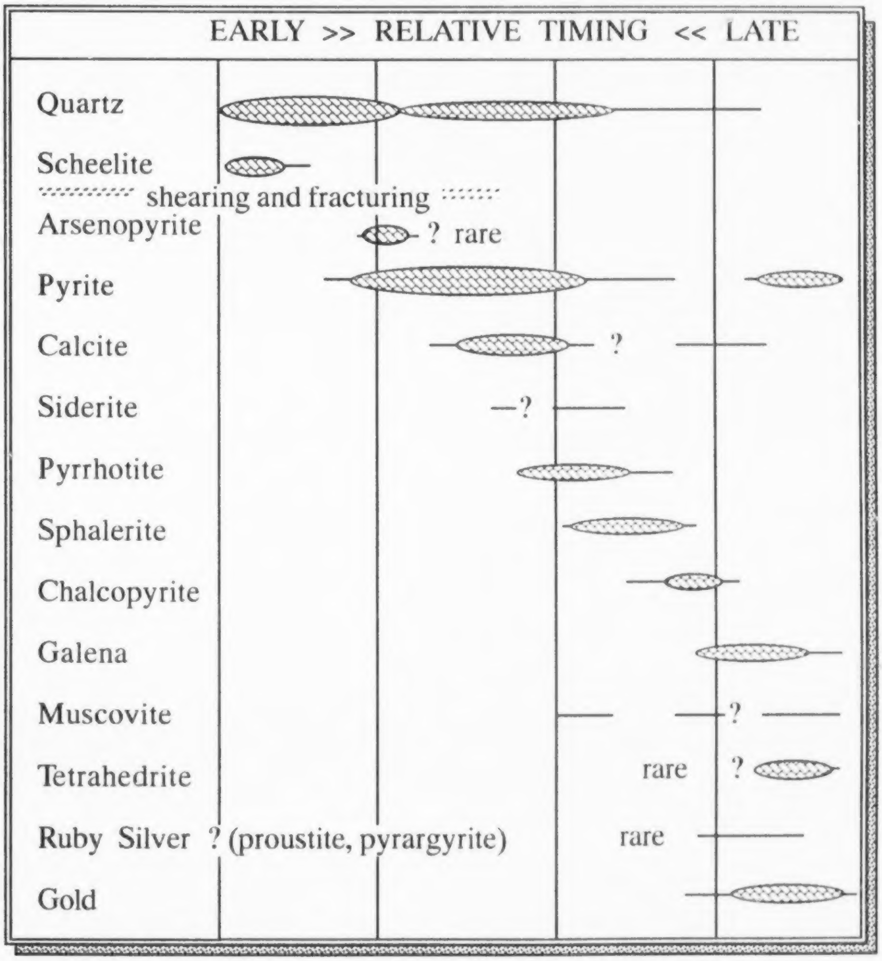

Figure 2.4 Paragenetic sequence as determined by M.C. Robinson (1949) with additions of muscovite and siderite from the current study.

CHAPTER III

FLUID INCLUSION RESEARCH

INTRODUCTION:

Hydrothermal quartz veins are a common feature of many geologic environments. Quartz ± carbonate veins are found throughout the Kootenay Arc and are associated with significant base and/or precious metal mineralization. The ability to characterize ancient hydrothermal systems is the principal motivation in fluid inclusion study and in particular, the study of those systems associated with commercial grades of mineralization. If it is possible to establish the pressure, temperature and composition of the fluids in the ancient hydrothermal system, it is also probable that spatial and temporal variations within the system can be documented.

Fluid inclusions offer the only direct means to study the fluids and the associated pressure-temperature parameters of ancient hydrothermal processes. Although the natural complexities of fluid-rock interactions preclude a true and complete understanding of the actual geological events, careful research and interpretation of the fluid inclusions can give geologists a more thorough understanding of a particular hydrothermal setting.

Hollister et al. (1981) suggest that prior to initiating a fluid inclusion research program, a clear understanding of the tectonic, metamorphic, igneous and hydrothermal evolution of the region is required so as to relate these specific events to the fluid inclusion research. In addition to having a good understanding of the regions geological history, knowledge of the paragenetic sequence is essential. Spatial variations in fluid characteristics can only be observed if a substantial vertical and horizontal representation of the rock suite is obtained. Ideally, petrographic evidence will relate the fluid inclusion research to the physio-chemical process being investigated.

To acquire maximum benefit from the research, fluid inclusions must be studied qualitatively and quantitatively. Before this can occur however, two fundamental assumptions regarding the inclusions must be considered (Roedder,1984; Burruss, 1981; Diamond,1986):

I. A fluid inclusion is a closed system of constant volume and composition.
II. The fluid inclusion was trapped as an homogeneous, single phase fluid.

For any fluid inclusion study to be valid, it is imperative that the researcher either demonstrate that these assumptions are correct or be able to recognize when these assumptions are invalid. Roedder (1984) considers exceptions to these assumptions and suggests that any post-trapping changes in fluid inclusion volume will affect the thermometrics of the inclusion. The actual volume change in quartz, the host for all inclusions in this study, is a function of thermal expansion and compressibility and as Roedder suggests, is negligible. Leakage or partial decrepitation of the inclusion due to natural phenomena is potentially one of the most significant sources of error. The fact that much of the vein material studied exhibits high strain and partial recrystallization suggests that data from these samples be interpreted with caution. Fortunately, most veins that have undergone post-trapping strain or metamorphism host few, if any, workable inclusions.

There are two major exceptions to the assumption that the fluid was trapped as an homogeneous single phase. These exceptions are: (a) the fluid was trapped as an immiscible, heterogeneous mixture of fluid phases and, (b) any fluid inclusion can recrystallize, "neck down", or "neck off", as to reduce high surface energy. This second process will result in the formation of two or more smaller inclusions that do not accurately represent trapping conditions. Microthermometric research of necked off inclusions will invariably result in invalid data. For the case of heterogeneous phase entrapment, microthermometric data can be valid and can be used for interpretation.

Mineralized and unmineralized quartz from discordant and foliation parallel (foliaform) veins of the Sheep Creek district were collected from mine dumps, outcrops and underground exposures. Subtle variations in quartz texture eventually proved to be important criteria for separating quartz with no or few workable inclusions from material which hosts workable inclusions. Massive homogeneous milky quartz, the most common type in the district, is generally filled with clouds of unworkable, microfine (<1.0μm) fluid inclusions. In most cases, quartz which exhibited minor optical clarity would contain workable inclusions. As has been previously mentioned, open space vuggy or comb quartz is exceedingly rare in the Sheep Creek Camp.

Of the more than 100 doubly polished quartz "wafers" (≅ 0.2 mm) which were made, thirty five samples, which contained inclusions large enough to observe (>3.0μm) fluid phases and phase changes, were chosen for microthermometry. In many instances the size of the inclusion was the major limiting factor regarding the number of phase transitions observed and with very small inclusions, (<5.0μm) the potential error in microthermometry becomes significantly high. Few inclusions of this size or smaller were studied and they generally revealed only a few phase transitions. As a result of this relatively poor return from the samples collected, only a few of the mineralized fracture veins were studied in detail, the results of which are held in comparison with those samples associated with gold or sulfide mineralization.

ANALYTICAL TECHNIQUE

A "FLUID INC." adapted U.S.G.S. Gas-Flow Heating/ Freezing System, with a Doric Trendicator 410A digital thermometric control system attached to a Leitz-Wetzlar microscope with 10X periplan oculars and 4X, 10X, 32X EF objective lenses was used for all microthermometric analyses. The heating-freezing stage was calibrated using a distilled water-ice bath, pure CO_2 inclusions in Alpine vein quartz, liquid nitrogen, and Merck standards. "Standard errors are ± 0.2C° for freezing values and ± 2.0C° for heating to 300C° (Rushton,1991).

Fields of inclusions suitable for heating/freezing studies were identified and mapped. Mapping of the inclusion fields was of primary importance for relocating individual inclusions or fields and for recording initial inclusion characteristics such as size, shape, origin and phase volumes. Upon completion of the mapping process, cooling (freezing) and heating runs were conducted. Inclusion decrepitation, (the rupturing of the inclusion due to internal overpressuring as a result of heating) proved to be a significant problem and this, in conjunction with the need to avoid any inclusion stretching errors (Reodder, 1984), suggested that cooling studies be completed prior to heating the inclusions above 50 C°.

PHASE TRANSITIONS

Fluid inclusion microthermometry is essentially the study of closed system phase transformations. The inherent worth of the non-destructive process of heating and cooling an isochoric-isoplethic system is entirely dependent upon the ability to observe and accurately record phase changes and to relate the observations to known phase equilibria. As the number of available components in a fluid system increase, the number of possible phases and phase transitions also increase. Phase equilibria have been well documented for many relevant unary systems (eg. CO_2, H_2O) and binary systems (eg.CO_2-H_2O, H_2O-NaCl, CO_2-CH_4, Burruss, 1981). Much recent work has extended documentation of such geologically significant ternary systems as H_2O-NaCl-CO_2, (Gehrig et al., 1979; Bowers and Helgeson,1983a) and it is believed that "Judicious use of an ideal mixing model for more complex fluids allows quantitative deductions on fluids as complex as the quaternary system CO_2-CH_4-H_2O-NaCl" (Burruss, 1981). The experimental and analytical complexities inherent in such multi-component systems suggest that these analyses will be semi-quantitative at best. Semi-quantitative and qualitative fluid inclusion research can however be useful regarding the interpretation of hydrothermal fluid-rock processes.

The following is a brief discussion of the phase transitions observed and recorded in this study as well as their possible implications.

COOLING

(i) Final Melting Temperature of Solid CO_2, Tm_{carb}:

Nucleation of any solid phases in fluid inclusions is extremely sluggish and for this reason all solid-liquid phase transitions are measured as final melting points, not freezing temperatures. If CO_2 is contained within an inclusion, it will freeze upon super-cooling at approximately -100°C and will melt at the invariant point for CO_2 of -56.6°C. If this phase change is observed to be sluggish (drawn out over a few degrees) and the final melt temperature is depressed below -56.6°C, additional miscible volatiles are present in the carbonic phase (Burruss,1981). Methane, nitrogen, hydrogen sulfide and higher order hydrocarbons are often associated with hydrothermal systems and are often found in the inclusions. Tm_{carb} can be used in conjunction with Th_{carb} (homogenization of the carbonic phase, to be discussed below) to estimate the density of the carbonic phase as well as the ratio of other volatiles in the CO_2 phase.

(ii) Final Melting Temperature of Clathrate Hydrate, Tm_{clath}:

A fluid system that contains CO_2 and H_2O will form clathrate hydrates when cooled sufficiently. Clathrate hydrates are compounds that consist of a lattice-work of water molecules that form cavities which are occupied by simple to complex volatiles (Seitz et al.,1987). The common formula for type I, CO_2 clathrate is $CO_2 * 5.75H_2O$ and the formation of this particular clathrate will affect the overall volume percent of CO_2 and H_2O at low temperature but will not ultimately affect compositional calculations. Clathrate formation in the system CO_2-CH_4-H_2O can significantly affect estimates of composition as these estimates are based upon the CO_2-CH_4 system. It is the differential partitioning of the volatile species between coexisting carbonic fluids and clathrate that stretches the assumption of Hollister and Burruss, (1976) that the ternary system CO_2-CH_4-H_2O can be treated as a binary CO_2-CH_4 system at low temperatures. Seitz et al. (1987) argue that it is the CH_4 that will partition into the clathrate whereas Parrish and Prousnitz (1972) suggest that the CO_2 will be the major guest species in these complex clathrates. From the work of

Seitz et al. (1987), an underestimation of 5-8% CH_4 in the volatile phase could result from the misinterpretation of microthermometric data in the presence of compex clathrate hydrates.

Quantitative CO_2 -H_2O clathrate equilibria studies as summarized by Hollister and Burruss (1976) and discussed by Burruss (1981), can denote the presence of a pure CO_2 -H_2O system. In most geologic situations however, NaCl or other similar electrolytes will be present and these added components will decrease "...the chemical potential of water, thereby lowering the temperature of formation of the clathrate hydrates" (Burruss 1981). The depression of clathrate dissociation below +10°C (the dissociation temperature for pure CO_2-H_2O clathrate at 50 bars pressure) can be used to estimate the salinity of the system. Salinity values in fluid inclusion research are generally presented as equivalent weight percent NaCl (eq.wt.% NaCl) and these values can be calculated for clathrate dissociation from the equation of Bozzo et al.,(1973).

$$\text{Eq.wt\% NaCl} = 15.52023 - 1.023420\Theta - 5.286 \times 10^{-2}\Theta^2$$

where Θ is the temperature of clathrate melting in degrees celsius.

Caution must be exercised with this method for estimating salinity as the presence of CH_4 will inhibit clathrate melting. (Katz et al.,1959; Burruss, 1981). These opposing effects of salinity and methane will result in erroneous salinity estimates. Clathrate dissociation temperatures that are greater than +10°C at pressures higher than 75 bars thus signify the presence of volatiles other than CO_2 within the clathrate lattice.

(iii) Temperature of CO_2 or Carbonic Phase Homogenization, Th_{carb}:

The temperature of homogenization of the carbonic phase in either two phase ($CO_{2(L)}$-$CO_{2(G)}$) or three phase ($CO_{2(L)}$-$CO_{2(G)}$-$H_2O_{(L)}$) inclusions is indicative of the density of the carbonic component as well as the overall ratio of CO_2 and other miscible volatile phases (eg.CH_4).

Two factors must be considered regarding the relationship between Th_{carb} and the density of the carbonic phase. In a system where CO_2 is the only volatile component, Th_{carb} is directly related to the density of the carbonic phase, which is a function of the pressure of entrapment (Shepherd et al.,1985). If the inclusion homogenizes to the vapor phase (dew curve homogenization) the bulk density is less than the critical density (0.468g cm^{-3}). If the inclusion homogenizes to the liquid phase (bubble curve), the density is greater than the critical density. Fading of the liquid-vapour meniscus is indicative of critical density. Density estimates for CO_2 in pure CO_2-H_2O inclusions were derived from

Figure 6.17 of Shepherd et al.(1985) (after Valakovich and Altunin (1968)) and a density calculation program written and compiled by Lynch (1989), from work by Parry (1986).

The homogenization temperatures of the carbonic phase is affected by the presence of other volatiles as well as internal pressures and distinguishing which of these two factors is operating, without the aid of destructive analysis, is difficult. In this study an arbitrary, Tm_{carb} of -57.6°C was used to indicate the purity of the CO_2 phase. It should be pointed out that density calculations of 'impure' carbonic inclusions by the above method would give incorrect results. Densities (molar volumes) and mole fraction CH_4 in the carbonic phase were therefore estimated using Shepherd et al.(1985) Figure 6.19 (after Heyen et al.,(1982)). The interdependence of Tm_{carb} and Th_{carb} is indicative of the volatile ratios and densities; the accuracy of such estimates is however difficult to establish. One reason for this relates to the question of volatile partitioning in the formation of clathrate. The temperature of final carbonic phase melting is recorded in the presence of clathrate, whereas Th_{carb} can be measured with or without the presence of clathrate. In contrast to the disparate temperatures for Th_{carb} (with clathrate) from Th_{carb} (no clathrate).recorded by Seitz et al.(1987), a general shift of less than one degree (+/-) was recorded in this study for Th_{carb} (clathrate) from Th_{carb} (no clathrate). As Tm_{carb} is measured in the presence of clathrate, Th_{carb} should also be measured in the presence of clathrate as the pairing of Th_{carb} (no clathrate) with Tm_{carb} yields erroneous numbers for volatile ratios and densities whereas the pairing of Th_{carb} (clathrate) with Tm_{carb} yields the composition and density of the *residual* carbonic fluid. In this study, Th_{carb} was the first measurement taken and was recorded in the absence of clathrate and this can result in an underestimation of 5-8 mole % CH_4 in the CO_2-CH_4 fraction, which can result in an underestimate of molar volume which will express itself as higher densities. The interpretation of the clathrate bearing inclusions must therefore account for possible errors in compositions and densities.

(iv) First Melt, Temperature of Eutectic, T_{eu}:

The temperature of first melt T_{eu}, is a function of the type of chlorides (KCl, NaCl, $CaCl_2$, $MgCl_2$) or other dissolved species in the aqueous phase of the fluid inclusion (Crawford,1981; Potter et al.,1978). The point to consider here is that this phase transition is extremely difficult to observe in most systems, except, fortunately enough, for some of the more exotic chlorides such as $CaCl_2$ or $MgCl_2$ or the combinations of these and NaCl.

(v) Final Melting Temperature of Ice,Tm_{ice}:

The final melting temperature of ice of a pure H_2O system will be +0.15°C (Crawford,1981) and depression of this temperature can be used to estimate the equivalent weight percent NaCl within the system. As the refractive index of ice is very nearly the same as that of water, this phase change is difficult to observe and the process of "cycling" is generally the only means for observing this phase change (Shepherd et al.,1985). 'Cycling' is the process of warming the inclusion until the vapor bubble seems to return to its original (pre-freezing) configuration, and then cooling the inclusion a few degrees. If the vapor bubble deforms within this range of cooling, ice remains in the inclusion. At this point the inclusion is warmed to a slightly higher temperature, approximately 0.3 ° higher than the first measurement and the process is repeated. In spite of the significant time associated with this process, it is the only means of recording Tm $_{ice}$ which can then be used to calculate eq.wt.% NaCl using the formula of Potter et al., (1979).

$$\text{Eq.wt\% NaCl} = 0.00 + 1.76958\Theta - 4.2384 \times 10^{-2}\Theta^2 + 5.2778 \times 10^{-4}\Theta^3 :$$

Θ is temperature in degree Celsius.

HEATING

(vi) Temperature of Total Homogenization, Th:

The observation of this phase change, which is either the collapse of the vapor bubble into the fluid (bubble curve homogenization) or the expansion of the vapor bubble to encompass the entire inclusion (dew curve homogenization) or the disappearance of the meniscus between the two phases (critical point homogenization) is the temperature of total homogenization (Burruss,1981). Provided that certain conditions are met, this value can be used to estimate the pressure and temperature of formation of the inclusion, ie; Pt (pressure of trapping) and Tt (temperature of trapping). These conditions are as follows: (1) The bulk density and the composition of the inclusion can be estimated (from cooling microthermometry). If this is the case an isochore (line of constant density,) is defined in P-T space and this line represents the range of P-T conditions over which a fluid of that density was trapped. (2) An independent value of either pressure or temperature (eg. by light stable isotope fractionation analysis, or a metamorphic pressure estimate). (3) If pure CO_2 and pure H_2O +/- NaCl fluids are simultaneously (and as homogeneous, single phases) entrapped, the point at which the isochores of these two inclusion types intersect will define the P-T of formation (Kalyuzhnyi and Koltun,1953; Roedder and Bodnar,1980). (4) If two partly immiscible fluids were trapped (boiling, phase separation) than each inclusion should homogenize at the same temperature and this temperature is the trapping temperature (Burruss,1981; Roedder and Bodnar,1980; Bowers and Helgeson, 1983). Pressure can be estimated from an appropriated P-T diagram.

(vii) Temperature of Decrepitation, Td:

If the internal pressure of the inclusion being heated exceeds the bounding pressure of the host mineral, the host will open along any incipient fractures. The observation of this phenomena is valuable on the grounds of recognizing that this phenomenon has occurred, but the actual temperature value cannot be directly associated with any pressure-temperature phase equilibria as decrepitation temperatures are as much a function of the host material as they are a function of the fluids within the inclusions. It is possible to derive some qualitative information from those inclusion that do decrepitate. The observance of the phases prior to decrepitation will suggest the general proximity of temperature of homogenization and the type of homogenization, (ie. bubble, or dew curve). Td values can be used as minimum homogenization temperatures (Walsh et al.,1988).

RESULTS OF THE FLUID INCLUSION RESEARCH:

Inclusion Classification:

Fluid inclusions in this study are classified on the basis of composition and according to their origin. Although many authors have chosen to classify inclusions as a function of the phase assemblage observed at room temperature, (20°C in this study) this arbitrary value would have produced a totally unnatural division in the most commonly observed inclusions of the Sheep Creek Camp. The classification scheme for this study is summarized in Figure 3.1.

Aqueous inclusions (Type A, Type As) are defined by the presence of one or two fluidphases and the absence of any observable volatile phase such as CO_2. No carbonic freezing or clathrate formation was observed in these inclusions. An arbitrary value of 8 eq.wt.% NaCl was chosen to differentiate between low salinity aqueous inclusions (Type A) and higher salinity aqueous inclusions (Type As). These inclusions may contain minor amounts of undetected volatile components other than H_2O.

Carbonic inclusions (Type C, Type Ch, and Type Cx) are defined by the presence of CO_2 with or without additional volatile phases,though they may contain in excess of 90 Vol.% H_2O. Type C inclusions are defined by the presence of H_2O and CO_2, whereas Type Ch inclusions are defined by the presence of H_2O and CO_2, and the presence of one or more additional volatile components in the carbonic phase. The presence or absence of additional volatile components was defined by choosing and arbitrary temperature of 1°C depression of Tm_{carb} from the triple point of pure CO_2. Values of -57.6°C or less indicate CH_4, N_2, H_2S, or other contamination and the inclusion would be classified as Type Ch.

If the inclusion contained no discernable aqueous phase and revealed carbonic phase freezing phenomena, (ie. the inclusion was not empty) it was classified as Type Cx. All inclusions observed in this study that were pure non-aqueous inclusions had depressed Tm_{carb} values which is indicative of a complex carbonic fluid. Th_{carb} values below 31.1°C (critical point for pure CO_2) and phase equilibria data suggest that CH_4 is the prominent additional volatile.

In addition to the classification of fluid inclusions on the basis of the inclusion composition, all inclusions were classified by their origin according to the criteria of primary, secondary and pseudosecondary inclusions as defined by Roedder (1984). The majority of inclusions chosen for microthermometry in this study were considered to be primary in spite of the considerable ambiguity and/or uncertainty involved. Although "a correct determination of the origin of fluid inclusions is crucial to any useful interpretation of P-V-T-X data derived", (Roedder,1984), it must be emphasized that the distinction between primary and pseudosecondary inclusions in these massive anhedral quartz veins is difficult.

The majority of the vein quartz in the Sheep Creek Camp is massive white quartz and is "...normally white because of the large number of healed shear planes in it, each outlined by thousands of tiny secondary inclusions" (Roedder, 1984). Secondary inclusions are found in all inclusion bearing samples and all of the inclusion types described above have been observed as secondaries. The obvious dearth of microthermometric data for secondary inclusions is both a function of geological process, ie. most secondaries are too small to see phases or phase changes, and 'artistic license'; the inclusions are so difficult to work that most values recorded aresuspect. The paradox thus exists; knowing that gold mineralization in this region is a late stage aspect of the evolution of the hydrothermal system, it is only reasonable to believe that the inclusions representative of this stage should be studied in detail and that "...most inclusions in most samples are secondary" and "...the safest presumption is that an inclusion is secondary until proven primary" (Roedder,1984). The greater emphasis of this study is on primary or pseudosecondary inclusions.

LOCAL OBSERVATIONS

For the purpose of analysis, the Sheep Creek Camp and surrounding district has been subdivided into eight locales (Figure 3.2). These locales are centered upon the Reno mine with the intention of determining if there is any variation in fluid inclusion characteristics from this core region of high-grade gold mineralization to those localities of lower grades and those of no observed mineralization.

Presented in Table 3.2 is a compilation of averages for all inclusions recorded; these data are summarized in Table 3.1. Frequency histograms are presented for Th_{carb}, eq.wt.% NaCl, Th-Td in Figures 3.3, 3.5, 3.6 respectively and Figure 3.4 being a scatter plot for Tm_{carb} vs. Th_{carb}.

RENO PERIPHERAL and Vsc #205:

Samples Vsc127 through Vsc131 produced a number of workable inclusions and yielded an assortment of inclusion types. The inclusion populations of samples Vsc131,130,129 and 127 are dominated by Ch and Cx inclusions. This contrasts with sample Vsc128,which has a predominance of aqueous and high salinity aqueous inclusions. Salinity estimates for Reno Peripheral inclusions range from 0 to 24% eq.wt.% NaCl (Table 3.2), with the majority of salinity values being less than 8%. Eutectic temperatures suggest that the high salinity inclusions contain complex chloride chemistry (Crawford, 1981). Figure 3.5 shows that the relationship of Tm_{carb} and Th_{carb} of Reno Peripheral inclusions is strongly influenced by the presence of CH_4 and from Table 3.2 it can be seen that CH_4 constitutes up to 40 mole % of these inclusions. Bulk inclusion densities range from 0.47 gm cm^{-3} for 'Cx2' inclusions to 1.12 gm cm^{-3} for 'As' inclusions. From the frequency histograms of Th and Td (Figure 3.6), it can be seen that there is a wide range in homogenization temperatures with a mean value of 301±50°C over 35 values and a slightly tighter range in decrepitation values with a mean of 279±36°C over 21 observations. Homogenization temperatures trend towards the high end for the aqueous inclusions with a significantly lower set of values for the higher salinity inclusions.

Sample Vsc113, pyritized quartz from the Calhoun vein, contained a number of very small 'Ch-Cx' inclusions and a few slightly larger aqueous inclusions. Bulk densities range from 0.53 gm cm^{-3} to 0.72 gm cm^{-3} for the 'Ch-Cx' inclusions and average 0.94± 0.3 gm cm^{-3} for the aqueous inclusions. Th for the aqueous inclusions average 276±25°C.

Vsc #205:

Visible gold, euhedral quartz, biotite, siderite, calcite and late muscovite are the major minerals that compose this sample from the #3 level of the Reno mine. The association of gold with quartz in this sample prompted an extensive fluid inclusion study and seven wafers were produced from different quartz crystals contained in the sample and each wafer supplied many good inclusions for microthermometry. Aqueous inclusions range from less than 2% eq.wt.% NaCl to the 8 % maximum and 'As' inclusions range up to 25 eq.wt.% NaCl with similar eutectic temperatures as observed in sample Vsc128D, suggesting the presence of calcium or magnesium chlorides. Carbonic inclusions contain variable CO_2-CH_4 ratios with CH_4 ranging from 3 mole % to 20 mole %, not including a pair of complexed inclusions, Vsc205/Eu/2, which exhibit phase transitions at -129°C (solid-liquid phase transition) and -86.2°C (solid-liquid phase transition) suggesting that these are complexed Cx inclusions.

As with inclusions from Reno Peripheral, the interdependence of Tm_{carb} and Th_{carb} indicates that lower Th_{carb} values are a function of CO_2 contamination by CH_4. Of note however is the trend towards lower Th_{carb} values without the associate lowering in Tm_{carb} which suggests that variable pressures are also recorded in these inclusions. Bulk density estimates for these inclusions range from a minimum of 0.52 gm cm^{-3} for high XCH_4 inclusions to a maximum of 1.04 gm cm^{-3} for high salinity aqueous inclusions with an average value for the whole field at 0.87±0.14 gm cm^{-3}. Total homogenization temperatures peak around 280°C, though the mean value is 257±53°C. As is the case for Reno Peripheral, the range in Th values is probably a result of not only variable pressures within the system (Kesler, 1991), but reflects the possibility of post-trapping deformation.

HIDDEN CREEK RIDGE:

Five barren (<3% pyrite) quartz veins, hosted by a variety of lithologies were investigated and all five types of inclusions were observed. Sample Vsc179 is an oblique-foliaform quartz vein in a finely crenulated siliceous argillite with chloritized biotite parallel to foliation, which is overprinted by biotite perpendicular to foliation. Minor amphibole is located near the vein and a clinozoisite phase rims the vein. The quartz is moderately undulose and saturated with secondary inclusions.

The Type A inclusions were dilute with a bulk density of 0.87 gm cm^{-3}. One decrepitation temperature of 285°C was recorded. Pseudosecondary and primary Ch, Cx inclusions with an X_{CH_4} range from 0.01 to 0.21 and an X_{CO_2} range from 0.07 to 0.80 produced only one Th value of 327°C and a mean decrepitation value of 251±25°C. The average bulk density for these Ch andCx inclusions is 0.92±0.03 gm cm^{-3} ranging from a low of 0.82 gm cm^{-3} to a high of 1.01 gm cm^{-3}.

Vsc188 is white, massive quartz from a 0.7m vein striking east and dipping 85° N. The quartz is coarse, anhedral and exhibits relatively low strain. Mineralogy of wallrock alteration includes biotite, euhedral zoned horneblende, altered plagioclase and late muscovite. The vein interfingers with the host rock which is silicified garnet-bearing argillaceous quartzite. Inclusions from this sample are Types A, As, and C with salinities ranging from 2.8% (clathrate) to 14% in the As inclusions. Consistent Th_{carb} values of 9-

11 °C give average bulk density values for 'C' inclusions of 0.94 gm cm^{-3} for Vsc188A and 0.97 gm cm^{-3} for chip B. Bulk densities for the low salinity inclusions range from 0.85 gm cm^{-3}- to 0.88 gm cm^{-3}- and for 'As' inclusions a range of 0.83 gm cm^{-3}- to 1.01 gm cm^{-3}. The bulk of the total homogenization temperatures recorded for Hidden Creek Ridge come from Type A and As inclusions from this sample and average 271±40°C. All 'C' inclusions decrepitated prior to homogenization.

Samples Vsc356 and Vsc357 are quartz carbonate veins from massive Laib limestone. The quartz is coarse to very fine grained, which is a function of the intense brittle-ductile strain recorded in these samples. Either late-stage quartz microveining or recrystallization and incipient recrystallization is common throughout these samples. Late calcite is also severely strained and microtourmaline floods the quartz in Vsc356. Tremolite is locally present in Vsc357. Small 'As2' inclusion in Vsc357 have an average salinity of 10.4±0.7 eq.wt.% NaCl. Only two homogenization values were recorded over a range of over 50°C (187 to 246°C). Vsc356 contains a set of 'Cx2' inclusions, as well as a complex of high X_{CH_4} inclusions with phase changes at -142.3°C and -70.9°C. The 'Cx2' inclusions exhibited remarkably consistent Tm_{carb} and Th_{carb} values, which equates to an X_{CH_4} of 0.31 and bulk densities of 0.75 gm cm^{-3}.

Sample Vsc383 is a coarse-grained tourmaline, muscovite, quartz-bearing vein hosted by massive argillaceous quartzite. The vein is not more than 10cm wide and pinches out over a lenght of approximately 1.5m. The close proximity of this vein to Hidden Creek migmatite and the eastern contact with the Salmo stock makes its origin uncertain. Nonetheless, Type A and C inclusions with salinities of 1-5% where observed. Many of the Type C inclusions were three phase or would nucleate a CO_2 vapor phase upon minimal cooling, (the lowest recorded Th_{carb} was +15.7°C). Tm_{carb} averages of -56.9 and -56.8 for the two chips suggest nearly pure CO_2 phases with bulk densities ranging from 0.83 gm cm^{-3} (one value) to 0.96 gm cm^{-3} with an overall average of 0.92 gm cm^{-3}. Homogenization temperatures for those 'C' inclusions that did not decrepitate averaged 301±2°C and total homogenization temperature values for 'A' inclusions averaged 314±3°C. Decrepitation values ranged from 261-318°C with a mean value of 277±28°C.

The variety of inclusion types observed in these five samples is an indication of the very complex nature of the hydrothermal history of this portion of the Kootenay Arc. Interestingly enough, total homogenization temperatures for the primary inclusions exhibit a moderate range of 80°C with a mean of 271± 40°C and the bulk densities are all high, at approximately 0.90 gm cm^{-3}.

RENO EAST, DONNYBROOK:

Sample Vsc361 is a barren quartz vein found crosscutting an altered felsic dyke. The vein is relatively unstrained and the fluid inclusions observed had consistent salinities of approximately 4 eq.wt.%NaCl, low X_{CO_2}, and X_{CH_4}, high densities ranging from 0.92 gm cm^{-3}- 0.96 gm cm^{-3} and decrepitation temperatures with a mean value of 296±3°C. Fluid inclusion compositions for this locale are remarkably consistent in that eighty percent of the inclusions are carbonic. The one secondary inclusion observed, (density of 0.98 gm cm^{-3}) homogenized at 192°C.

Sample Vsc364, found in the Donnybrook mine workings, is one of the two methane bearing samples from this locale. The sample is vuggy, coarse grained, smoky quartz with pyrite and limonite. Primary Ch inclusions had fairly high methane fractions, low bulk densities (0.61 gm cm^{-3}), elevated clathrate dissociation temperatures (+15.1°C), decrepitation temperatures average 308±16°C and the one total homogenization value is 295°C. Sample Vsc367, hosted by siliceous argillite and located east of the Donnybrook fissure, along the ridge north of Reno Mountain peak, contained few workable inclusions and these inclusions exhibited methane-bearing cooling characteristics and bulk densities of 0.88 gm cm^{-3} and 0.95 gm cm^{-3}. One small aqueous inclusion had a salinity of 6% and a bulk density of 0.97 gm cm^{-3}. No total homogenization or decrepitation phenomena were observed in these inclusions. The remaining portion of the sample set from this locale, Vsc366, Vsc368 and Vsc372 were essentially low X_{CH_4}, high X_{H_2O} Type Ch inclusions with relatively high densities. Th (mean of 330±30°C) and fairly high mean decrepitation temperatures where recorded from these samples. Primary aqueous inclusions observed from this locale gave relatively high total homogenization temperatures of 327±19°C.

Two points of interest can be made regarding this set of inclusions. First, the methane fraction in the carbonic inclusions becomes negligible towards the east and this depletion phenomena seems to be intimately related to the absence of argillaceous or carbonaceous lithologies in the eastern region. Secondly, the total homogenization and decrepitation temperatures are slightly elevated compared to the other locales.

PANTHER LAKE; FAR EAST:

Farther to the east, the vein material from sample Vsc102, Vsc110, and Vsc150 is coarse grained, slightly strained barren quartz. Most of the inclusions observed were high density, H_2O-rich carbonic inclusions with salinities averaging 5.3±0.8 eq.wt.% NaCl. The very few total homogenization temperatures observed have a mean value of 305±10°C with one temperature of 185°C. Inclusion decrepitation proved to be a serious problem with this group, ie. most of the inclusions exploded from 168-309°C. The few aqueous inclusions had slightly elevated salinities approaching 11% eq.wt.% NaCl and bulk densities with values greater than 0.91 gm cm^{-3}. In addition to the high densities and the propensity for decrepitation, the absence of methane in these far field inclusions is notable.

GOLD BELT YELL MOM:

The Gold Belt, Yellowstone and Motherlode mines, centrally located in the Sheep Creek Camp, produced approximately 150,000 ounces of gold from 300,000 tons of ore (Mathew,1953). Repeated attempts to locate workable fluid inclusions in mine dump, outcrop and underground vein samples proved difficult as most samples contained only clouds of very small inclusions. 9Ys3-2, taken from the core of the active workings in the Yellowstone property, contained a few small secondary aqueous inclusions. The vein material is a very tight homogeneous blue-grey, fine grained material that is petrologically similar to the quartzites in the region. Pyrite flooding and fracture filling characterizes the type of mineralization observed in many of the samples from this locale. The four inclusions observed in this material were low salinity, secondaries characterized by a wide range of Th values, (174-315°C) and high densities. No carbonic inclusions were observed.

None of the mineralized samples from the Motherlode mine dump site contained workable inclusions. Sample Vsc022, a foliaform barren quartz vein from the Nugget Member of the Quartzite Formation, contained a number of workable Type C inclusions. Elevated Th_{carb}, elevated Tm_{carb} and depressed Tm_{clath} values confirm the absence of methane in these inclusions. Clathrate temperatures were used to estimated salinities which range from less than 3% to 7% eq.wt% NaCl. An average bulk density of 0.93 gm cm^{-3} over a range of 0.83 gm cm^{-3} to 0.97 gm cm^{-3} and a mean total homogenization temperature of 307±5.6°C were recorded for this highly strained and recrystallized quartz sample. Note that significant strain and recrystallization was observed in both barren and sulphide rich samples from the Motherlode area and post trapping strain and/or metamorphism is one possible reason for the dearth of workable inclusions. Much of the sulphide is euhedral unstrained pyrite and sphalerite which suggests that the mineralization was late with respect to veining and deformation.

Samples Vsc345 and Vsc346, found near the adit of the Gold Belt 8000 vein, contained a few workable inclusions. Except for one Th value of 396°C, the small Type A inclusions decrepitated above 374°C. These values, in comparison with the rest of the fluid inclusion study, suggest post trapping deformation and leakage. Three inclusions from Vsc346 (one 'A' and two 'C') gave an average total homogenization temperature of 253±26°C. The aqueous inclusion had a low salinity and a depressed homogenization temperature (224°C), where as the carbonic inclusions (nearly pure CO_2 at $X_{CO_2} = 0.85$) homogenized at 265 and 271°C with slightly lower bulk densities of 0.77 gm cm^{-3}. Salinity estimates from clathrate were recorded as 4 and 6% NaCl and X_{CH_4} was less than 0.04.

The remaining sample from this locale,Vsc352, was found in the Reno Formation calcareous argillite near the confluence of Twilight and Sheep Creek east of the Motherlode mill site. This quartz carbonate vein contained a few high density, high X_{H_2O} carbonic inclusions with slightly elevated salinities (6%). No decrepitation or homogenization temperatures were recorded for these inclusions. The one aqueous inclusion observed from this sample homogenized to liquid at 329°C.

STAG LEAP +; The Salmo-Creston Transect:

The Stag Leap transect crosses the southern portion of the Sheep Creek Anticline, the Western Anticline, the Laib Syncline and in the east, the Windermere metasediments. This southern set of inclusions is characterized by high variability in composition and densities

Sample RB121, from east of the Laib Syncline, is locally saturated with 'C' inclusions. These carbonic inclusions contain little to no methane, have variable carbonic phase volumes and a salinity range of 0-9% (mean of 4.7±1.7 eq.wt.% NaCl). Interestingly enough, most of these inclusions homogenize and mean values of 253±12 and 326±52°C were recorded for chip RB121b and RB121c respectively. Densities for the 'C', 'Ch' and 'Cx' inclusions varied from a low of 0.60 gm cm^{-3} to a high of 0.96 gm cm^{-3}. Samples Vsc224 and Vsc234 contain similarly variable carbonic inclusions except that these samples, located west of the Sheep Creek Anticline had significantly depressed Th_{carb} which is suggestive of either higher pressures or the presence of additional volatiles, (CH_4 ?). Tm_{carb} values were not depressed however (see Figure 3.5), which suggests that methane is not present and that variable internal pressures are responsible for the observed Th_{carb} values. Vsc224 exhibits minimal strain and only minor incipient recrystallization where as sample Vsc232, located adjacent to Vsc234, is a complex of recrystallized quartz and calcite within a muscovite,staurolite, biotite schist. Clinozoisite rims the recrystallized quartz-carbonate vein.

All inclusions recorded from Vsc228 were relatively high salinity, primary and pseudosecondary aqueous types with no indication of a carbonic phase. This quartz-carbonate vein is coarse grained, exhibits no stress related extinction or recrystallization. The late calcite and chlorite observed in this sample are similarly pristine. In contrast to the higher bulk salinities recorded, the bulk densities from these inclusions range from a low of 0.63 gm cm^{-3} to 1.01 gm cm^{-3} with a mean of 0.86±0.11 gm cm^{-3}. All inclusions studied in Vsc228 homogenized to liquid between 247 and 347°C with mean values of 282±37 and 279±26°C for chips A and B.

Variable H_2O phase-carbonic phase ratios were also observed in RB123. Carbonic phase homogenization temperatures were similarly variable and minor depression of Tm_{clath} is indicative of CH_4 presence. RB123, located west of the Western Anticline, exhibited depressed clathrate dissociation temperatures regardless of the possible presence of methane and these temperatures equate to an average salinity of 8 eq. wt. %NaCl. Except for the two high XH_2O inclusions in this group (Th of 199 and 175°C) all inclusions decrepitated prior to homogenization at temperatures ranging from 230 to 279°C.

BILLINGS CREEK, MNT. WALDIE, ACTIVE # 265:

As has been previously discussed, the mineralization in the Ore Hill and Sumit mines of the Billings Creek locale is hosted by limestones along the same set of northeasterly trending faults as are the mines in the rest of the camp. The only significant lead-zinc production for the camp is from this locale and the gold-silver ratios reversed from the >1 values recorded from the other mines. The mineralization is similar though not identical to the common quartzite fissure veins though, "...it can scarcely be doubted that both are derived from a common source" (Mathews,1953). Sample Vsc094 is from dendritic quartz veining with minor pyrite in a grey-green (Reno) quartzite which is presumed to be atypical for these mines.

Inclusions found within this sample were invariably either 'Cx', or 'Ch' inclusions with depressed Tm_{carb}, depressed Tm_{clath} and in spite of the methane contamination, gave depressed clathrate temperatures suggestive of significant salinities. Calculations from clathrate melting relations give values of 4 and 8 eq.wt.% NaCl.and these values are minimums if methane contamination (XCH_4=0.03) is considered. A range of bulk densities (0.65 gm cm^{-3}-0.89 gm cm^{-3}) was recorded for these inclusions though the majority had values greater than 0.75 gm cm^{-3}. All 'Ch-Cx' inclusions decrepitated prior to homogenization at an average value of 258±30°C

Mount Waldie, Vsc042:

A small quartz vein with very minor galena, hosted by grey-green quartzite (Quartzite Formation) was found on the north side of Waldie Creek along a cliff face near the Weasal Creek fault. Cooling studies revealed low eutectic temperatures (approximately -38°C), and "crazy paving" ice textures, which are indicative of complex chlorides (Shepherd et al., 1985). Both Tm_{clath} and Tm_{ice} were significantly depressed and gave average salinity values of 20 and 22 eq.wt.% NaCl respectively. Volatile fractions in all these inclusions were relatively low with XCO_2 of 0.15 being the highest recorded value.

Only 'As' inclusions homogenized prior to decrepitation and all homogenization was to the liquid phase ranging from 214 to 307°C (six values) with a mean value of 264±36°C. It was not possible to determine the type or types of chlorides from microthemometric analysis alone.

Active #265

An attempt was made to investigate veins from the west of the camp between the Western Anticline and the H.B.mine. The dominant lithology in this region is the Active Formation,which is composed of fractured recessive argillites (brecciated slates) and arenaceous, carbonaceous argillites. Active #265 is a barren white, oxide stained, concordant quartz vein found in the brecciated argillite. Pyrite occurs in both the near-adjacent wall rock and to the east in a boudinaged quartz vein. Fluid inclusion research confirmed the presence of non-aqueous volatiles, which were suspected from the pungent odor that this sample produced when fractured. As the Th_{carb} values for these inclusions were not elevated above the critical temperature for pure CO_2, these inclusion do not contain H_2S. The majority of inclusions are of the Ch and Cx type with significantly lowered Tm_{carb} and Th_{carb} values, where as Tm_{clath} values are all above +10°C. All salinity estimates are from ice melting temperatures and in the presence of clathrate these values would represent maximums. A density range of approximately 0.5 gm cm^{-3} was recorded from 28 inclusions with an average value of 0.8±0.14 gm cm^{-3}. Homogenization temperatures are, for the most part, higher than observed in the Sheep Creek Camp (325±44°C) though decrepitation values were similar at 270±31°C. Aqueous inclusions from this sample gave an average salinity of 8.6 eq.wt.% NaCl, are all high density and have rather low Th values (176±36°C) suggesting either secondary origins, significant changes in fluid dynamics, post-trapping alteration of the inclusions or statistical bias from a rather small data set.

GEOBAROMETRY AND GEOTHERMOMETRY; INTERPRETATIONS AND INTERDEPENDENCIES:

COMPOSITION of the FLUID INCLUSIONS

As has been discussed above, non-destructive analysis, has allowed for compositional estimates. In this study, estimations of fluid compositions span a very broad range including low salinity aqueous fluids, high salinity complex chloride solutions, non-aqueous ($CO_2+CH_4\pm N_2$ (?)) fluids and complexed mixtures of chloride bearing aqueous -

volatile fluids. In addition to these components, it is only logical to believe that other components such as S, Ca, Mg and Si, were potentially associated with the fluid regime and that these additional elemental components would influence the physicochemical nature of the fluid. For the purpose of discussion, the simplified compositional estimates documented in this study will hopefully be sufficient. In spite of this simplistic overview of compositions, significant errors in estimates can occur and these errors will seriously impact upon interpretation.

BULK DENSITIES.

Interpretation of trapping temperature (Tt) and trapping pressure (Tp) is often the most sought after aspect of a fluid inclusion project. In most investigations, neither pressure nor temperature can be determined from the inclusions alone as most inclusions are trapped as supercritical fluids and therefore, trapping pressure or temperature must be estimated from independent evidence such as, depth of burial at time of fluid entrapment, mineralogical equilibria data or light stable isotope geothermometry. The process of interrelating pressure and temperature to establish the 'pressure correction' necessary to determine trapping temperatures or pressures is dependent upon estimates of bulk fluid densities. These estimates are ultimately based upon compositional estimates and experimental/ theoretical equilibria data.

EXPERIMENTAL AND THEORETICAL P-V-T-X DATA:

It is often considered convenient to use experimental P-V-T-X data to interpret complex natural fluid systems (Burruss,1981). It must be emphasized though, that minor changes in fluid compositions, temperatures or pressures (see Figure 3.7) can have significant consequences regarding the fluid regime and the specific P-V-T-X properties. Another problem that plagues this type of research is what compositional estimates does the researcher chose for interpretation, mean values for given inclusion types from specific locales or regions or P-V-T-X data of individual inclusions and then using a consolidation of these individual interpretations for discussion. The latter process would probably produce a more realistic estimate of the P-T regime however the labor inherent in such an activity makes it unrealistic and therefore most inclusionists seem to choose the former, which no matter how carefully done, produces broad and possibly dilute interpretations.

INDEPENDENT 'Tt' AND 'Pt':

Independent trapping pressures and/or independent trapping temperatures are often used for interpretation and discussion of homogenization data (Roedder,1984). In this study, the complex tectonic history can only be used to suggest what has occurred and because the temporal relationship of the veins and the local/regional orogenic history has not been fully explored, i.e., no date for mineralization has been established, neither metamorphic or burial depth criteria can be used as independent geothermometers. Structural and petrographic evidence suggest that the Sheep Creek fissure mineralization is structurally late (post-metamorphic) so any attempt at establishing independent pressures or temperatures from metamorphic facies analyses, would be wrong. Archibald et al. (1983,1984) have presented an argument for periods of intense and rapid tectonic evolution of the region and it is therfore arguable that the Sheep Creek Camp did at one or more times experience high temperature-pressure. As is discussed below, (cf.Cpt. 4) the use of light stable isotope geothermometry in this region, could further the interpretation of the fluid inclusion research. The protracted tectonic evolution of the region has however produced such geological complexity that the issue of isotopic equilibration (necessary to establish geothermometry) cannot be assumed, and as is documented, rarely encountered.

This semi-quantitative, qualitative fluid inclusion study of the Sheep Creek veins has resulted in four significant observations.

I. Fluid pressures throughout the camp, though moderately variable, were at the time of vein precipitation (and probably at the time of ore deposition) high to very high, possibly exceeding 1.5 kbars, which if correct suggests deep crustal burial (1.5 kbars=15 km assuming hydrostatic pressures, or 5.4 km assuming lithostatic pressures)

II. Much of the spatial, microthermometric and compositional evidence supports the assertion that saline aqueous-volatile fluids underwent the process of phase separation and that this process occurred at relatively high pressures and temperatures. Gold mineralization and/or sulphide precipitation could have been a direct consequence of this fluid effervescence.

III. Post trapping deformation of the inclusions and metamorphic overprinting of the quartz or quartz-carbonate veins have resulted in a natural sorting mechanism (inclusions are generally too small to study) which limits the potential error in interpretation and could also be considered as an exploratory tool.

IV. Complex volatile inclusions (CO_2-CH_4) have not been observed in the eastern portions of the study area and a 'methane front' may possibly exist. This front could be structurally, metasomatically or/and lithologically controlled.

DISCUSSION:

To evaluate pressure relations for the Sheep Creek veins, Figure 3.7 is presented for a number of varying CO_2-H_2O-NaCl fluid compositions (Bowers and Helgeson,1983b). These phase diagrams are referred to by the letters A through H which correspond to increasing CO_2 contents. Variable salinities are presented as mole fractions. Figure 3.8 shows homogenization and decrepitation temperatures against mole fraction CO_2 and solvus curves for 6 eq.wt.% NaCl. Both of these diagram sets along with Figure 3.10 and inclusion data values for specific locales, from Table 3.2, are used for pressure estimates. As no independent trapping pressures or temperatures are available and significant variability in inclusion compositions is the norm, this activity of pressure estimates are only approximate.

For sample Vsc179 from the Hidden Creek Ridge locale, if an estimate of Tt is set at the Th value, the type Ch inclusions were trapped at 327°C and have a composition estimate of X_{CO_2}= 0.7, X_{CH_4}= 0.12 and a minimum value of X_{NaCl}= 0.01. Such an inclusion set plotted onto the miscibility field of Figure 3.7G at a density of 0.85 gm cm^{-3} would give a pressure of approximately 1.7 kbars assuming 0% NaCl. If an X_{NaCl}= 0.019 is considered the Th value lies in the two phase region of the appropriate diagram (Fig.3.7H). The shape of the miscibility curve does not allow for an estimate of pressure for these compositions. If the isochores are projected into the immiscible region (isochores plot along same slopes as for Fig.3.7G) and Tt=Th (as is the case for trapping a fluid undergoing phase separation), an absolute minimum pressure of 1.6 kbars is recorded from Th at 250°C and a maximum value of 2.2 kbars is appropriate for 350°C. If Th for Vsc188 is considered at 270°C, 8°C lower than recorded decrepitation values, and a composition of X_{CO_2}= 0.1 and X_{NaCl}= 0.02 are given, Figure 3.7D shows that these inclusions represent immiscibility. If the temperature of trapping was at 300°C, the intersection of the 0.90 gm cm^{-3} isochore will give a pressure estimate of approximately 1.2 kbars and if the 0.95 gm cm^{-3} isochore is considered the pressure estimate is approximately 1.8 kbars. As sample Vsc356 is host to a set of pure CO_2-CH_4 inclusions, no Th value is recorded and the 'pressure correction' estimated for Th_{carb} will be very large. If it is assumed that these inclusions were trapped cogenetically at a temperature of 270°C, Figure 3.10 gives a pressure of trapping of 1.2 kbar. An alternative approach to the pressure problem would be to consider the simpler H_2O-NaCl system. From Figure 3.10 (from Fig. 9.6, Roedder,1984) Vsc179, Type As, with a Th value of 295°C, an eq.wt.% NaCl of 10% (low) and a range of bulk densities of 0.89 to 0.95 gm cm^{-3} (low), pressure estimates range from 600 bars to 1.6 kbars.

From Table 3.2, it can be seen that the data for sample Vsc #205 varies considerably. If these inclusions were trapped from an homogeneous fluid, the data suggest a pressure range from 1.0 kbar at 308°C for 0.70 gm cm^{-3} for Ch inclusions with no NaCl, to approximately 1.4 kbars for Type As inclusions which homogenize at 290°C. Type Ch inclusions from sample Vsc#205G/B had a Th value of 290°C and a composition estimate of $X_{CO_2}=0.76$, $X_{CH_4}=0.10$ and $X_{NaCl}=0.02$. Using Figure 3.7G and assuming no NaCl, a pressure estimate of 1.1 kbars is recorded. If the X_{NaCl} component is considered the inclusions will plot well into the immiscibility field of Figure 3.7H and no pressure value can be determined until Tt is raised above 400°C which would result in a pressure of 1.7 kbars. These elevated pressures and temperatures are possible but the more likely explanation for their occurrence is that these inclusions are end members of phase separation as is suggested by Figure 3.8. Also worthy of consideration is that the methane component (excluded from discussion to this point) will force the two phase region to even higher temperatures (Burruss, 1981; Hollister and Burruss, 1976; Roedder,1984). The salient observation here is that an extreme trapping temperature (greater than 500°C) would be necessary to keep this type of fluid mixture miscible.

The Panther Lake-Far East group of inclusions has a relatively homogeneous character and this partially simplifies discussion. Sample Vsc150 with an average density of 0.90 gm cm^{-3}, a composition estimate of $X_{CO_2}= 0.20$, $X_{NaCl}= 0.02$ and an average homogenization temperature of approximately 270°C can be plotted on Figure 3.7C and a trapping pressure of approximately 1.3 kbars is recorded. If Figure 3.7D is used for this exercise an homogenization temperature of 270°C falls outside of the one phase field and immiscibility is suggested. Observation of the miscibility plot, Figure 3.8 for the Panther Lake, Far East locale, suggests that this was not the case and the probability of a higher, 'pressure corrected' temperature estimate for trapping is required in which case a possible Tt of 325°C will give a trapping pressure of 1.5 kbars.

A continuation of this pressure speculation process shows that for the majority of inclusions observed in this study, Ph values (no independent pressure or temperature estimates therefore no Pt values) fall within the one to two kilobar range. Further estimations of 'pressure correction' and any attempt at establishing Tt from this process is not warranted as a result of the paucity of appropriate P-V-T-X data, the variable nature of the observed inclusion compositions and the significant loss of potential Th data as a result of decrepitation. The inclusion study suggests trapping pressures in excess of one kilobar and trapping temperatures in excess of 300°C.

From a purely petrographic point of view, the observation of nearly pure CO_2 inclusions (CO_2±CH_4) within fields of H_2O-NaCl±(CO_2-CH_4) inclusions indicate either immiscibility of an earlier mixed CO_2-H_2O phase, H_2O loss from earlier mixed CO_2-H_2O fluids or the mixing and subsequent trapping of different fluids either cogenetically or at different times. Figure 3.8 reveals that those locales that are spatially associated (located near to) with the Reno vein, Reno Peripheral, Hidden Creek Ridge, Reno East, Donnybrook and Vsc#205, all exhibit both low X_{CO_2} and high X_{CO_2} inclusions. As has been argued, the probability of phase separation of a fluid, which results in these observed compositions, is high and this suggests that deposition of vein-hosted ore in the Reno vein was asociated with phase separation of a complex aqueous-volatile fluid (Walsh et al.,1988; Roedder, 1984; Ramboz, 1982; Kesler,1991). It is widely believed that 'bonanza' type high-grade zones, the most commonly observed type of Au mineralization in the Reno vein, have "...formed as a result of the gross change in the chemistry of the ore fluids upon boiling or effervescence (Roedder,1984)". The likelihood of this phenomenon is high, as the separation of an homogeneous H_2O-NaCl-(CO_2±CH_4) fluid can occur under a wide range of crustal conditions as a result of minor changes in temperature or pressure and "...pressure could have fluctuated widely between lithostatic and hydrostatic conditions in response to possible fluid overpressures and related movement along deep fractures" (Walsh et al.,1988; Sibson et al.,1988). Gold grades are observed to decrease at depth along the vein structure and this could reflect the probability of immiscibility occurring at shallower depths.

The two inclusion sets, Panther Lake-Far East and Stag Leap+ show high variability in CO_2:H_2O ratios and minimal methane contamination (from Figure 3.4, Tm_{carb} vs.Th_{carb} diagrams). Fluid immiscibility is not suggested for these regions as few end member volatile phase inclusions were observed. This lack of observation may however be simply a function of a small data set. Minor pressure variation are proposed to account for the observed ranges in Th_{carb} (densities) for these locales. The actual density variability is minimal however and this probably reflects minimal pressure fluctuations which is on one hand, incompatible with the overall evolution of the fluid regime of the region yet may be on the other hand, totally consistent with local temporal and spatial fluid characteristics.

The last and possibly most significant observation gleaned from this fluid inclusion study is the absence of methane bearing inclusions to the east of the Sheep Creek Anticline or similarly put, the presence of methane bearing inclusions to the west of the structure, in the mineralized region of the camp. The significance of this 'methane front' and additional comments regarding the fluid inclusion study are made in Chapter V.

Fluid Inclusion Classification
Sheep Creek Camp

Aqueous Inclusions

Type A - H_2O rich, two phase, oval to amorphous, generally high temperature , low salinity

Type As - H_2O rich, two phase, oval to amorphous, variable homogenization temperature, > 8 Eq. Wt.% NaCl

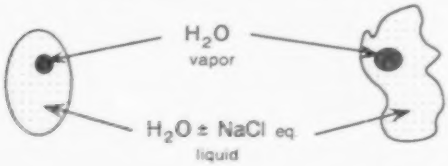

Carbonic Inclusions

Type C - $H_2O + CO_2 \pm NaCl$ bearing, three phase, euhedral to amorphous, $Tm_{carb} > -57.6$ C°

Type Ch - $H_2O + CO_2 \pm CH_4 \pm NaCl$ bearing, three phase at °C < Th_{carb} $Tm_{carb} < -57.6$ C°

Type Cx - $CO_2 \pm CH_4$ bearing inclusions, two phase, no detectable H_2O

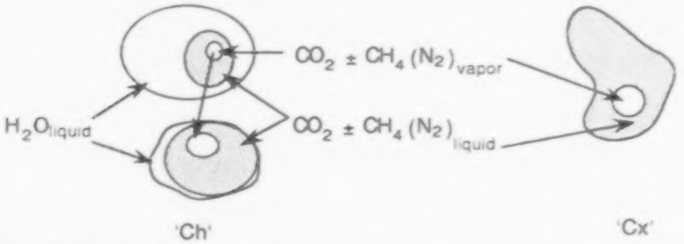

Note that all inclusions can be subclassified according to Primary, Secondary or pseudosecondary origin. The following inclusion types are thus characterized:

Primary; A, As, C, Ch, Cx
Secondary; A2, As2, C2, Ch2, Cx2
Pseudosecondary; Ap2, Asp2, Cp2, Chp2, Cxp2

Figure 3.1 Classification scheme for Sheep Creek inclusions.

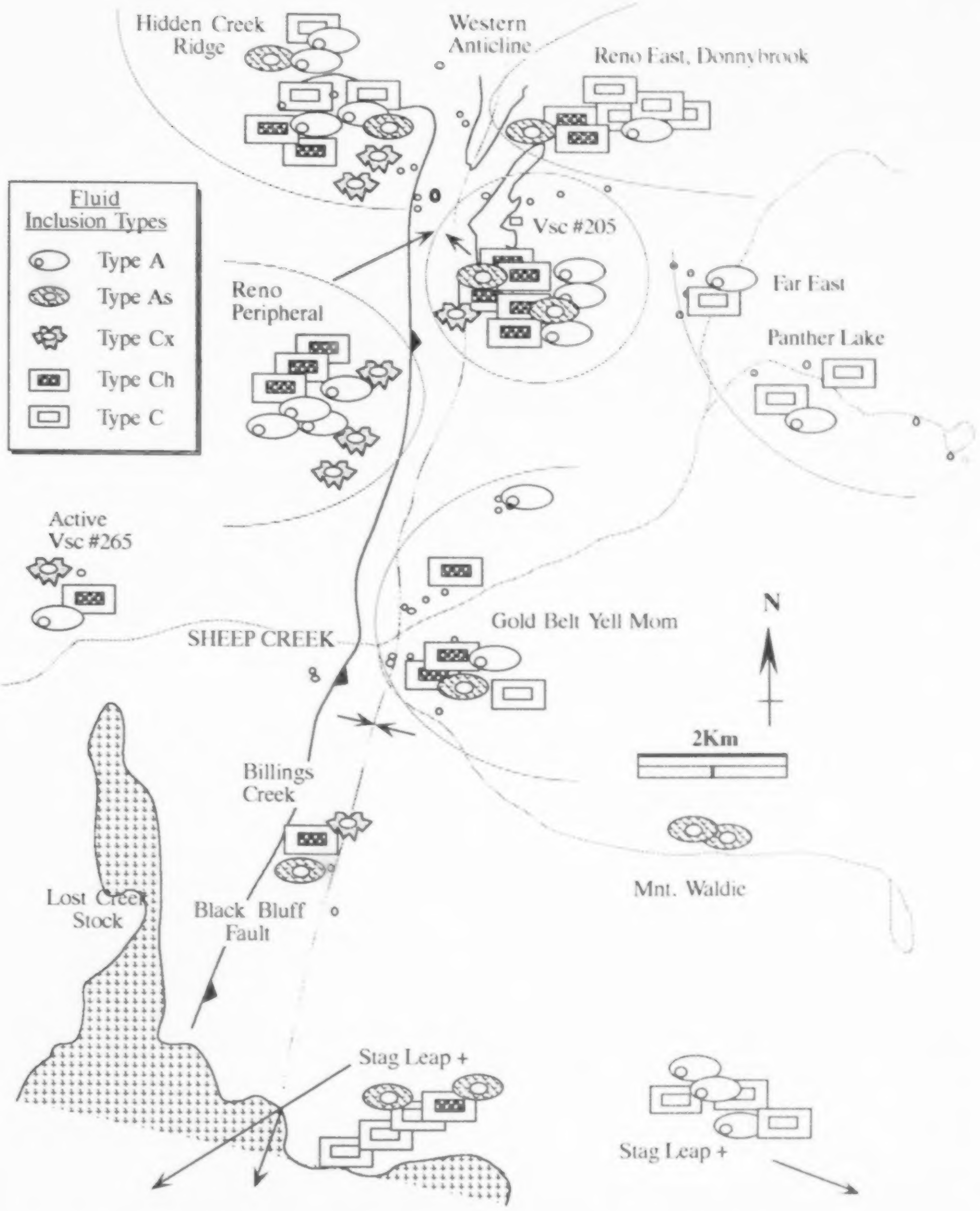
Hidden Creek Ridge
Western Anticline
Reno East, Donnybrook
Fluid Inclusion Types
Type A
Type As
Type Cx
Type Ch
Type C
Vsc #205
Far East
Reno Peripheral
Panther Lake
Active Vsc #265
SHEEP CREEK
Gold Belt Yell Mom
N
2Km
Billings Creek
Lost Creek Stock
Black Bluff Fault
Mnt. Waldie
Stag Leap +
Stag Leap +

Figure 3.2 Fluid inclusion localities and summary of inclusion compositions from the Sheep Creek Gold Camp.

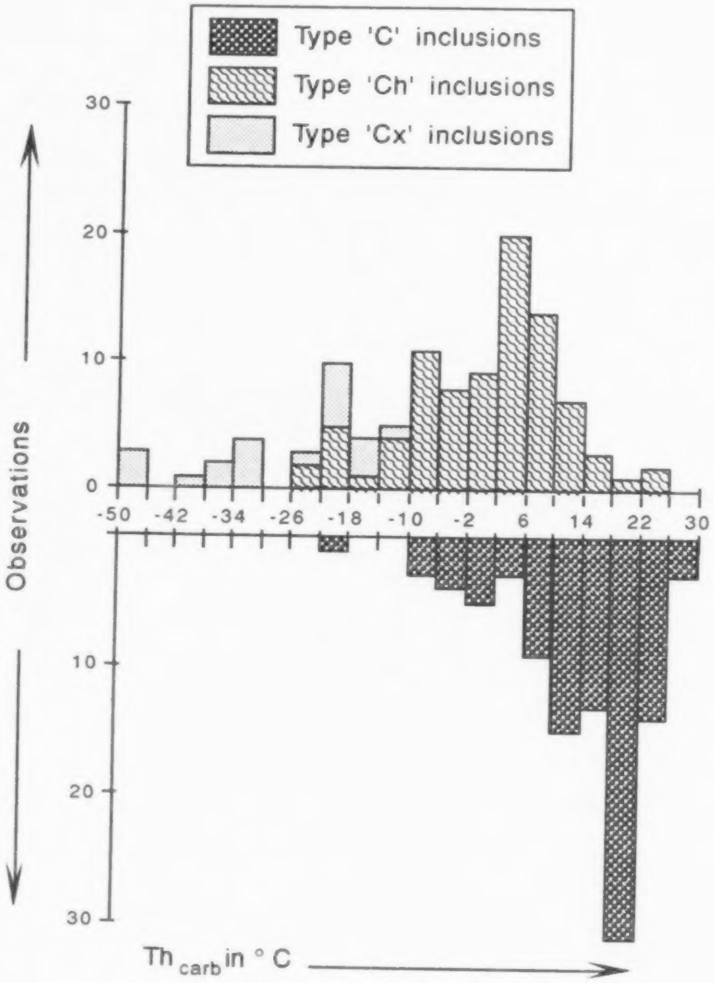

Figure 3.3 Temperature of Carbonic Phase Homogenization. Values for Type C, Ch and Cx inclusions.

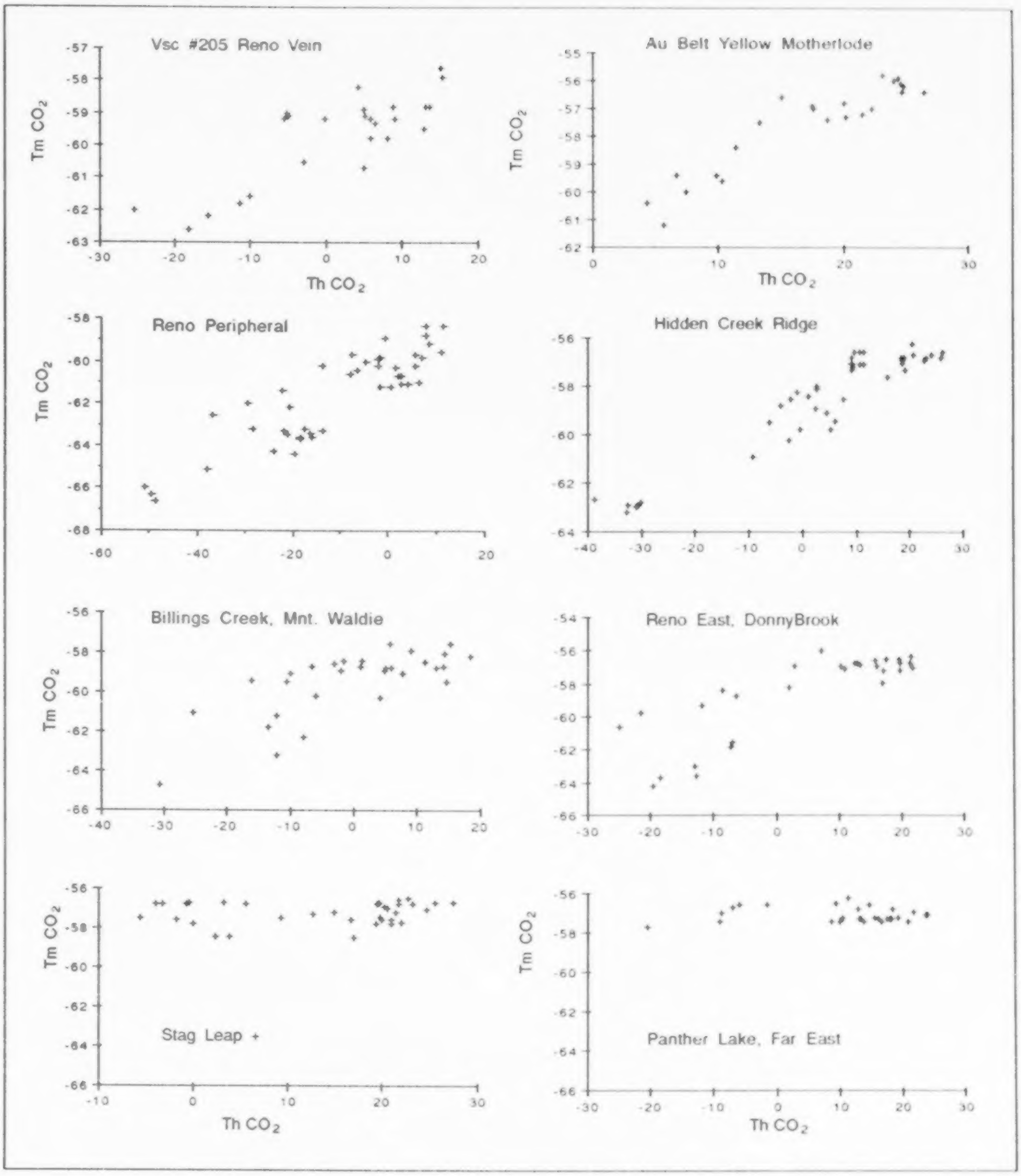

Fig. 3.4. Temperature (in degrees Celsius) of carbonic phase melting Vs. carbonic phase homogenization for CO_2 +/- CH_4 inclusions (Type C, Ch, Cx). Figures are for each of the eight locales of the Sheep Creek as described in the text. Depression of melt and homogenization temperature is indicative of an additional volatile phase, commonly methane or nitrogen. Plots for Stag Leap + and Panther Lake, Far East show no remarkable volatile component with shift in homogenization temperature being due to variation in bulk inclusion density.

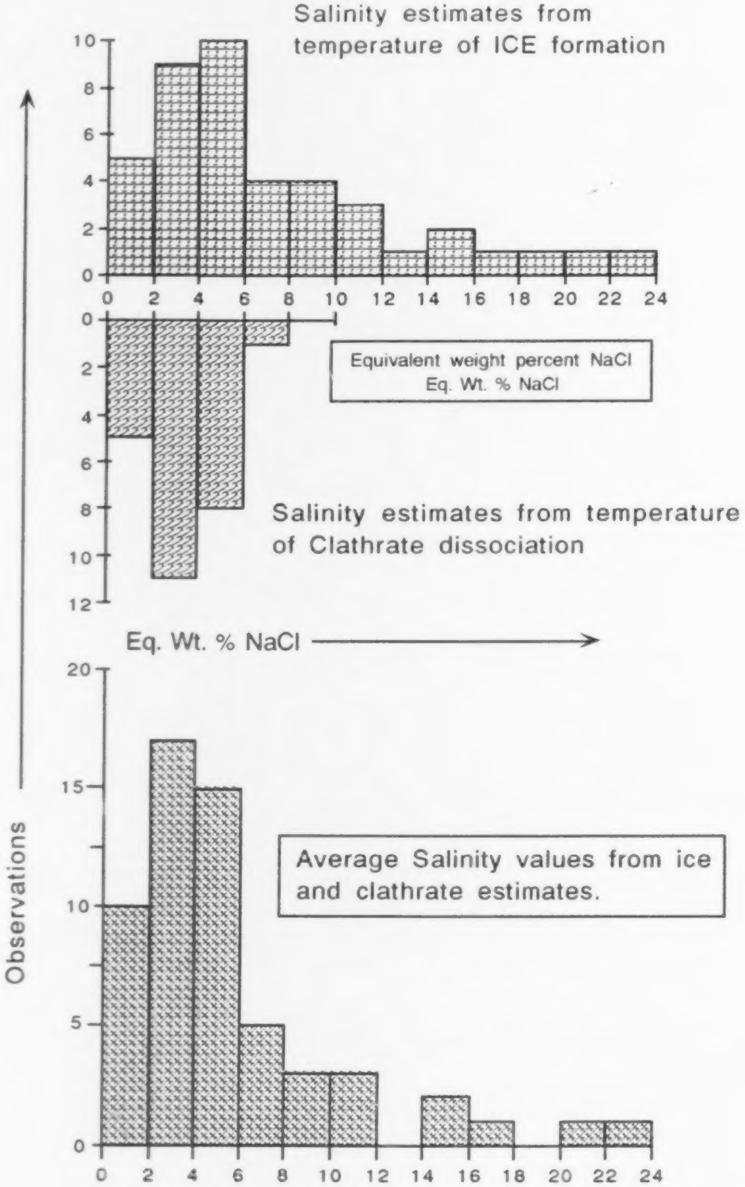

Figure 3.5 Salinity estimates for the Sheep Creek Campp

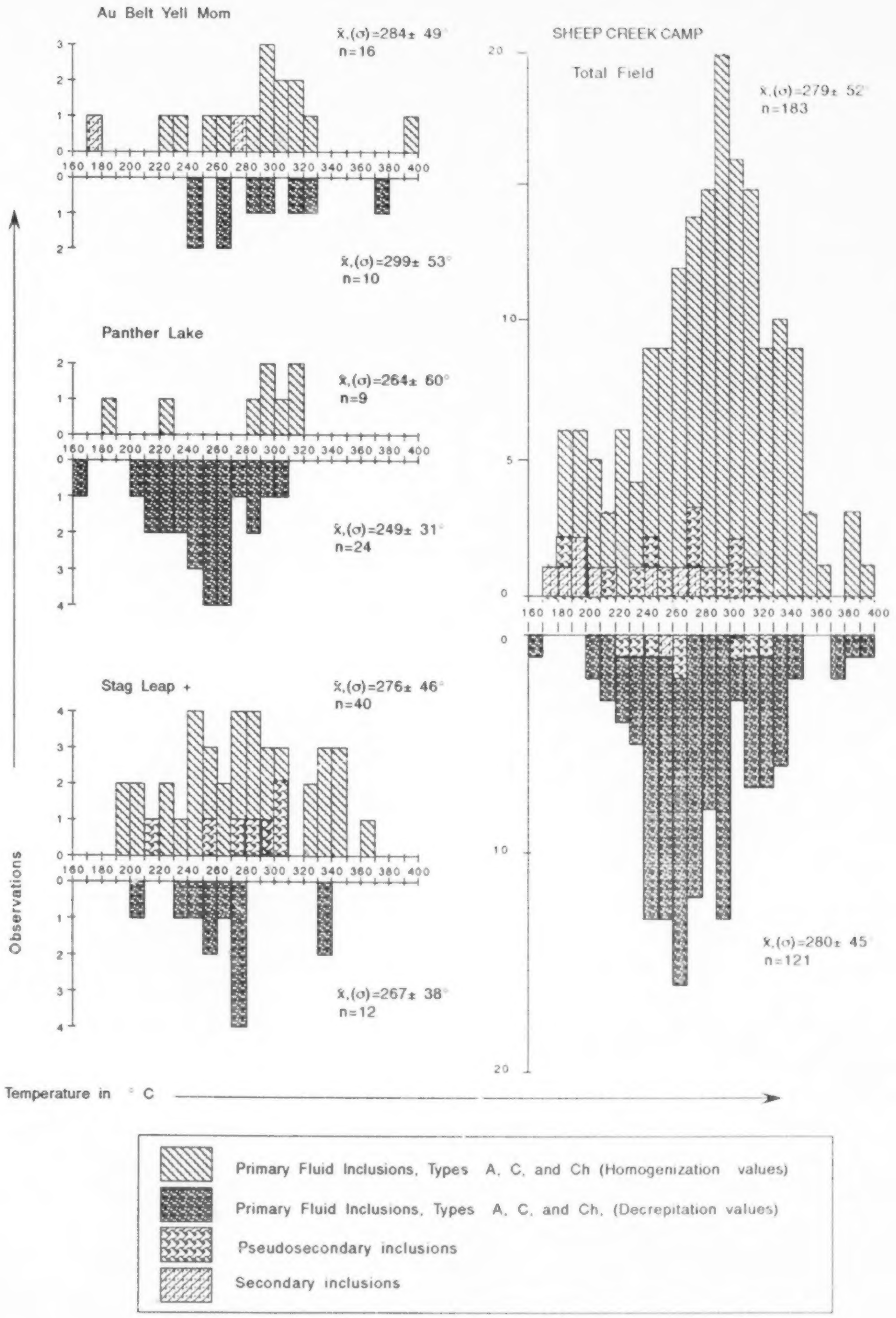

Fig. 3.6a. Total homogenization and decrepitation observations for type A, C and Ch inclusion as observed in the indicated localities of the Sheep Creek Camp with occurrence plot for the total field.

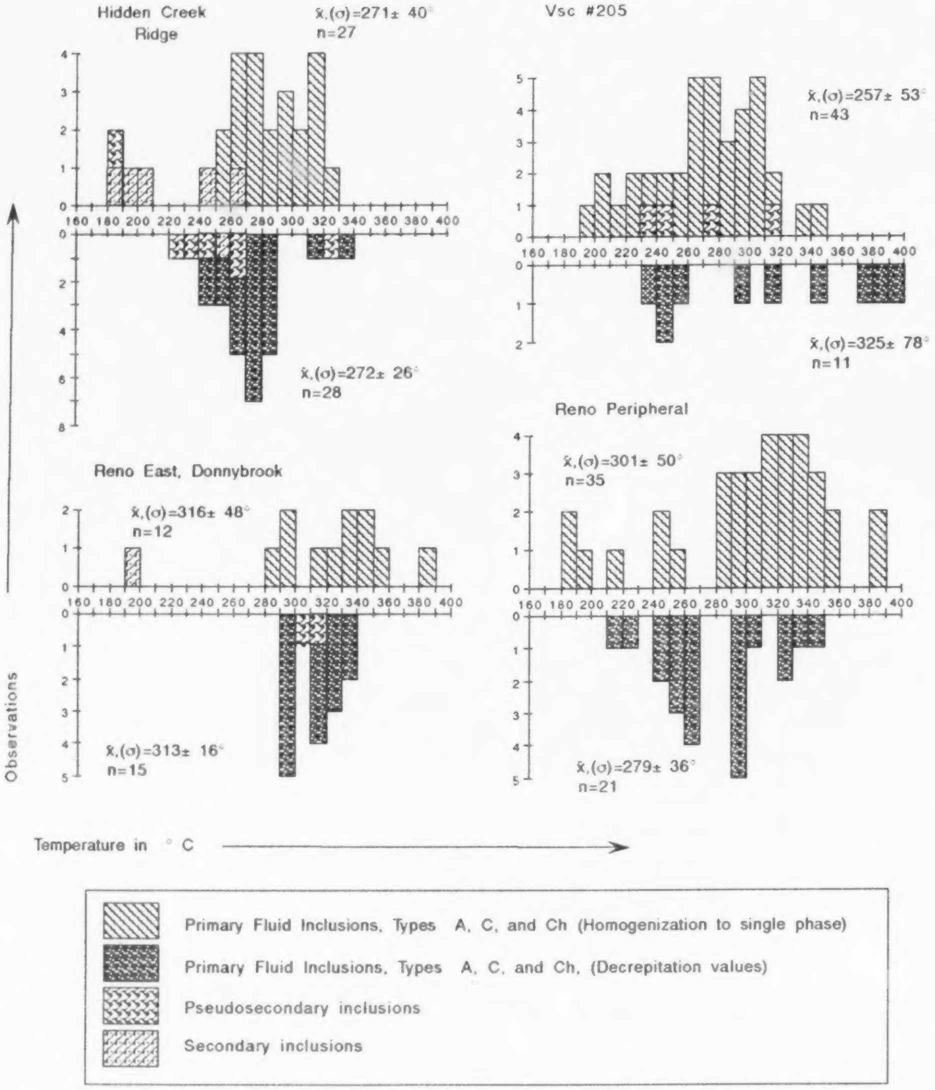

Fig. 3.6b. Total homogenization and decrepitation observations for type A, C and Ch inclusions as observed in the indicated localities of the Sheep Creek Camp.

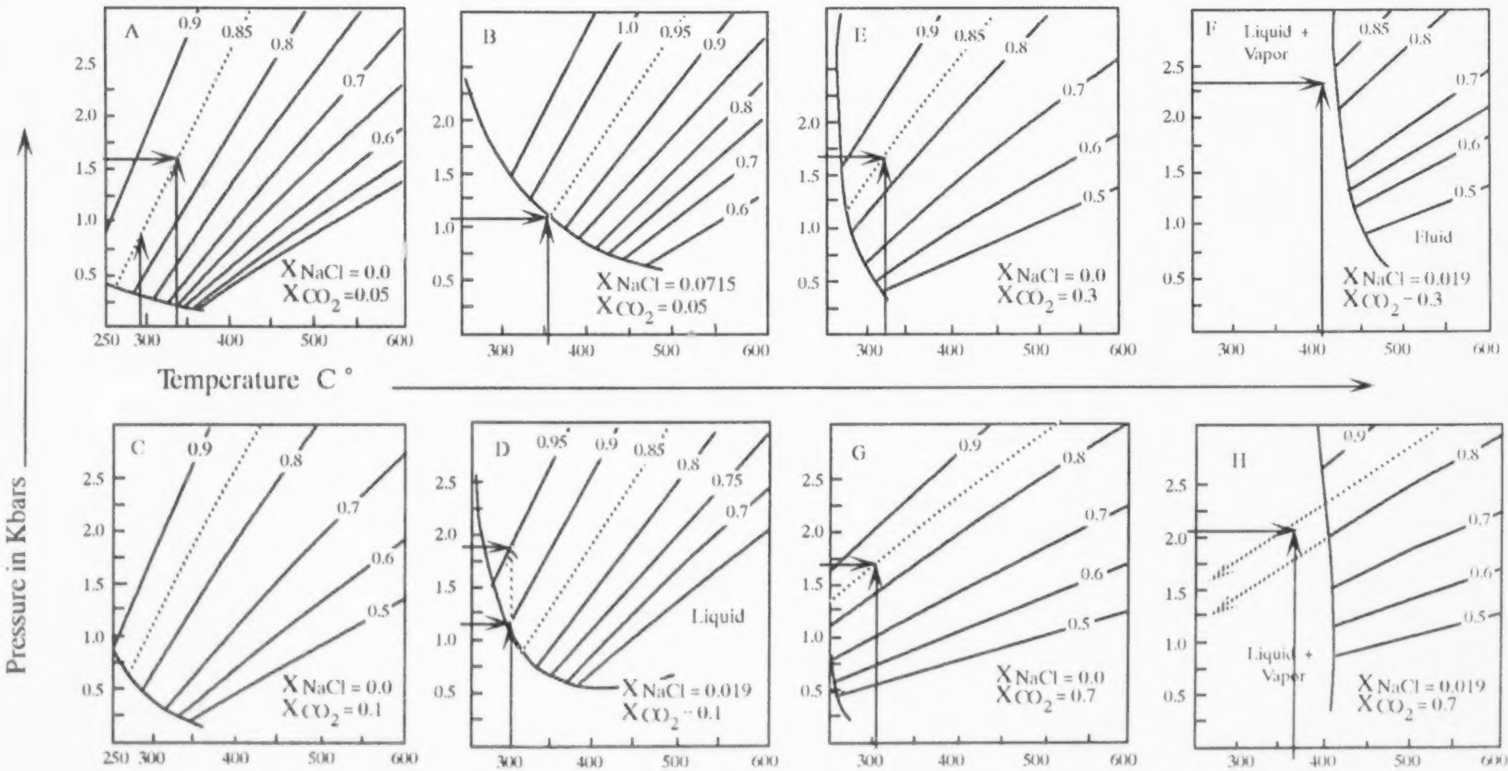

Figure 3.7. Isochores and miscibilty gap diagrams for the system water, carbon dioxide and eq.wt.% NaCl Bulk compositions are labeled as mole fractions, isochores are densities in g cm-3. Letters refer to specific composition possibilites as designated in the text. Diagrams redrawn from Bowers and Helgeson (1983a).

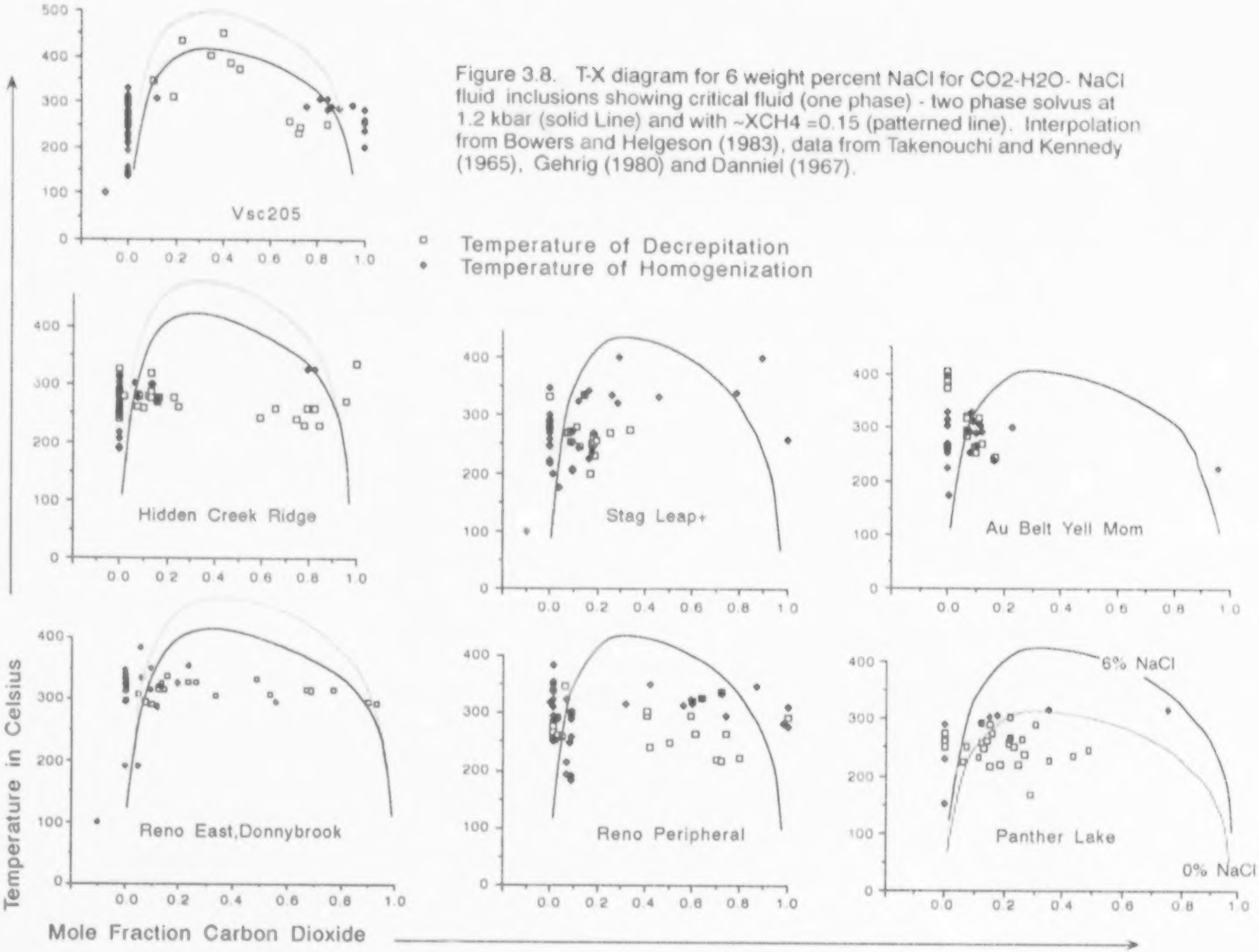

Figure 3.8. T-X diagram for 6 weight percent NaCl for CO2-H2O- NaCl fluid inclusions showing critical fluid (one phase) - two phase solvus at 1.2 kbar (solid Line) and with ~XCH4 =0.15 (patterned line). Interpolation from Bowers and Helgeson (1983), data from Takenouchi and Kennedy (1965), Gehrig (1980) and Danniel (1967).

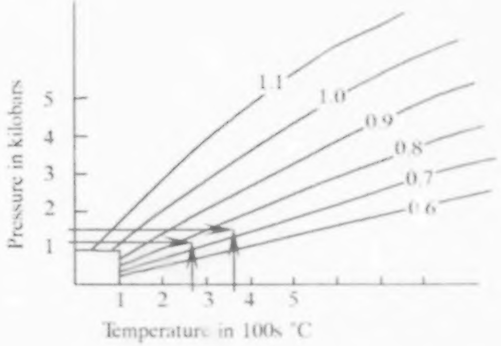

Figure 3.9. Isochores in the system CO2, (densities in g/cc). Partial diagram redrawn from Swanenberg (1979) with data from Juza et al. (1965), Kennedy and Holser (1966), and Shmonov and Shmulovich (1974). Pressure estimate for sample Vsc#356 as discussed in the text.

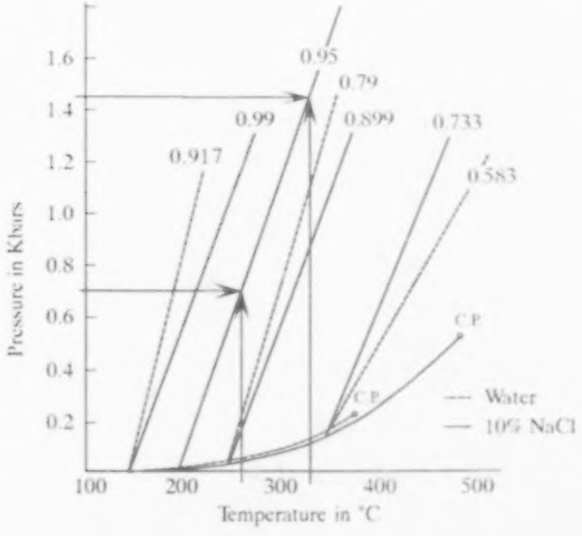

Figure 3.10 Pressure estimate at Th for sample Vsc#179 as discussed in text. Partial phase diagrams for water and 10% NaCl solution, showing the liquid-vapor curves and appropriate isochores in g/cc. Diagram redrawn from Roedder (1984), data from Sourirajan and Kennedy (1962), Burnham et al. (1969), Keenan et al. (1969) and Haas (1976)

Table 3.1 Fluid Inclusion Data Summary; AVERAGES *(p.1)*

Sample	Type	V%H2O	V%Carb	TmCarb	TmIce	TmClath	ThCarb	Td	Th	NaCl	Density	XCO2	XCH4	XH2O	XNaCl
Panther Lake-Far East															
110Ave CO2	C	72.0	28.0	-56.6		7.5	14.8	232		5	0.97	0.11	n/d	0.87	0.02
102 Ave CO2	C	46.0	54.0	-57.0	-7.4	9.0	-8.7	226	314	11	1.00	0.34	0.01	0.59	0.05
150AveCO2	C	53.0	46.8	-57.3		7.2	16.3	267	262	5	0.90	0.21	0.01	0.76	0.02
150Ave 2	A	90.0	0.0					274		7	0.93	n/d	n/d	0.98	0.02
Billings Crk-Mnt Waldie															
Vsc042	C-Ch	78.0	26.0							20	1.06	0.08	0.01	0.84	0.08
Vsc042	As	93.8	0.0		-21.8					22	1.08	n/d	n/d	0.92	0.08
Vsc042	Ch	77.5	26.0	-58.8	-19.5		13.1			22	1.05	0.07	0.01	0.83	0.09
Vsc094A	Cxp2-Ch	0.7	99.3	-58.9			-1.9			n/d	0.81	0.86	0.12	0.02	n/d
Vsc094B	Ch	27.9	64.9	-61.8	-10.6		-13.5	258	301	15	0.75	0.35	0.14	0.44	0.08
Reno-East, Donnybrook															
Vsc372	C	76.7	23.3	-56.7		8.6	12.5	290	315	3	0.97	0.09	n/d	0.89	0.01
Vsc364	Ch	17.5	82.5	-58.7			-6.2	317		6	0.85	0.60	0.07	0.30	0.04
Vsc368	C/A	70.0	30.0	-57.2		8.6	19.8	317	322	3	0.94	0.12	0.01	0.87	0.01
Vsc364A	Ch/Chp2	19.0	81.4	-63.0		15.1	-12.9	308		n/d	0.61	0.35	0.18	0.47	n/d
Vsc361A	C/A	86.7	13.3	-56.5	-3.5	8.3	17.5	309	192	4	0.99	0.05	n/d	0.94	0.01
Vsc366A	C/As	53.2	46.8	-56.8	-11.9	8.1	13.5	328	358	4	0.93	0.23	n/d	0.75	0.02
Hidden Creek Ridge															
Vsc188/A	C	77.7	17.3	-56.6		8.2	11.4	283	278	4	0.94	0.07	0.00	0.91	0.01
Vsc188/B	As, A2, A	88.6	0.0	-57.1	-7.1	8.6	10.7	282	253	10	0.95	n/d	n/d	0.97	0.03
Vsc188/C	C	65.0	35.0	-57.1	-10.2	8.2	9.1	278	268	4	0.97	0.16	0.01	0.82	0.02
Vsc188/D	A	79.0	0.0		-2.5			262	271	4	0.81	n/d	n/d	0.99	0.01
Vsc179	Chp2	17.7	82.3	-58.4	-9.8	9.8	1.1	258		14	0.94	0.69	0.07	0.15	0.09
Vsc179	As	89.3	0.0					256	293	14	0.99	n/d	n/d	0.95	0.05
Vsc179/B	Ch	7.8	92.2	-59.8	-0.5	9.2	-0.4	258	327	2	0.82	0.70	0.13	0.16	0.01
Vsc179/B	A	87.0	1.0					285		1	0.87	n/d	n/d	1.00	0.00
Vsc 383	C	59.7	40.3	-56.9		7.6	22.8			5	0.91	0.17	n/d	0.81	0.02
Vsc 383	A	90.0	0.0		-2.6					5	0.93	n/d	n/d	0.98	0.02
Vsc 383/B	C	67.8	32.2	-56.8	-1.2	8.3	18.8	277	302	3	0.94	0.13	n/d	0.86	0.01
Vsc 383/B	A	88.3	0.0					241	314	2	0.89	n/d	n/d	0.99	0.01
Vsc356 A	Ch	0.0	100.0	-62.9			-32.6		n/d	n/d	0.75	0.69	0.31	n/d	n/d
Vsc357/ A	As	93.0	0.0		-6.8			253	216	10	1.00	n/d	n/d	0.97	0.03
Reno-Peripheral															
Vsc113	C	2.5	98.3	-60.7	-1.7	10.2	2.0		280	3	0.66	0.74	0.22	0.02	0.02
Vsc113	A	92.5	0.0		-1.7					3	0.94	n/d	n/d	0.99	0.01
Vsc128/A	A	87.0	0.0						341	3	0.89	n/d	n/d	0.99	0.01
Vsc128/B	A	87.0	0.0					268	383	3	0.89	n/d	n/d	0.99	0.01
Vsc128/C	Cx		100.0	-62.0	-16.3		-29.4			n/d	0.78	0.73	0.27	n/d	n/d
Vsc128D	As	91.4	0.0	0.0	-20.4		-21.5		245	23	1.07	0.00	0.00	0.92	0.08

Table 3.1 (continued) **Fluid Inclusion Data Summary; AVERAGES** *(p.2)*

Sample	TYPE	V%H2O	V%Carb	TmCarb	TmIce	TmClath	ThCarb	Td	Th	NaCl	Density	XCO2	XCH4	XH2O	XNaCl
Reno-Peripheral															
Vsc129	Ch	19.2	80.8	-59.2	-1.4		8.7	295.9	322.1	2	0.75	0.50	0.08	0.41	0.01
Vsc127	Cxp2	0.0	100.0	-63.7	-3.1	10.8	-18.2	294.0	308.4	n/d	0.53	0.63	0.37	n/d	n/d
Vsc127	A	91.8	0.0		-3.1					5	0.95	n/d	n/d	0.98	0.02
Vsc130	Cx, Ch	23.8	72.9	-63.2	-4.7	10.1	-28.4	322.0	313.7	7	0.78	0.38	0.18	0.40	0.03
Vsc131	Ch	31.9	68.1	-60.2	-3.7	13.1	-1.8	240.5	347.8	n/d	0.81	0.34	0.08	0.58	0.00
Vsc #205															
CO2,'c'	Ch	40.0	60.0	-62.0				400.8		n/d	0.80	0.23	0.12	0.65	n/d
H2O,'c'	A, As	91.4	0.0		-6.3		-15.1		193.7	9	0.97	n/d	n/d	0.97	0.03
H2O,A,B	As	89.7	0.0		-13.4			331.8	289.8	16	1.00	n/d	n/d	0.95	0.05
CO2,A,B	*Ch*	*53.0*	*45.0*				0.8			*n/d*	*0.85*	*0.18*	*0.04*	*0.78*	*n/d*
H2O,B1	As	86.4	0.0		-17.4			248.8	225.4	20	1.00	0.00	0.00	0.93	0.07
CO2,C	Cx	0.0	100.0	-59.1			-3.9		253.3	n/d	0.81	0.87	0.13	n/d	n/d
H2O,D	A	87.5	0.0		-1.8				246.3	3	0.89	0.00	0.00	0.99	0.01
CO2,G/A	Ch, Cx	6.4	94.2	-59.4		11.1	10.2	251.0	308.0	3	0.68	0.71	0.13	0.14	0.02
H20,G/A	A	91.7	0.0		-1.8				221.3	3	0.93	0.00	0.00	0.99	0.01
CO2,G/B	Ch	6.3	93.7						289.8	3	0.73	0.76	0.10	0.12	0.02
H20,G/B	A	91.2	0.0		-1.9	9.8	8.5		291.4	3	0.93	0.00	0.00	0.99	0.01
Stag-Leap+															
Rb123b	C, Ch	68.5	28.9	-58.3		5.9	6.0	259.6	187.0	8	0.96	0.13	0.01	0.83	0.03
Rb121	C	56.9	41.9	-56.8	-6.7	7.4	23.2			5	0.89	0.18	n/d	0.80	0.02
R.B.121 B	A/C/Ch	75.0	25.0	-57.0	-3.4	9.1	20.5		252.6	2	0.95	0.09	n/d	0.90	0.01
R.B.121 C	A/Ch	48.1	50.6	-57.6	-2.8	8.3	20.0		335.6	4	0.88	0.24	0.01	0.72	0.02
Vsc224	C	62.1	37.9	-56.8	-4.9	8.7	5.6	200.0	244.4	3	0.96	0.18	n/d	0.81	0.01
Vsc234	C	71.3	28.8	-57.2	-6.8	8.7	14.9		242.4	10	0.80	n/d	n/d	0.97	0.03
Vsc228 A	As	83.3	0.0		-5.6				282.0	9	0.89	n/d	n/d	0.97	0.03
Vsc228 B	Asp2	81.1	0.0		-4.8				277.4	8	0.86	n/d	n/d	0.97	0.03
GoldBelt Yell Mom															
9Ys3-2	A,As	92.0	0.0		-3.5				251.9	6	0.96	n/d	n/d	0.98	0.02
Vsc022	C	70.0	30.0	-56.1		7.4	24.6	318.5	307.0	4	0.93	0.11	n/d	0.88	0.01
VscGb01A	Ch, A	66.0	34.0	-60.0	-0.4	9.1	7.4	271.0	291.0	1	0.87	0.10	0.03	0.87	0.00
VscGB01B	C	75.0	25.0	-57.0		7.7	17.6	252.5	268.2	5	0.97	0.10	0.00	0.88	0.02
Vsc345A	A	90.0	0.0		-1.2			388.9	396.0	2	0.91	n/d	n/d	0.99	0.01
Vsc346 A	C, A	4.0	96.0	-57.3		7.6	20.1		253.2	5	0.77	0.91	0.05	0.01	0.04
Vsc352 A	Ch, A	80.0	20.0	-58.4		6.9			329.4	6	1.00	0.08	0.01	0.90	0.02
Active 265	A	61.0	37.0		-0.8			307.7	303.1	3	0.89	0.30	n/d	0.73	0.02
Active 265	Ch	43.7	55.9	-61.2	-5.5	13.2	-7.1	270.2	324.5	4	0.81	0.29	0.10	0.60	0.02

Table 3.2 Fluid Inclusion Data Summary for Locale: ACTIVE #265

Sample	Type	V%H2O	V%Carb	TmCarb	TmIce	TmClath	ThCarb	Td	Th	NaCl	Density	XCO2	XCH4	XH2O	XNaCl
Vsc265	Chp2	7.0	93.0	-59.6		13.7	9.7			3	0.67	0.69	0.14	0.15	0.02
	Cx	0.0	100.0	-61.8			-30.1			3	0.72	0.76	0.28	0.00	0.02
	Ch	80.0	20.0							3	0.97	0.07	0.00	0.91	0.01
	Chp2	25.0	75.0							3	0.85	0.49	0.03	0.47	0.02
	Ch	40.0	60.0	-63.5			-12.9			3	0.65	0.15	0.11	0.73	0.01
	Ch	20.0	80.0	-62.1			-6.5			3	0.53	0.29	0.19	0.51	0.01
Vsc265	Ch	65.0	35.0	-60.7		>10.0	6.3	253.2		3	0.82	0.08	0.03	0.88	0.01
	Ch	85.0	15.0		-10.3			278.3		14	1.04	0.05	0.00	0.90	0.05
	Ch	80.0	20.0	-61.2		>10.0	-2.4		365.1	3	0.93	0.05	0.02	0.92	0.01
	Ch	38.0	62.0	-60.2		>10.0	-0.6	232.4		3	0.83	0.29	0.07	0.63	0.01
	Ch	55.0	45.0	-60.9		>10.0	-3.5	247.6		3	0.86	0.16	0.05	0.78	0.01
	Ch	60.0	40.0	-61.5		>10.0	-7.6	271.0		3	0.88	0.13	0.05	0.81	0.01
	Ch	65.0	35.0	-60.6		>10.0		325.0	325.0	3	0.91	0.13	0.03	0.83	0.01
	Ch	85.0	15.0		-4.4			324.8		7	1.00	0.05	0.00	0.93	0.02
	Ch	65.0	35.0	-60.0		13.7	-3.5		370.4	3	0.93	0.13	0.03	0.83	0.01
	Ch	70.0	30.0	-60.5		14.2	2.7		361.0	3	0.90	0.09	0.03	0.87	0.01
	Cx	1.0	99.0	-62.3		14.3	-23.6		264.7	3	0.69	0.71	0.31	0.00	0.02
	Ch	10.0	90.0	-61.8			-27.1	248.3		3	0.79	0.58	0.22	0.18	0.02
	Ch	10.0	90.0	-61.4		12.4	-20.1			3	0.77	0.59	0.21	0.19	0.02
	Chp2	20.0	80.0	-61.3		13.0	-1.6	261.5		3	0.55	0.32	0.16	0.50	0.01
	Chp2	98.0	2.0		-3.8			259.4	255.5	6	1.03	0.01	n/d	0.97	0.02
	Chp2	85.0	5.0		-3.4				317.0	6	0.92	0.02	n/d	0.96	0.02
	Ch	17.0	83.0	-60.2		11.3	7.1		337.0	3	0.67	0.47	0.12	0.39	0.02
	Ch	20.0	80.0							3	0.79	0.46	0.15	0.38	0.02
	Ch	16.0	84.0	-61.8			-28.6			3	0.83	0.51	0.19	0.29	0.02
	Ch	30.0	70.0	-62.1			-21.8			3	0.80	0.32	0.14	0.52	0.01
	Ch	12.0	88.0	-60.6			9.0			3	0.51	0.47	0.17	0.35	0.02
	Ch	65.0	35.0	-61.0			12.1			3	0.79	0.06	0.03	0.89	0.01
Vsc265	Ap2	95.0	0.0		-3.2				150.9	5	0.98	n/d	n/d	0.98	0.02
	A	95.0	0.0		-9.4				136.3	13	1.04	n/d	n/d	0.96	0.04
	A/Chp2	85.0	2.0			11.0			213.3	3	0.88	0.01	n/d	0.98	0.01
	A	90.0	0.0		-7.7				204.3	11	0.97	n/d	n/d	0.96	0.04
	A	85.0	0.0		-7.4			264.0		11	0.92	n/d	n/d	0.96	0.04

Table 3.2 Continued **Fluid Inclusion Data Summary for Locale: Billings Creek-Mnt Waldie**

Sample	TYPE	V% H2O	V% Carb	TmCarb	TmIce	TmClath	ThCarb	Td	Th	NaCl	DENSITY	XCO2	XCH4	XH2O	XNaCl
Vsc042	C	80.0	20.0	-57.6		-6.2	5.8	225.0		20	1.08	.08	n/d	.84	.08
Quartz	Ch	65.0	35.0	-57.9		-4.7	9.2	225.0		20	1.02	.15	.01	.75	.09
Vein	Ch	75.0	25.0	-58.1	-5.0		14.5	225.0		21	1.04	.09	.01	.82	.08
	C	85.0	15.0	-57.6		-2.9	15.4			18	1.07	.05	n/d	.88	.07
	Ch	85.0	15.0	-58.5	-5.0	-3.6	11.4			25	1.11	.05	.01	.85	.10
	As	95.0	.0		-22.4				307.0	24	1.12	n/d	n/d	.91	.09
	As	90.0	.0		-21.9				291.0	24	1.06	n/d	n/d	.91	.09
	As	95.0	.0		-23.3				284.0	24	1.12	n/d	n/d	.91	.09
	As	95.0	.0		-19.7				253.0	25	1.13	n/d	n/d	.91	.09
Vsc042	Ch	85.0	15.0	-58.7		-5.0	14.2	268.0		19	1.07	.04	.01	.88	.07
	Ch	80.0	20.0	-59.5			14.7			19	1.02	.05	.01	.87	.07
	Ch	70.0	30.0	-58.2			18.4			19	.98	.10	.01	.82	.08
	Ch	75.0	25.0	-58.9			5.0			19	1.04	.09	.01	.82	.08
	As	95.0	.0		-20.3				236.0	23	1.11	n/d	n/d	.92	.08
	As	95.0	.0		-19.4				214.0	22	1.11	n/d	n/d	.92	.08
illings Cr	Cxp2	.0	100.0	-59.4			-16.0			n/d	.89	.86	.14	n/d	n/d
Vsc094A	Cxp2	.0	100.0	-59.1			-10.0			n/d	.86	.87	.13	n/d	n/d
	Cxp2	.0	100.0	-58.7			-6.5			n/d	.71	.89	.11	n/d	n/d
Quartz	Chp2	5.0	95.0	-60.2			-5.8			n/d	.78	.71	.16	.13	n/d
Vein	Chp2	3.0	97.0	-58.7			1.2			n/d	.83	.83	.09	.08	n/d
	Cxp2	.0	100.0	-58.8			6.0			n/d	.77	.88	.12	n/d	n/d
	Cxp2	.0	100.0	-58.8			5.2			n/d	.79	.88	.12	n/d	n/d
	Cxp2	.0	100.0	-58.4			1.4			n/d	.83	.90	.10	n/d	n/d
	Cxp2	.0	100.0	-58.4			-1.4			n/d	.85	.90	.10	n/d	n/d
	Cxp2	.0	100.0	-58.6			-3.1			n/d	.84	.90	.10	n/d	n/d
	Cxp2	.0	100.0	-59.1			7.8			n/d	.72	.86	.14	n/d	n/d
Vsc094B	Ch	5.0	78.0	-59.5			-10.5	229.0		n/d	.84	.75	.13	.12	n/d
	Ch	20.0	75.0	-61.2			-12.2	231.0		n/d	.79	.44	.14	.41	n/d
	Ch	80.0	17.0	-64.7		5.8	-30.6	303.0		8	.97	.05	.03	.89	.03
	Ch	77.0	20.0	-63.2		8.3	-12.1	266.0		4	.89	.04	.03	.92	.01
	Cx	.0	100.0	-60.3			4.3			n/d	.71	.79	.21	n/d	n/d
	Cx	.0	100.0	-62.3			-7.8			n/d	.65	.67	.33	n/d	n/d
	Ch	13.0	64.0	-61.1			-25.3	261.0		5	.82	.58	.17	.21	.03
	As	87.0	.0		-10.6				301.0	15	.97	.00	.00	.95	.05

Table 3.2 Continued. **Fluid Inclusion Data Summary for Locale: GOLDBELT YELL MOM**

Sample#	TYPE	V%H2O	V%CO2	TmCarb	TmIce	TmClath	ThCarb	Td	Th	% NaCl	Density	XCO2	XCH4	XH2O	XNaCl
9Ys3-2	A2s	93	0		-4.8				174.0	8	0.98	n/d	n/d	0.97	0.03
	A2	95	0		-2.5					4	0.98	n/d	n/d	0.99	0.01
	A2	90	0		-3.3				267.0	5	0.93	n/d	n/d	0.98	0.02
	A	90	0		-3.3				314.7	5	0.93	n/d	n/d	0.98	0.02
Vsc022	C	70	30	-55.8		7.3	23.1		303.0	5	0.94	0.11	n/d	0.87	0.02
	C	80	20	-55.9		8.3	24.4	320.0		3	0.96	0.07	n/d	0.92	0.01
	C	80	20	-56.0		7.4	24.0	317.0		5	0.97	0.07	n/d	0.91	0.02
	C	75	25	-56.2		8.3	24.8		311.0	3	0.94	0.09	n/d	0.90	0.01
	C	50	50	-56.4		6.7	26.5			7	0.83	0.21	n/d	0.79	n/d
	C	65	35	-56.4		6.6	24.7			7	0.90	0.13	n/d	0.87	n/d
VscGb01A	Ch	60	40	-59.4		8.8	9.9	243.0		2	0.87	0.14	0.03	0.83	0.01
	Ch	80	20	-59.6		9.3	10.3	294.0	291.0	2	0.94	0.06	0.01	0.92	0.01
	Ch	42	58	-60.4			4.3		299.6	2	0.79	0.23	0.06	0.70	0.01
	Ch	75	25	-61.2			5.7	283.0		2	0.86	0.05	0.02	0.93	0.01
	Ch	75	25	-59.4		9.3	6.6			1	0.93	0.08	0.01	0.90	n/d
	A2	90	0		-0.4				271.0	1	0.90	n/d	n/d	1.00	n/d
	A	90	0					264.0		2	0.91	n/d	n/d	0.99	0.01
	A	90	0						302.5	2	0.91	n/d	n/d	0.99	0.01
VscGB01B	C	75	25	-57.0		7.6	22.2	263.0		5	0.96	0.09	n/d	0.89	0.02
	C	80	20	-56.8		7.7	20.0		253.0	5	0.98	0.07	n/d	0.91	0.02
	C	75	25	-56.9		7.8	17.5		289.8	4	0.97	0.10	n/d	0.89	0.01
	C	80	20	-56.6		7.8	15.0		291.9	4	0.98	0.08	n/d	0.91	0.01
	C	65	35	-57.5		7.4	13.3	242.0	238.0	5	0.96	0.15	0.01	0.82	0.02
Vsc345A	A	85	0		-1.3			403.7		2	0.86	n/d	n/d	0.99	0.01
	A	90	0		-0.7			374.0		1	0.90	n/d	n/d	1.00	0.00
	A	95	0		-1.5				396.0	3	0.97	n/d	n/d	0.99	0.01
Vsc346 A	A	90	0		-0.4				223.7	1	0.90	n/d	n/d	1.00	0.00
	C	5	95	-57.2		8.2	21.5		265.0	4	0.76	0.87	0.04	0.06	0.03
	C	7	93	-57.4		6.9	18.7		271.0	4	0.79	0.82	0.04	0.11	0.03
Vsc352 A	Ch	90	10	-58.4		7.2	11.4			5	1.00	0.03	0.00	0.95	0.02
	Ch	70	30	-58.5		6.6				7	0.96	0.12	0.01	0.85	0.03
	A	85	0						329.4		0.88	n/d	n/d	1.00	0.00

TABLE 3.2 Continued. **Fluid Inclusion Data Summary for Locale: Panther Lake-Far East**

Sample	TYPE	V% H2O	V% Carb	TmCO2	TmIce	Tm Clath	ThCO2	Td	Th	%NaCl	Density	XCO2	XCH4	XH2O	XNaCl
Vsc150	As	90.0	2.0		-5.5	6.8		262.0	148.0	7	0.94	n/d	n/d	0.98	0.02
	C	28.0	72.0	-57.4		7.6	16.7	246.0		5	0.86	0.46	0.02	0.49	0.03
	C	70.0	30.0	-57.4		7.4	21.0	260.0		5	0.95	0.12	0.01	0.86	0.02
	C	65.0	35.0	-57.3		7.0	18.3	289.4		6	0.95	0.15	0.01	0.82	0.02
	C	70.0	30.0	-57.3		7.1	18.1	293.4	291.1	6	0.97	0.12	0.01	0.85	0.02
	C	55.0	45.0	-57.3		4.8	17.5	303.0		9	0.94	0.21	0.01	0.74	0.04
	C	45.0	55.0	-57.4		6.9	13.9	289.0		6	0.92	0.29	0.01	0.67	0.03
	C	50.0	50.0	-57.2		7.3	10.5	237.8		5	0.94	0.26	0.01	0.71	0.02
	C	65.0	35.0	-57.3		6.9	13.5	274.0		6	0.96	0.15	0.01	0.82	0.02
Vsc150b	C	63.0	37.0	-57.1		7.7	23.9		299.7	5	0.91	0.15	0.01	0.83	0.02
	C	50.0	50.0	-57.2		7.5	15.5	264.6		5	0.92	0.25	0.01	0.72	0.02
	C	55.0	45.0	-57.4		7.3	8.7	250.7		5	0.96	0.22	0.01	0.74	0.02
	C	60.0	40.0	-57.2		7.4	19.4		303.6	5	0.93	0.17	0.01	0.80	0.02
	C	57.0	43.0	-57.4		8.4	10.1	256.3		3	0.95	0.21	0.01	0.77	0.01
	C	29.0	71.0	-57.1		7.7	24.1	235.6		5	0.81	0.42	0.02	0.54	0.03
	C	35.0	65.0	-57.3		7.5	13.1			5	0.91	0.39	0.02	0.57	0.02
	A	90.0	0.0							5	0.94	n/d	n/d	0.98	0.02
	A	95.0	0.0							5	1.00	n/d	n/d	0.98	0.02
	A	84.0	0.0							5	0.88	n/d	n/d	0.98	0.02
Vsc102	C	50.0	50.0	-56.6		8.6	-5.8	168.0		5	1.00	0.28	n/d	0.69	0.02
	C	40.0	60.0	-57.4		10.3	-8.9		bub 185	5	1.00	0.37	0.02	0.59	0.02
	C	70.0	30.0	-56.6		7.6	-1.5	262.0		5	1.01	0.14	0.00	0.84	0.02
	C	15.0	85.0	-57.7		10.4	-20.5		313.0	5	1.03	0.71	0.04	0.21	0.03
	C	55.0	45.0	-56.7		8.2	-6.9	219.0		5	1.01	0.24	n/d	0.73	0.02
	A	85.0	0.0		-6.8			209.0		10	0.92	n/d	n/d	0.97	0.03
	A	90.0	0.0		-7.6			249.7		11	0.97	n/d	n/d	0.96	0.04
	A	90.0	0.0		-7.7			251.0		11	0.97	n/d	n/d	0.96	0.04
		88.0	0.0						315.0	5	0.92	n/d	n/d	0.98	0.02
Vsc110	C	70.0	30.0	-56.5		7.6	9.3	248.0		5	0.98	0.13	n/d	0.85	0.02
	C	85.0	15.0	-56.2		7.4	11.3	224.0		5	1.00	0.06	n/d	0.93	0.02
	C	60.0	40.0	-56.8		7.6	13.0	220.0		5	0.95	0.19	n/d	0.79	0.02
	C	65.0	35.0	-56.8		7.5	18.5	217.0		5	0.94	0.15	n/d	0.83	0.02
	C	80.0	20.0	-56.9		7.4	21.8	252.0		5	0.97	0.07	n/d	0.91	0.02

TABLE 3.2 Continued. **Fluid Inclusion Data Summary for Locale: Vsc#205** *(p.1)*

Sample	F.I. Type	V% H2O	V% CO2	Tm Carb	TmIce	Tm Clath	Th Carb	Td	Th	% NaCl	Density	XCO2	XCH4	XH2O	XNaCl
Vsc205	As	90.0	0.0		-13.5				207.7	18	1.02	n/d	n/d	0.94	0.06
Euhedral'c'	As	95.0	0.0		-7.9				193.4	12	1.03	n/d	n/d	0.96	0.04
	A2	90.0	0.0		-0.9				156.8	2	0.91	n/d	n/d	0.99	0.01
	As	95.0	0.0		-12.2				306.5	16	1.06	n/d	n/d	0.95	0.05
	A2	90.0	0.0		-1.1				138.2	2	0.91	n/d	n/d	0.99	0.01
	A2	90.0	0.0		-0.4				139.4	1	0.90	n/d	n/d	1.00	0.00
	As	90.0	0.0		-7.9				213.6	12	0.98	n/d	n/d	0.96	0.04
	Ch	65.0	35.0	-62.0		* Critical>	-25.4	346.0		n/d	0.79	0.06	0.04	0.89	n/d
	Ch	20.0	80.0	-62.2		* Critical>	-15.7	373.0		n/d	0.52	0.28	0.20	0.53	n/d
	Ch	25.0	75.0	-62.6		* Critical>	-18.2	450.9		n/d	0.55	0.23	0.17	0.60	n/d
	Ch	50.0	50.0	-61.6			-10.0			n/d	0.86	0.19	0.07	0.74	n/d
	Ch	25.0	75.0	-61.8			-11.4		348.0	n/d	0.69	0.34	0.13	0.53	n/d
	Ch	55.0	45.0	-61.6			-10.0	433.3		n/d	0.87	0.16	0.06	0.77	n/d
Vsc205/A	Ch	70.0	25.0	-60.4					308.6	n/d	0.90	0.10	0.02	0.88	n/d
	A	90.0	0.0		-4.9				271.0	8	0.95	n/d	n/d	0.97	0.03
	A	90.0	0.0		-5.0				266.4	8	0.95	n/d	n/d	0.97	0.03
	As	90.0	0.0		-17.4				267.8	21	1.04	n/d	n/d	0.92	0.08
	As	85.0	0.0		-21.6				277.9	24	1.00	n/d	n/d	0.91	0.09
	A	90.0	0.0					297.7			0.95	n/d	n/d	1.00	0.00
Vsc205/B	As	90.0	0.0		-18.9				331.0	22	1.05	n/d	n/d	0.92	0.08
	As	87.0	0.0		-19.6				314.9	22	1.01	n/d	n/d	0.92	0.08
	As	90.0	0.0		-19.5				261.7	22	1.05	n/d	n/d	0.92	0.08
	A	95.0	0.0		-0.1				309.1	1	0.95	n/d	n/d	1.00	0.00
	Ch	60.0	40.0	-60.5			-2.8	311.1		n/d	0.89	0.15	0.04	0.81	n/d
	Ch	30.0	70.0	-58.2			4.4	386.6		n/d	0.83	0.40	0.04	0.57	n/d
Vsc205/B1	As	90.0	0.0		-22.7				247.0	25	1.07	n/d	n/d	0.91	0.09
	As	90.0	0.0		-23.4				260.0	25	1.07	n/d	n/d	0.91	0.09
	As	90.0	0.0		-23.8				232.8	25	1.07	n/d	n/d	0.91	0.09
	As	95.0	0.0		-15.2				228.0	19	1.08	n/d	n/d	0.93	0.07
	As	75.0	0.0		-7.4			248.8		11	0.81	n/d	n/d	0.96	0.04
	As	85.0	0.0		-23.8				229.0	25	1.01	n/d	n/d	0.91	0.09
	As	80.0	0.0		-5.3				155.8	8	0.84	n/d	n/d	0.97	0.03
Vsc205/C	Cx	0.0	100.0	-59.0			-5.1		283.8	n/d	0.83	0.87	0.13	n/d	n/d
	Cx	0.0	100.0	-59.1			-5.0		239.0	n/d	0.83	0.87	0.13	n/d	n/d
	Cx	0.0	100.0	-59.2			-0.2		203.0	n/d	0.78	0.86	0.14	n/d	n/d
	Cx	0.0	100.0	-59.2			-5.4		261.0	n/d	0.79	0.86	0.14	n/d	n/d
	A	85.0	15.0		-2.0				279.7	3	0.87	n/d	n/d	0.99	0.01

TABLE 3.2 Continued. **Fluid Inclusion Data Summary for Locale: Vsc#205** *(p.2)*

Sample	F.I. Type	V% H2O	V% CO2	Tm Carb	TmIce	Tm Clath	Th Carb	Td	Th	% NaCl	Density	XCO2	XCH4	XH2O	XNaCl
Vsc205/D	Ch	60.0	40.0	-59.8			5.9			n/d	0.87	0.14	0.03	0.83	n/d
	A	85.0	0.0		-4.1					7	0.89	n/d	n/d	0.98	0.02
	A	90.0	0.0		-2.3				246.3	4	0.92	n/d	n/d	0.99	0.01
	A	90.0	0.0		-0.5					1	0.90	n/d	n/d	1.00	0.00
	A	85.0	0.0		-0.4					1	0.85	n/d	n/d	1.00	0.00
Vsc205G/A	Ch	10.0	90.0	-58.8		11.9	13.2	244.0		n/d	0.71	0.64	0.09	0.27	n/d
	Ch	12.0	88.0	-60.7		12.3	5.1	257.0		n/d	0.64	0.51	0.16	0.32	n/d
	Ch	5.0	95.0	-59.8		9.4	8.1			n/d	0.65	0.69	0.15	0.15	n/d
	Ch	7.0	93.0	-58.8			9.0		308.0	n/d	0.73	0.71	0.10	0.19	n/d
	Ch	8.0	92.0	-59.2			9.2			n/d	0.71	0.68	0.10	0.22	n/d
	Cx	0.0	100.0	-58.8		10.8	13.7			n/d	0.68	0.88	0.12	0.00	n/d
	Ch	3.0	97.0	-59.5			12.9			n/d	0.59	0.74	0.15	0.11	n/d
	Ap2	90.0	0.0		-1.8				259.7	3	0.92	n/d	n/d	0.99	0.01
	Ap2	90.0	0.0		-2.4				258.4	4	0.92	n/d	n/d	0.99	0.01
	A2	95.0	0.0		-1.1				145.7	2	0.96	n/d	n/d	0.99	0.01
Vsc205G/B	Ch	7.0	93.0	-58.9		9.3	5.1		283.0	2.8	0.76	0.74	0.10	0.14	0.02
	Ch	3.0	97.0	-59.3		8.9	6.5		294.0	2.8	0.70	0.81	0.14	0.03	0.02
	Ch	10.0	90.0	-57.9		10.8	15.4		291.0	2.8	0.73	0.70	0.06	0.23	0.02
	Ch	5.0	95.0	-57.6			15.2		287.0	2.8	0.73	0.83	0.05	0.09	0.02
	Ch	3.0	97.0	-59.2		10.6	6.0		294.0	2.8	0.71	0.81	0.14	0.03	0.02
	Ch	4.0	96.0	-59.1		8.7	5.2			2.8	0.72	0.79	0.12	0.06	0.02
	Ch	12.0	88.0	-59.2		10.7	5.9	231.0		2.8	0.74	0.62	0.10	0.26	0.02
	Ap2	90.0	0.0		-0.9				310.8	2	0.91	n/d	n/d	0.99	0.01
	A	90.0	0.0		-1.4				301.0	2	0.91	n/d	n/d	0.99	0.01
	A	95.0	0.0						293.0	3	0.97	n/d	n/d	0.99	0.01
	A	93.0	0.0		-2.3				278.0	4	0.96	n/d	n/d	0.99	0.01
	A	90.0	0.0		-2.7				274.0	5	0.93	n/d	n/d	0.98	0.02
	A	89.0	0.0		-2.1					4	0.91	n/d	n/d	0.99	0.01
/sc205/Eu/2	Cx	0.0	100.0	-86.2			-129.1								
	Cx	0.0	100.0	-86.2			-129.1								

TABLE 3.2 Continued. **Fluid Inclusion Data Summary for Locale: Reno Peripheral** *(p.1)*

Sample	Type	V% H2O	V% Carb	Tm Carb	TmIce	Tm Clath	Th Carb	Td	Th	% NaCl	Density	XCO2	XCH4	XH2O	XNaCl
Vsc113	Cx	0.0	100.0	-60.6			-7.7			n/d	0.70	0.79	0.21	n/d	n/d
	Ch-Cx	2.0	98.0	-61.1		9.7	2.9			n/d	0.68	0.69	0.25	0.06	n/d
	Cx	0.0	100.0	-61.1			4.4			n/d	0.67	0.73	0.27	n/d	n/d
	Cx	0.0	100.0	-59.7			5.6			n/d	0.66	0.83	0.17	n/d	n/d
Calhoun	Ch-Cx	3.0	100.0	-61.0		10.7	6.4			n/d	0.53	0.65	0.24	0.11	n/d
	Cx	0.0	100.0	-61.2			0.8			n/d	0.58	0.73	0.27	n/d	n/d
	Ch	10.0	90.0	-60.3			1.7		294.0	n/d	0.72	0.59	0.15	0.26	n/d
	A	90.0	0.0		-1.7				247.3	3	0.92	n/d	n/d	0.99	0.01
	A	95.0	0.0		-2.4				285.7	4	0.98	n/d	n/d	0.99	0.01
	A	95.0	0.0		-0.9				292.8	2	0.96	n/d	n/d	0.99	0.01
Vsc128/A	A	85.0	0.0						347.5	3	0.87	n/d	n/d	0.99	0.01
	A	80.0	0.0						337.0	3	0.81	n/d	n/d	0.99	0.01
	A	90.0	0.0						335.0	3	0.92	n/d	n/d	0.99	0.01
	A	85.0	0.0						334.0	3	0.87	n/d	n/d	0.99	0.01
	A	95.0	0.0						352.0	3	0.97	n/d	n/d	0.99	0.01
Vsc128/B	A	90.0	0.0						383+	3	0.92	n/d	n/d	0.99	0.01
	A	85.0	0.0					276.0		3	0.87	n/d	n/d	0.99	0.01
	A	90.0	0.0					259.0		3	0.92	n/d	n/d	0.99	0.01
	A	90.0	0.0						383+	3	0.92	n/d	n/d	0.99	0.01
Vsc128/C	Cx	0.0	100.0	-62.6			-36.8				0.76	0.67	0.33	0.00	0.00
	Cx	0.0	100.0	-61.4			-22.0				0.78	0.75	0.25	0.00	0.00
	As	95.0	0.0		-16.3					20	1.09	n/d	n/d	0.93	0.07
	A	95.0	0.0												
Vsc128D	Cx	0.0	100.0	-63.3			-21.5		274.4	n/d	0.62	0.65	0.35	n/d	n/d
	As	90.0	0.0		-22.1				255.4	24	1.06	n/d	n/d	0.91	0.09
	As	90.0	0.0		-21.4				301.3	24	1.06	n/d	n/d	0.91	0.09
	As	90.0	0.0		-22.3				187.0	24	1.06	n/d	n/d	0.91	0.09
	As	95.0	0.0		-22.6			299.7	286.3	24	1.12	n/d	n/d	0.91	0.09
	As	90.0	0.0		-22.6				179.4	24	1.06	n/d	n/d	0.91	0.09
	As	96.0	0.0		-16.2				190.8	20	1.10	n/d	n/d	0.93	0.07
	As	85.0	0.0		-15.6				211.0	20	0.97	n/d	n/d	0.93	0.07
	As	95.0	0.0						321.6	20	1.08	n/d	n/d	0.93	0.07
Vsc129	Ch	20.0	80.0	-58.3			11.7		311.1	n/d	0.78	0.50	0.06	0.44	n/d
	Ch	30.0	70.0	-59.8			7.3	303.6		n/d	0.74	0.33	0.07	0.59	n/d
	Ch	10.0	90.0	-60.2			5.6	336.0	331.3	n/d	0.66	0.58	0.15	0.28	n/d
	Ch	15.0	85.0	-58.8			8.1	327.0	324.0	n/d	0.75	0.56	0.08	0.36	n/d
	Ch	25.0	75.0	-58.3			8.1	249.0		n/d	0.81	0.44	0.05	0.50	n/d
	Ch	15.0	85.0	-59.6			11.3	264.0		n/d	0.66	0.50	0.11	0.39	n/d
	A	90.0	0.0		-1.4					2	0.91	n/d	n/d	0.99	0.01

TABLE 3.2 Continued. **Fluid Inclusion Data Summary for Locale: Reno Peripheral** *(p.2)*

Sample	Type	V% H2O	V% Carb	Tm Carb	TmIce	Tm Clath	Th Carb	Td	Th	% NaCl	Density	XCO2	XCH4	XH2O	XNaCl
Vsc127	Cxp2	0.0	100.0	-64.3			-24.0			n/d	0.59	0.62	0.38	n/d	n/d
	Cx2	0.0	100.0	-64.4			-19.4			n/d	0.47	0.58	0.42	n/d	n/d
	Cx2	0.0	100.0	-63.6			-15.9			n/d	0.49	0.60	0.40	n/d	n/d
	Cxp2	0.0	100.0	-63.4			-16.0			n/d	0.48	0.60	0.40	n/d	n/d
	Cxp2	0.0	100.0	-63.6			-18.4			n/d	0.53	0.62	0.38	n/d	n/d
	Cxp2	0.0	100.0	-63.3			-13.6			n/d	0.46	0.61	0.39	n/d	n/d
	Cxp2	0.0	100.0	-63.2			-17.3			n/d	0.53	0.63	0.37	n/d	n/d
	Cxp2	0.0	100.0	-63.5			-21.0			n/d	0.57	0.63	0.37	n/d	n/d
	A	93.0	0.0		-0.8	10.8			316.0	1	0.93	n/d	n/d	1.00	0.00
	A	95.0	0.0		-5.3			294.0	287.0	8	1.00	n/d	n/d	0.97	0.03
	A	91.0	0.0						321.7	4	0.93	n/d	n/d	0.99	0.01
	A	88.0	0.0						309.0	4	0.90	n/d	n/d	0.99	0.01
Vsc130	Cx	0.0	100.0	-66.6			-48.8			n/d	0.70	0.55	0.45	n/d	n/d
	Cx	0.0	100.0	-65.1			-37.6			n/d	0.76	0.61	0.39	n/d	n/d
	Ch	30.0	70.0	-58.9		9.6	-0.5			n/d	0.85	0.39	0.06	0.55	n/d
	Ch	40.0	60.0	-60.4		10.9	-6.2		313.7	n/d	0.81	0.26	0.06	0.68	n/d
	Cx	0.0	100.0	-66.0			-50.7			n/d	0.73	0.56	0.44	0.00	n/d
	Cx	0.0	100.0	-66.3			-49.4			n/d	0.73	0.56	0.44	0.00	n/d
	Ch	35.0	65.0	-62.2		10.1	-20.5	295.0		n/d	0.83	0.29	0.12	0.59	n/d
	Ch	85.0	15.0	-60.2		9.6	-13.7	349.0		n/d	0.96	0.05	0.01	0.94	n/d
	A	95.0	0.0		-4.7			254.7		7	1.00	n/d	n/d	0.98	0.02
Vsc131	Ch	8.0	92.0	-60.0			-4.5	223.0		n/d	0.76	0.65	0.14	0.20	n/d
	Ch	12.0	88.0	-59.7		12.2	-7.5	217.0		n/d	0.81	0.61	0.12	0.28	n/d
	Ch	11.0	89.0	-59.9			-2.0	264.0		n/d	0.78	0.60	0.13	0.26	n/d
	Ch	5.0	95.0	-59.8			-1.6		344.0	n/d	0.77	0.72	0.15	0.13	n/d
	Ch	85.0	15.0	-61.2		13.1	-1.4	258.0		n/d	0.94	0.04	0.01	0.95	n/d
	Ch	12.0	88.0	-60.3			1.6	220.0		n/d	0.73	0.56	0.14	0.30	n/d
	Ch	90.0	10.0	-60.7			2.8	261.0		n/d	0.96	0.02	0.01	0.97	n/d
	A	95.0	0.0		-3.7				351.6	6					

TABLE 3.2 (continued) **Fluid Inclusion Data Summary for Locale: Hidden Creek Ridge**

Sample	Type	V% H2O	V% Carb	Tm Carb	TmIce	Tm Clath	Th Carb	Td	Th	% NaCl	Density	XCO2	XCH4	XH2O	XNaCl
Vsc188/A	C	63.0	27.0	-56.6		8.0	9.7	287.0		4	0.88	0.13	n/d	0.85	0.01
	C	80.0	20.0	-56.6		8.3	10.6	279.0		3	0.98	0.08	n/d	0.91	0.01
	C	90.0	5.0	-57.1		8.7	11.4	281.0		3	0.96	0.02	n/d	0.97	0.01
	A	83.0	0.0		-2.7				263.0	4	0.85	n/d	n/d	0.99	0.01
	A	86.0	0.0						317.0	3	0.88	n/d	n/d	0.99	0.01
	A	84.0	0.0						254.0	3	0.86	n/d	n/d	0.99	0.01
Vsc188/B	As	95.0	0.0		-5.8				294.2	9	1.01	n/d	n/d	0.97	0.03
	As	75.0	0.0		-10.2			284.0		14	0.83	n/d	n/d	0.95	0.05
	As2	85.0	0.0		-10.3				271.4	14	0.94	n/d	n/d	0.95	0.05
	A	90.0	0.0						265.0	9	0.95	n/d	n/d	0.97	0.03
	Asp2	87.0	0.0		-7.5				188.9	11	0.94	n/d	n/d	0.96	0.04
	A2	95.0	0.0		-4.3				191.4	7	1.00	n/d	n/d	0.98	0.02
	As	85.0	0.0		-4.5				207.7	7	0.89	n/d	n/d	0.98	0.02
	A	90.0	0.0						295.6	5	0.93	n/d	n/d	0.98	0.02
	A	95.0	0.0						313.6	5	0.98	n/d	n/d	0.98	0.02
	C	73.0	27.0	-57.1		8.6	10.7	281.0		3	0.97	0.11	n/d	0.87	0.01
Vsc188/C	As	85.0	0.0		-10.2				260.0	14	0.94	n/d	n/d	0.95	0.05
	C	70.0	30.0	-57.2		8.1	9.3	278.0		4	0.98	0.13	0.01	0.85	0.01
	C	65.0	35.0	-57.3			9.1	278.0		4	0.97	0.16	0.01	0.82	0.02
	C	55.0	45.0	-57.0				278.0		4	0.95	0.23	n/d	0.76	0.02
	C	65.0	35.0	-57.0		8.2	9.0	278.0	276.0	4	0.97	0.16	n/d	0.82	0.02
	C	70.0	30.0	-56.8		8.4	9.1	278.0		3	0.97	0.13	n/d	0.86	0.01
Vsc188/D	A	70.0	0.0		-2.3				272.0	4	0.72	n/d	n/d	0.99	0.01
	A	80.0	0.0		-2.9			262.0	258.0	5	0.83	n/d	n/d	0.98	0.02
	A	75.0	0.0		-2.8				284.0	5	0.77	n/d	n/d	0.98	0.02
	A	85.0	0.0		-1.9				273.0	3	0.87	n/d	n/d	0.99	0.01
	A	85.0	0.0		-2.6				267.0	4	0.87	n/d	n/d	0.99	0.01
Vsc179	Chp2	83.0	17.0	-58.1		8.8	2.6	262.5		3	1.01	0.07	0.01	0.92	0.01
	Chp2	2.0	98.0	-58.5			7.5			n/d	0.87	0.86	0.09	0.05	n/d
	Chp2	8.0	92.0	-58.8		10.1	-4.0	260.0		n/d	0.94	0.74	0.09	0.17	n/d
	Chp2	2.0	98.0	-58.5			-2.2			n/d	0.94	0.86	0.09	0.05	n/d
	Chp2	10.0	90.0	-58.0		10.3	2.6	230.7		n/d	0.92	0.72	0.06	0.22	n/d
	Chp2	7.0	93.0	-58.2			-1.1	228.8		n/d	0.93	0.77	0.07	0.16	n/d
	Chp2	12.0	88.0	-58.9		9.9	2.3	241.3		1	0.92	0.66	0.09	0.25	n/d
	Asp2	87.0	0.0		-11.4			325.6	302.8	15	0.97	n/d	n/d	0.95	0.05
	As	91.0	0.0		-9.3				283.7	13	1.00	n/d	n/d	0.96	0.04
	As	90.0	0.0		-8.6			256.0		12	0.98	n/d	n/d	0.96	0.04

TABLE 3.2 (continued) **Fluid Inclusion Data Summary for Locale: Hidden Creek Ridge** *(p.2)*

Sample	Type	V% H2O	V% Carb	Tm Carb	TmIce	Tm Clath	Th Carb	Td	Th	% NaCl	Density	XCO2	XCH4	XH2O	XNaCl
Vsc179/B	Ch	7.0	93.0	-60.2			-2.5			n/d	0.94	0.69	0.16	0.15	n/d
	Ch	21.0	79.0	-59.1			4.5	243.8		n/d	0.91	0.52	0.07	0.40	n/d
	Ch	13.0	87.0	-59.4		9.2	6.1		327.3	2	0.85	0.70	0.12	0.17	0.01
	Ch	3.0	97.0	-59.8			5.1	272.6		2	0.88	0.80	0.16	0.03	0.01
	Ch	3.0	97.0	-59.5			-6.1			n/d	0.96	0.80	0.13	0.07	n/d
	Ch	0.0	100.0	-60.9			-9.2	338.0		n/d	0.97	0.79	0.21	0.00	n/d
	A	87.0	0.0		-0.7			284.8		1	0.87	n/d	n/d	1.00	0.01
	A	87.0	2.0		-0.3					1	0.87	n/d	n/d	1.00	0.01
Vsc 383	C	65.0	35.0	-57.3		7.7	19.2			5	0.94	0.14	0.01	0.83	0.02
	C	70.0	30.0	-56.7		7.5	24.0			5	0.95	0.12	n/d	0.86	0.02
	C	68.0	32.0	-56.8		7.5	23.1			5	0.93	0.12	n/d	0.86	0.02
	C	60.0	40.0	-56.8		7.9	25.8			4	0.91	0.17	n/d	0.82	0.02
	C	22.0	78.0	-57.0			18.6			n/d	0.83	0.52	0.02	0.47	0.00
	C	73.0	27.0	-56.6		7.6	26.2			5	0.93	0.09	n/d	0.89	0.02
	A	95.0	0.0		-2.6					4	0.98	0.00	n/d	0.99	0.01
	A	85.0	0.0							n/d	0.85	0.00	n/d	1.00	0.00
Vsc 383/B	C	50.0	50.0	-56.8		8.2	18.8	260.9		4	0.90	0.24	n/d	0.74	0.02
	C	68.0	32.0	-56.9		7.4	18.6	317.9		5	0.95	0.13	n/d	0.85	0.02
	C	74.0	26.0	-56.7		8.3	20.7	259.7		4	0.96	0.10	n/d	0.89	0.01
	C	65.0	35.0	-57.6		9.7	15.7	269.0		1	0.93	0.15	0.01	0.84	0.00
	C	83.0	17.0	-56.2			20.4		303.4	1	0.96	0.06	n/d	0.94	0.00
	C	67.0	33.0	-56.8		8.1	18.3		299.7	4	0.95	0.14	n/d	0.85	0.02
	A	90.0	0.0		-0.7				312.4	1	0.90	n/d	n/d	1.00	0.00
	A	90.0	0.0		-1.3				316.2	2	0.91	n/d	n/d	0.99	0.01
	A	85.0	0.0		-1.1			241.0		2	0.86	n/d	n/d	0.99	0.01
Vsc356 A	Cx	0.0	100.0	-62.8			-30.1			n/d	0.75	0.69	0.31	n/d	n/d
	Cx	0.0	100.0	-63.0			-31.0			n/d	0.75	0.69	0.31	n/d	n/d
	Cx	0.0	100.0	-62.9			-30.7			n/d	0.75	0.69	0.31	n/d	n/d
	Cx	0.0	100.0	-62.7			-38.6			n/d	0.76	0.70	0.30	n/d	n/d
	Cx	0.0	100.0	-63.2			-32.7			n/d	0.75	0.69	0.31	n/d	n/d
Vsc357/ A	As	90.0	0.0		-7.5			252.6	245.7	11	0.97	n/d	n/d	0.96	0.04
p28	As	95.0	0.0		-6.7				187.2	10	1.02	n/d	n/d	0.97	0.03
	As	90.0	0.0		-6.3					10	0.96	n/d	n/d	0.97	0.03
Vsc356 B	Cx		0.0	Th (y) =-70.9 ; Th (x) = 145											

TABLE 3.2 (continued) **Fluid Inclusion Data Summary for Locale: Reno East-Donnybrook**

Sample	TYPE	V% H2O	V% C02	Tm Carb	TmIce	Tm Clath	Th Carb	Td	Th	%NaCl	Density	XCO2	XCH4	XH2O	XNaCl
Vsc366 A	C	85.0	15.0	-57.2		7.9	17.1		383.3	4	0.99	0.05	n/d	0.93	0.01
	C	30.0	70.0	-56.9		7.7	3.0	332.0		5	0.94	0.47	0.01	0.49	0.03
	C	65.0	35.0	-56.9		8.0	16.1	338.0		4	0.95	0.15	n/d	0.83	0.02
	C	14.0	86.0	-56.6		9.0	15.9	314.0		2	0.83	0.68	0.01	0.30	0.01
	C	50.0	50.0	-56.7		7.9	13.0	327.0		4	0.93	0.26	n/d	0.72	0.02
	C	75.0	25.0	-56.5			19.5		350.0	n/d	0.94	0.10	n/d	0.90	n/d
	As	80.0			-11.9				340.2	16	0.89	n/d	n/d	0.95	0.05
Vsc361 A	C	80.0	20.0	-56.7		8.5	21.4	294.0		3	0.96	0.07	n/d	0.92	0.01
	C	90.0	10.0		-4.0			298.0		6	0.94	0.00	n/d	0.98	0.02
	C	90.0	10.0	-56.3		8.1		317.0		4	0.92	0.00	n/d	0.99	0.01
	A2	95.0			-3.1				192.0	5	0.98	0.00	n/d	0.98	0.02
Vsc364 A	Ch	18.0	82.0	-61.8	-3.2	14.4	-7.1		295.0	5	0.59	0.39	0.17	0.42	0.02
	Ch	7.0	93.0	-61.5		14.6	-6.9	317.0		n/d	0.54	0.55	0.23	0.23	n/d
	Ch	2.0	98.0	-63.7		15.9	-18.4	293.0		n/d	0.55	0.59	0.34	0.07	n/d
	Ch	3.0	97.0	-64.2		15.2	-19.5	296.0		n/d	0.54	0.57	0.33	0.10	n/d
	Ch	65.0	35.0	-63.6		15.3	-12.8	325.0		n/d	0.83	0.08	0.05	0.87	n/d
Vsc368 A	C	65.0	35.0	-57.0		14.3	21.9	317.0		n/d	0.91	0.14	0.01	0.86	n/d
	C	75.0	25.0	-57.9			17.0			n/d	0.95	0.09	0.01	0.90	n/d
	C	55.0	45.0	-56.7		8.5	19.8			3	0.90	0.20	0.00	0.78	0.01
	C	70.0	30.0			8.6			347.8	3	0.71	n/d	n/d	0.99	0.01
	C	85.0	15.0			7.9			294.5	4	0.87	n/d	n/d	0.99	0.01
	A	90.0							312.5	n/d	0.90	n/d	n/d	1.00	n/d
	A	95.0							334.0	n/d	0.95	n/d	n/d	1.00	n/d
Vsc364	Chp2	40.0	60.0	-58.2		13.4	2.1	307.0		n/d	0.86	0.30	0.03	0.67	n/d
	Cxp2	0.0	100.0	-58.4			-8.5			n/d	0.85	0.91	0.09	0.00	n/d
	Chp2	30.0	70.0	-58.7			-6.4			n/d	0.88	0.41	0.05	0.54	n/d
	Cxp2	0.0	100.0	-59.3			-11.8			n/d	0.82	0.86	0.14	n/d	n/d
	A	90.0						326.0		n/d	0.90	n/d	n/d	1.00	0.00
Vsc372	C	60.0	40.0	-56.0		8.7	7.2		325.4	3	0.96	0.19	n/d	0.79	0.01
	C	85.0	15.0	-56.9		8.8	10.2		334.0	3	0.99	0.06	n/d	0.93	0.01
	C	80.0	20.0	-57.1			10.9			n/d	0.97	0.08	n/d	0.92	0.00
	C	75.0	25.0	-57.6		8.4		290.0		3	0.97	0.10	n/d	0.89	0.01
	C	70.0	30.0	-56.3			21.5		286.0	n/d	0.92	0.12	n/d	0.88	0.00
	C	90.0	10.0	-56.4		8.3				3	0.92	0.00	n/d	0.99	0.01
	A	93.0			-0.2					1	0.93	0.00	n/d	1.00	0.00
Vsc367 A	Ch ?	60.0	40.0	-59.7		14.8	-21.5			n/d	0.95	0.17	0.04	0.79	0.00
	A	95.0			-3.5					6	0.97	n/d	n/d	0.98	0.02
	Ch ?	33.0	67.0	-60.6			-25.0			n/d	0.88	0.34	0.10	0.56	0.00

TABLE 3.2 Continued. **Fluid Inclusion Data Summary for Locale: STAG LEAP +** *(p.1)*

Sample	F.I. Type	V% H2O	V% Carb	TmCarb	TmIce	TmClath	ThCarb	Td	Th	% Na Cl	Density	XCO2	XCH4	XH2O	XNaCl
R.B. 121	Cx	0	100	-56.9			20.3			n/d	0.76	0.97	0.03	n/d	n/d
	Cx	0	100	-56.8			21.7			n/d	0.74	0.98	0.02	n/d	n/d
	C2	80	20			7.5				5	0.83	n/d	n/d	0.98	0.02
	C2	60	40	-56.7		7.3	27.5			5	0.88	0.15	n/d	0.83	0.02
	C2	60	40	-56.7		6.9	25.5			6	0.90	0.16	n/d	0.81	0.02
	C2	85	15		-9.9	4.9				9	0.90	n/d	n/d	0.97	0.03
	C	80	20	-57.2		9.3	21.5			2	0.96	0.07	n/d	0.92	0.01
	Ap2	90	0		-3.4					6	0.94	n/d	n/d	0.98	0.02
R.B.121 B	A	75	0		-3.0			332.0	249.0	5	0.77	n/d	n/d	0.98	0.02
	A	85	0		-3.4				244.6	6	0.88	n/d	n/d	0.98	0.02
	A	80	0		-3.7				245.9	6	0.83	n/d	n/d	0.98	0.02
	C	75	25	-57.0		9.1	20.5		271.0	2	0.95	0.09	n/d	0.90	0.01
R.B.121 C	A	95	0		-2.8				288.7	5	0.98	n/d	n/d	0.98	0.02
	C	5	83	-56.8		8.1	19.5		401.7	4	0.69	0.87	0.02	0.08	0.03
	C	87	13	-57.5		8.1			301.8	4	0.89	n/d	n/d	0.99	0.01
	Ch	63	37	-57.8		7.9	21.0		343.2	4	0.93	0.15	0.01	0.82	0.02
	C	80	20	-57.5		8.4			281.1	3	0.81	n/d	n/d	0.99	0.01
	C	70	30	-57.6		8.5	21.0		325.0	3	0.94	0.11	0.01	0.87	0.01
	C	45	55	-57.8		8.2	19.4		422.0	4	0.89	0.27	0.02	0.69	0.02
	C	45	55	-57.4			19.8		321.6	n/d	0.87	0.27	0.01	0.72	0.00
	Ch	28	72	-57.7		8.3	22.1		330.9	3	0.82	0.43	0.03	0.53	0.02
	Ch	10	90	-58.5		8.7	17.0		339.6	3	0.82	0.71	0.07	0.20	0.02
Vsc224	C	60	40	-56.7		8.6	19.7		234.0	3	0.92	0.17	n/d	0.81	0.01
	C	55	45	-57.1		8.2	24.7			4	0.88	0.19	0.01	0.79	0.02
	C	50	50	-56.8		9.1	-3.2			2	0.98	0.28	n/d	0.71	0.01
	C	65	35	-56.7		8.4	3.3	200.0		3	0.98	0.17	n/d	0.82	0.01
	C	65	35	-56.8		9.0	-3.9			2	0.99	0.17	n/d	0.82	0.01
	C	80	20	-56.8		8.7	-0.7		254.7	3	1.00	0.09	n/d	0.90	0.01
	C	60	40	-56.7		8.9	-0.4			2	0.98	0.20	n/d	0.79	0.01
	A	97	0		-4.9				222.0	8	1.03	n/d	n/d	0.97	0.03

TABLE 3.2 Continued. **Fluid Inclusion Data Summary for Locale: STAG LEAP +** *(p.2)*

Sample	F.I. Type	V% H2O	V % Carb	TmCarb	TmIce	TmClath	ThCarb	Td	Th	% Na Cl	Density	XCO2	XCH4	XH2O	XNaCl
Vsc234	C	75	25	-56.6	-6.8	8.3	21.8		204.1	3	0.95	0.09	n/d	0.90	0.01
	C	75	25	-56.5	-6.7	8.3	22.7		206.0	3	0.95	0.09	n/d	0.90	0.01
	Ch	70	30	-58.4		10.6	2.4	335.8	334.4	0	0.97	0.13	0.01	0.85	0.00
	C	65	35	-57.3		7.4	12.7		225.0	5	0.96	0.15	0.01	0.82	0.02
Vsc228 A	As	75	0		-5.7				299.9	9	0.80	n/d	n/d	0.97	0.03
	As	80	0		-5.8				259.5	9	0.85	n/d	n/d	0.97	0.03
	As	85	0		-6.1				280.3	9	0.90	n/d	n/d	0.97	0.03
	As	95	0		-4.9				247.0	8	1.00	n/d	n/d	0.97	0.03
	As	90	0		-5.3				258.0	8	0.95	n/d	n/d	0.97	0.03
	As	75	0		-5.7				347.0	9	0.80	n/d	n/d	0.97	0.03
Vsc228 B	Ap2	70	0		-4.8					8	0.74	n/d	n/d	0.97	0.03
	Ap2	90	0		-4.2				260.0	7	0.94	n/d	n/d	0.98	0.02
	Ap2	60	0		-4.3				300.5	7	0.63	n/d	n/d	0.98	0.02
	Ap2	85	0		-4.7				270.4	7	0.89	n/d	n/d	0.98	0.02
	Asp2	95	0		-5.6				216.6	9	1.01	n/d	n/d	0.97	0.03
	Asp2	90	0		-5.2				300.2	8	0.95	n/d	n/d	0.97	0.03
	Asp2	65	0		-5.3				292.4	8	0.69	n/d	n/d	0.97	0.03
	Ap2	75	0		-4.4				289.6	7	0.79	n/d	n/d	0.98	0.02
	A	85	0						274.0	7	0.89	n/d	n/d	0.98	0.02
	A	90	0						270.2	7	0.94	n/d	n/d	0.98	0.02
	A	87	0						299.9	7	0.91	n/d	n/d	0.98	0.02
Rb123a	C	80	20	-57.5		8.0	-5.6	270.0		4	0.98	0.07	n/d	0.91	0.01
	C	70	30	-57.5		5.6	9.3	245.0		8	0.97	0.12	0.01	0.84	0.03
	C	50	50	-57.6		7.3	16.7	270.0		5	0.90	0.24	0.01	0.73	0.02
	C	40	60	-57.8		8.0	0.0	275.0		4	0.87	0.32	0.02	0.64	0.02
	C	60	40	-57.6		6.0	-1.7	251.0		8	0.94	0.17	0.01	0.78	0.03
	C	60	40			7.0		262.2		6	0.93	0.17	0.01	0.79	0.02
Rb123b	Ch	70	30	-61.8			0.0	279.0		7	0.91	0.08	0.03	0.86	0.02
	C	95	5	*-58		4.0	22.1		199.0	11	1.06	0.01	n/d	0.95	0.04
	C	90	10	*-58		5.2	9.0		175.0	9	1.04	0.03	n/d	0.93	0.03
	Ch	60	40	-58.4		3.7	3.9	230.0		11	0.96	0.17	0.02	0.76	0.05
	Ch	79	21			4.3		254.5		10	1.01	0.07	0.01	0.88	0.04

CHAPTER IV

STABLE ISOTOPE RESEARCH

INTRODUCTION:

Light stable isotope research has and is continuing to contribute much to the broad science of petrology and fluid-rock interaction. The expansion of the number of isotope research facilities and consequently the available data pool has allowed for the present breadth of application to geological problems and the level of understanding necessary to interpret this flood of isotope data. Variations in isotope ratios of oxygen, carbon, sulfur and hydrogen aid considerably in understanding certain aspects of hydrothermal processes, serve to define temperatures and mechanisms of mineral formation as well as the provenance or state of origin of the minerals, fluids and rocks. Oxygen, carbon and hydrogen isotopic signatures of the sample suite from the Sheep Creek Camp have contributed much to the understanding of the genesis and post-depositional nature of the vein system.

The sensitivity of stable isotope variability is a function of the elements isotopic species capacity to partition unequally (fractionate) between two or more co-existing phases. This is due to mass dependent differences in the element's physicochemical behavior and this "fractionation normally varies inversely with temperature and (is) independent of pressure" (Field and Fifarek, 1985). To adequately address any geological problem, (hydrogeologic, hydrothermal processes and alteration, ore deposits, etc.) through the use of isotope research, it is necessary to address questions of initial isotopic signatures; what level of isotopic exchange (approach to equilibration) is recorded in the samples and to what degree are water-rock interactions, heating and cooling processes, fluid mixings or fluid phase separations (boiling, effervescence) being represented.

As is the case with fluid inclusion research, the array of interconnected and often times chaotic influences upon the genesis of the isotopic signatures, demands an ever increasing data pool and careful regard for the associated geology. The similarities of the isotopic signatures recorded at the Sheep Creek and those recorded from numerous mesothermal Au vein systems studied can add much to the understanding of this mineral deposit and its association with larger scale rock-fluid systems. As a small portion of an ongoing study of Cordilleran rock and vein isotope geochemistry, the Sheep Creek Camp proved to be an excellent isotopic research project on the grounds of the good geological work and interpretation done in the area, the accessibility to portions of the vein system and the complex tectono-thermal history of the district.

Mineralized and unmineralized vein quartz and quartzites were analysed for $\delta^{18}O$ values. Many of these same samples were analysed for δD ratios from the ancient waters entrapped in the fluid inclusions. Carbonate-bearing veins and carbonate-rich host rocks were analysed for $\delta^{13}C$ and $\delta^{18}O$ ratios. Those rocks that contained appreciable amounts of fluid inclusion bound CO_2 and/or CH_4 have been analysed for $\delta^{13}C$ from CO_2 and, as an analytical first, $\delta^{13}C$ and δD from the methane. Although recent analyses of the volatile (carbonic) phases in these veins have produced an interesting assortment of $\delta^{13}C$ and δD values, the limited data set and the 'tuning' of the analytical process allows only for data presentation at this time.

Summary of Isotope Data

The oxygen data from quartz veins are remarkably consistent with those values expected for these types of systems (Kerrich, 1987). The quartzite oxygen values vary less than 2‰ over a region of approximately 300 km^2. Deuterium/hydrogen ratios from water in quartz-hosted fluid inclusions range over 90‰ and D/H ratios from inclusion decrepitation techniques performed on purified whole-rock quartzites range over 70‰ with the quartz veins being relatively depleted compared to the quartzites. Vein carbonates, predominantly calcite, have a relatively tight range in $\delta^{13}C$ values with a mean of -2.5±1.3‰ over a range of -5.8 to-0.4‰ and the wall rock carbonates (calcite) are comparatively enriched in both $\delta^{13}C$ and $\delta^{18}O$. A few quartz-calcite pairs have been analyzed and it is believed that some post-depositional isotope exchange is responsible for the disequilibrium observed in these pairs. Non-coeval mineral deposition may account for the observed disequilibria.

Following a brief discussion of methodology and relevant data presentation conventions, the data, possible interpretations and some comparisons with similar mesothermal systems are discussed.

ANALYTICAL TECHNIQUE and METHODOLOGY

Quartz is one of the best minerals for $\delta^{18}O$ isotopic analysis because of its tendency to concentrate ^{18}O relative to it's parent fluid and relative to other minerals and its tendency to be relatively insensitive to low temperature (<500°C) post-depositional exchange processes (Taylor, 1979; Field and Fifarek, 1985).

Quartz samples were initially chosen to establish a broad coverage of the field area. Additional analyses were chosen on the basis of testing trends in $\delta^{18}O$ and to complement fluid inclusion data .

Oxygen was liberated from fine crushed (-40 mesh) aqua regia purified quartz samples by the BrF_5 (bromine pentafluoride) technique of Clayton and Mayeda (1963). The oxygen was then reacted with carbon at approximately 850°C and the CO_2 was analyzed on a Micromass 602D Nier-type isotope ratio mass spectrometer (Nier,1947; Maheux,1989). The isotope ratio data are presented in δ-notation in per-mil values: ie. **$\delta x‰ = (Rx/Rs - 1) \times 10^3$** which is an expression of the sample ratios (Rx) deviation from a specific standard ratio (Rs), in this case either SMOW (standard mean ocean water) or PDB (Pee Dee Belemnite).

Deuterium/ hydrogen analyses were performed on inclusion fluids liberated from approximately 4 gram samples of coarse crushed quartz. The samples were bathed in aqua regia and then dehydrated to remove surface waters. These samples were dried in vacuum at 150°C for 24 hrs and then thermally decrepitated to a temperature of 1100°C. The waters collected were reduced with zinc metal to generate H_2 for analysis. δD values are reported relative to SMOW. In some cases CO_2 was isolated from the inclusion fluids and analysed for $\delta^{13}C$ values. Interestingly, a few inclusions had sufficient CH_4 for isotopic analysis. These inclusions were first identified in the fluid inclusion study and were then decrepitated as above. Those gases that were not frozen by liquid nitrogen were first absorbed on zeolite and subsequently oxidized at 800°C in a CuO packed column.

Vein and host-rock carbonates (calcites) were reacted with phosphoric acid (H_3PO_4) at an ambient temperature of 25°C for approximately 24 hours (after the technique of McCrea, 1950) Purified siderite were similarily reacted but for extended periods of three and six months. $\delta^{13}C$ values from carbonates and inclusions bearing CO_2 and/or CH_4 are presented relative to the PDB standard (Craig,1957) and $\delta^{18}O$ from carbonates are reported relative to SMOW.

RESULTS OF ISOTOPE ANALYSES

A compilation of isotopic data acquired for this study is presented in Table 4.1. Errors in analyses are ± 0.2‰ for $\delta^{18}O$ and $\delta^{13}C$ from quartz, carbonates and inclusion analyses and ±4‰ for δD values from fluid inclusions (Nesbitt, pers.comm.). Repeat analyses are listed directly in Table 4.1.

Quartz Oxygen:

$\delta^{18}O$ values from quartz veins range between 11.1 and 25.8‰ and from the condensed sample set which excludes values from Vsc193 (24.0‰) and Vsc265 (25.8 and 22.7‰), a mean value of 14.4 ± 3 ‰ from 55 analyses is obtained. Sample Vsc193 was excluded from the statistical calculations as this sample exhibits late, essentially epithermal chalcedony textures and Vsc265 was removed from the group because of its complex fluid inclusion characteristics. The significance of the clustering near 14 ‰ is related to the fact that the sample set includes an heterogenous mixture of unmineralized samples, mineralized samples bearing minor pyrite, mineralized veins with complex sulfide mineralogy and discordant and foliation parallel veins. A summary of the data for quartz and quartzite oxygen ratios is presented in Figure 4.1a.

A closer inspection of the data reveals an association of low $\delta^{18}O_{qtz\ veins}$ values with quartzite of siliceous greywacke host rock lithologies. This isolated portion of the sample set includes samples Vsc001, 002, 006, 007, 008b, 023, 042, 043, 107, 150, 224, and Vsc417. The $\delta^{18}O$ values from this set range from 11.1 to 13.3 ‰ with a mean of 12.3±0.8 ‰. These samples are consistently unmineralized except for isolated grains of galena in samples Vsc007 and Vsc042.

The remaining analyses are from veins that are either hosted by rocks of more argillaceous, carbonaceous or calcareous characteristics or mine workings, where the host rock is unknown. The range in $\delta^{18}O$ values from these veins is nearly 10 ‰; however, only two values are greater than 16.4 ‰. A mean value from this group, including the two high values is 14.9±2.0 ‰ and excluding these two values, 14.6±1.0 ‰.

Five quartzite samples were also analysed for $\delta^{18}O$. These rocks gave values ranging from 11.0 to 12.8 ‰ with a mean value of 11.7±0.7 ‰. This tight range in $\delta^{18}O$ values of rocks which were collected from a broad region including the extreme northern and southern portions of the field area, suggests that either metamorphic reequilibration of the isotopic signature of the protoliths entailed near homogeneous P-T conditions, the sandstone protolith was composed of isotopically homogenous quartz grains or that the quartzites have isotopically equilibrated with a post-metamorphic hydrothermal system involving large-scale circulation of an homogeneous fluid.

$\delta^{18}O_{Fluid}$; Isotopic Composition of Vein-Forming Fluids:

As was shown from the fluid inclusion study, temperatures of vein formation can be approximated from the temperatures of homogenization (Th values) from inclusions that represent a system of fluid phase separation. Although additional temperature constraints are difficult to make because of the minimal control on inclusion composition analyses and the lack of phase equilibria data for such complex fluid systems, it has been confirmed by a number of similar studies that these systems form at temperatures from approximately 250 to 350° C (Nesbitt et al., 1989). Values between 275-350° C were chosen as formation temperatures with choice of temperature being based upon parameters dictated by fluid inclusion characteristics. It is important to recognize that only a few of the quartz isotope numbers are from samples which allowed for inclusion analysis. Therefore formation temperatures for many of the samples were estimated by their proximal or textural association with better known samples.

Using the equation of Matsuhisa et al. (1979), for quartz water fractionation:

$$\Delta_{Qtz\text{-}H_2O} = 3.34\ (10^6/T^2) - 3.31$$

where T is temperature in degrees Kelvin

at the above estimated temperatures, the $\delta^{18}O_{Fluid}$ value of the vein-forming fluids have been calculated and are presented in Figure 4.1b. The mean value of 7.3±1.5‰ established by this process is about 0.3 ‰ lower than if an assumed temperature of 300° C was used for the calculations. The $\delta^{18}O_{Fluid}$ value of 7.3±1.5‰ is important in that it falls within the limits of the isotopic values of metamorphic, magmatic and evolved meteoric waters. In fact, this value could be adjusted by ± 2.5 ‰ and still reflect these three potential fluid sources (Taylor, 1974; Nesbitt et al.,1989).

Regional trend in $\delta^{18}O_{Quartz}$ values:

Figure 4.3 is a plot of $\delta^{18}O_{Quartz}$ values onto section line A-B as is depicted in Figure 4.2. The trend in decreasing $\delta^{18}O_{Quartz}$ values from west to east is evident. Any interpretation of this trend must consider the possibilities of variabilty in initial $\delta^{18}O_{Fluid}$, variability in the temperatures of quartz vein formations and variations in fluid-rock ratios. Even though it is not possible to directly transfer the documented regional trend of increasing metamorphic isograds (as discussed in chapter II) towards the Kootenay Lake (Archibald,1984) to the Sheep Creek Camp, it is possible that temperatures of formation were moderately higher in the eastern sector (refer to decrepitation temperatures of high density CO_2 bearing inclusions in the eastern portion of the research area). The higher temperatures of formation in the east would result in a smaller quartz-water fractionation and this is possibly what is being recorded in the $\delta^{18}O_{Quartz}$. Alternatively, the increasing abundance of quartzite towards the east and the increase of calcareous and argillaceous host rocks in the west could play a major role in the variability of the isotopic nature of the parent fluid and consequently the trend observed is a result of local lithological heterogeneities. Variability in original $\delta^{18}O$ compositions of these host rocks as well as the variability in primary and secondary permeabilities in these rocks would affect the isotopic composition of the fluids that have interacted with them.

A third possible explanation of the observed trend is that phase separation (as has been documented to have occurred in the region) produced local enrichments in $\delta^{18}O_{Fluid}$ resulting in the observed enrichments in quartz veins from this locale.

Questions remain regarding the extreme enrichment in $\delta^{18}O$ of some of the quartz veins from the study area (those removed from the statistical analysis). It is believed that both of these high $\delta^{18}O$ veins are not directly related to the primary veining process in the region and that they occurred at a later (lower temperature) period of the tectono-thermal history of the camp when the entire lithological package was being influenced by remnant hydrothermal activity.

Hydrogen Isotopes, of Veins, Rocks and Minerals:

The isotopic study of minerals and fluids from ancient hydrothermal systems relies heavily upon the $\delta^{18}O$-δD isotopic couplet. That all these vein systems are directly dependent upon the presence of waters of one form or another, and that both of the constituent elements can be isotopically characterized, renders this elemental pair as one of the most powerful tools for the interpretation of water-rock-mineral systems (Taylor, 1987; Nesbitt, 1989; Field and Fifarek, 1985).

Deuterium/hydrogen analyses of quartz vein hosted fluid inclusion waters, muscovite and sericite, whole rock quartzites (fluid inclusions and/or phyllosilicates) and CH_4 bearing fluid inclusions have allowed for rigorous constraints to be applied to the possible sources of the hydrothermal waters and have opened an intriguing area of isotopic research (δD_{CH4} from fluid inclusions). δD analyses of waters and gases liberated from thermally decrepitated fluid inclusions hosted by barren and mineralized quartz veins have resulted in a broad range of depleted δD values. Figure 4.4 summarizes the quartz vein and quartzite δD analyses. Much discussion regarding the applicability of this type of decrepitation analysis has occurred and at this time the bulk sampling of primary, secondary and psuedosecondary inclusions is not considered to adversely affect the interpretation of the δD values as they relate to the origins of the fluids and the formation of these types of veins (Pickthorn et al., 1987; Nesbitt et al., 1987).

A mean value of -129±21‰ from 47 analyses of quartz veins has been recorded and the extreme range of δD values (90‰) observed indicates that the physicochemical dynamics of hydrogen within these types of systems is more complicated than may be immediately apparent. The range in δD values recorded from surface waters and the remarkable sensitivities of hydrogen/deuterium fractionation to varying surface conditions support the interpretation that as surface waters (meteoric) penetrate into the brittle crust, these variations in δD will be manifest in the minerals from which we acquire our data. Fluid origin, D/H evolution under conditions of variable rock types, variable primary and secondary permeabilities and porosities and variable water:rock ratios (ie. rock dominated or fluid dominated systems) can all play significant roles in the genesis of the primary deuterium signature of the minerals. Post-depositional hydrogen diffusion and/or mineral recrystallization (incipient recrystallization to metamorphic overprinting) can also affect the deuterium/hydrogen ratios.

The overall depleted signature, relative to magmatic and metamorphic waters, of the veins from Sheep Creek Camp is indicative of a meteoric or formation waters origin. It is also interesting to note that "formation waters from sedimentary basins at high latitudes tend to plot along trends that intersect the meteoric water line at lower $\delta^{18}O$ and δD values (which)...strongly suggests that meteoric water comprises an important fraction of the formation waters in such basins" (Longstaff,1987; Clayton et al., 1967). A comparison of the Sheep Creek inclusion water δD values with other Cordilleran mesothermal vein system is presented in Figure 4.6. In all of these systems it has been shown that the deuterium signature is meteoric and that as a consequence of the fact that the principal source of the hydrogen is the meteoric water and at moderate to low water-rock ratios (≥ 0.1) the influence of the rock upon the hydrogen component of the hydrothermal waters is minimal. Water-rock exchange processes have not significantly affected the δD values and the hydrothermal fluids have essentially retained the primary meteoric δD compositions. As is depicted in Figure 4.6, the latitudinal trend from deuterium depleted systems in the northern reaches of the Cordillera (eg. Klondike) to the less depleted systems in the south (eg. Sheep Creek, Coquihalla, (all systems have meteoric signatures)) further enhances the argument that these veins are ultimately related to surface fluids.

δD analyses of fluid inclusions from purified quartzites are summarized in Table 4.1 and presented in Fig. 4.4. Although the moderately depleted mean value of -96±18‰ for this suite of samples could be interpreted as a meteoric signature, the relative enrichment observed in these rocks (as compared to quartz inclusion values) suggest that the interpretation cannot be this simplistic. Except for sample Vsc 383, 205, 034 which are muscovite and sericite separates, the δD values from the quartzite suite can only be viewed as whole-rock analyses. Although the samples were purified, the minor presence of sericite must be considered and the values recorded from these decrepitation analyses are possibly a combination of both ancient waters in quartzite grain bound inclusions and hydroxyl deuterium released from the metamorphic sericite. Alternatively, the values may in fact reflect formational inclusion fluids; however as the source of the quartz in these massive pure quartzites is only partially understood (Smith and Gehrels,1991; Smith,1990) any speculation upon the ultimate provenance of these fluids would be highly suspect.

The lack of any direct correlation between δD values from quartz vein fluid inclusions and the δD values recorded for quartzites indicates that there was little δD evolution of the vein forming fluids. That some of the quartzite samples have relatively depleted δD signatures suggests that phyllosilicate deuterium exchange with the hydrothermal fluids may have occurred, and this could possibly help to explain the scatter of δD values observed.

Interpretation of the δD values obtained from the phyllosilicates of samples Vsc034 (-95 and-92 ‰), Vsc383 (-77 and -73 ‰) and Vsc205 (-58 ‰) is similarly complex (plotted on figure 4.4). Vsc034 is a sample of a quartz-sericite phyllitic bed bound by the massive pure Motherlode quartzites. The -93 ‰ mean is possibly a hydrothermally altered metamorphic signature similar to those suggested for the quartzites that have similar δD values. The δD value could also simply reflect a primary metamophic signature although the -93‰ value is depleted relative to the accepted metamorphic deuterium range. Vsc383 was initially considered to be a complex hydrothermal vein crosscutting the metasediments, but discussions pertaining to it's ultimate origin included the possibility of this quartz, tourmaline and muscovite vein as being a pegmatite associated with the nearby, eastern edge of the Salmo stock. The δD values near -75 ‰ are compatible with a magmatic origin however, the elevated $\delta^{18}O$ values of 12.9 ‰ (quartz) and 12.7‰ (muscovite) suggest that either this vein (pegmatite) is not of magmatic origin or that it has undergone some degree of post-depositional $\delta^{18}O$ drift, as has been recognized to be relatively common to the magmatic bodies in this region (Magaritz and Taylor, 1986).

The hydrothermal character of sample Vsc205 strongly suggested that the muscovite contained within the sample would reflect an hydrothermal δD signature. δD values from fluid inclusions from the quartz samples have averaged -133 ‰ and this has been interpreted as being a meteoric signal, however the -58 ‰ value recorded from the muscovite does not directly support the meteoric interpretation. Petrographic analysis shows that the muscovite in this sample is the last mineral to form and that this late muscovite is therefore not coeval with the quartz. The question remains, what does the -58 ‰ value mean, and how relevant is it to the overall interpretation of the isotopic nature of the Sheep Creek Camp.

Preliminary δD analyses of methane from fluid inclusions have resulted in a small and rather scattered data set with δD_{CH_4} values ranging from -243‰ to -138‰. That the analytical procedure is still being fine tuned, the values show little reproducibility and that the data set is small, suggests that the simple reporting of findings will suffice at this time and interpretations should probably be taken lightly, or avoided. The possible analytical importance of this procedure is however quite significant and it should therefore be pursued further.

QUARTZ-MUSCOVITE GEOTHERMOMETRY

If it were such that the two muscovite-quartz pairs, samples Vsc383 and Vsc205 were formed contemporaneously and that they had achieved a state of isotopic equilibrium, it would be possible to apply one of the available quartz-muscovite fractionation equations and calculate a temperature of formation. This process can be applied to any one of a number of mineral pairs as long as isotopic equilibrium can be proved and the empirical or experimental fractionation equations are available. Temperatures derived from mineral pair geothermometry can then be used in conjunction with fluid inclusion studies for 'pressure corrections', (cpt.III) or be compared to metamorphic isograds to accentuate discussion on possible temperature regimes.

The following discussion on isotope pair geothermometry has been included to demonstrate that the mineral pairs represent disequilibrium and this may be a function of not only disequilibrium between the mineral pairs but may also represent a lack of equilibrium between the minerals and the mineralizing fluids.

Sample Vsc 205 has a $\Delta_{\text{Quartz-Muscovite}}$ ($\Delta_{\text{Q-M}}$) value of 3.0 ‰ and this value, using the equation of Bottinga and Javoy (1975): $\Delta_{\text{Q-M}} = 2.25\ (10^6/\ T^2)\ \text{-}0.6$ (where T is temperature in degrees Kelvin) gives an equilibrium temperature of formation of approximately 510° C. Using the equation of Chacko (pers. comm.): $\Delta_{\text{Q-M}} = -0.0418 + 1.54X + 0.013X^2 - 0.0061X^3$, (where X is (T) in degrees Kelvin) a formation temperature of 435° C is recorded for this pair at equilibrium. One additional calculation, using a fractionation equilibrium equation for quartz-muscovite cited in Field and Fifarek (1985), (Friedman and O'Neil,1977 and Matsuhisa, 1979): $\Delta_{\text{Q-M}} = 0.96\ (10^6/T^2)\ \text{-}0.58$ for temperatures between 250 - 500° C results in a formation temperature of 355°C. From fluid inclusion analyses, the estimated temperature of formation of the quartz is low compared to all of the above equations; Th ≅ 260°C; from inclusions that suggest formation from phase separation

Application of these same three equations to the quartz-muscovite pair from sample Vsc383 ($\Delta_{\text{Q-M}} = 0.2$ ‰) results in temperature that are in excess of 1000° C, which are to high for any reasonable type of crystallization scenarios and it is therefore argued that this mineral pair also represents isotopic disequilibrium.

If it were the case that the mineral pair from Vsc205 was in isotopic equilibrium, one or more of the above equations could be used to estimate the temperature of formation.

CARBONATES: $\delta^{13}C$ and $\delta^{18}O$; Veins and Calcareous Host Rocks:

Figure 4.7 is a scatter plot of $\delta^{13}C$ and $\delta^{18}O$ values from vein carbonates and associated calcareous (limestones and carbonate rich argillites) lithologies. The relatively tight clustering of values for both the vein calcites and the wall rock carbonates (which actual range in compositions from essentially pure limestones to slightly calcareous argillites) indicate that there is either some direct correlation between the veins and the calcareous host rocks or that there has been a large scale reequilibration of the isotopic ratios in these minerals. The general depletion of both $\delta^{13}C$ and $\delta^{18}O$ in the veins relative to the host rocks strongly suggests on the one hand that there is a relationship between these two carbonate systems. As is discussed below, the likelihood that both of these carbonate systems have reequilibrated as a result of post-depositional thermal or hydrothermal processes is similarily probable.

For the sake of discussion however, a preliminary assumption that the isotopic values recorded are preserved from the time of vein carbonate precipitation. In all cases , except for sample Vsc 205_{siderite}, the vein carbonates are calcites. No chemical analyses of the calcites have been performed and therefore no compositional data is available, however carbonate research at the Blue Bell mine north of the Sheep Creek (Ohmote and Rye, 1970,Table A1) shows significant variability in (Ca, Mg, Fe and Mn) compositions and it is probable that similar variability in calcite compositions would be observed at the Sheep Creek Camp. The most significant geological observation at the Sheep Creek is the general paucity of carbonate in the vein system and that most of the carbonate veins were either proximal to or intimately contained by carbonate bearing host rocks.

From twenty four analyses of 18 calcite (one siderite) samples, an average $\delta^{13}C$ of -2.5±1.3 ‰ over a range of -5.8 to -0.4 ‰ was recorded. These values are only slightly depleted relative to vein carbonate $\delta^{13}C$ values observed in the Rocky Mountains to the east of the camp, and moderately enriched (+5‰) relative to most analyses of vein carbonates north of the 51° parallel west of the Rocky Mountain Trench and west of the Kootenay Arc suture zone (Nesbitt and Muehlenbachs, in prep). A mean value of +16.8 ±2.7‰ over a range of $\delta^{18}O$ values of +7.0 to +21.4 ‰ is considerably more variable and depleted than the homogeneity observed in the Rocky Mountain vein carbonates, however the one anomalously low $\delta^{18}O$ value contrasts with the otherwise tight clustering of oxygen values between 14 and 21 ‰.

The results of 13 analyses of 8 host rock samples gives a $\delta^{13}C$ range of -9.3 to 0.34 ‰ with a mean value of -1.9±2.4 ‰ and a tight $\delta^{18}O$ range of approximately four per mil from +18.9 to 22.7 ‰ with a mean value of 20.5±1.1 ‰. Considering the overall variability in host rock composition, the relative homogeneity of $\delta^{13}C$ and $\delta^{18}O$ values recorded from these calcareous units is quite striking. The mean $\delta^{13}C$ value for these calcareous units can be further tightened by removing sample Vsc218b which is suspected to have a significant reduced carbon component as contamination in the sample. The overall package is slightly depleted from the typical values of Rocky Mountain limestones and dolomites which range from 0.0 to 1.5 ‰. In contrast however are the $\delta^{18}O$ values recorded for the Sheep Creek calcareous units which are significantly depleted relative to those values (23 to 29 ‰) recorded for the Rocky Mountain calcareous units.

Geothermometry of the quartz-calcite pairs from the Sheep Creek Camp and district is not considered to be viable two reasons, the most significant reason being that through petrological observations, all quartz carbonate pairs display some form of post-depositional alteration (recrystallization, strained and contorted calcite, calc-silicate formation at calcite-quartz boundaries) and, as can be observed from Figure 4.8, many of the quartz-calcite pairs display gross disequilibrium in $\delta^{18}O$ values. Only sample Vsc232 has a $\Delta_{Qtz\text{-}Cc}$ that suggests equilibrium near 330° C however the petrology of the sample is clearly indicative of post-depositional alteration. Not having any knowledge of carbonate compositions and by not having any strict confidence in the state of isotopic equilibrium suggests that any thermometric calculations presented would be suspect.

What the carbonate study does reveal though is that there is a very close correlation of vein isotopes and host rock isotopic compositions. For example, Vsc352 is a barren quartz-calcite vein hosted by an argillaceous limestone unit, Vsc353. The $\delta^{13}C$ and $\delta^{18}O$ values for these two samples (-1.0:+20.3‰ and -1.3:+20.1‰ respectively) are essentially identical. Similarly, Vsc357, a quartz-carbonate vein has a $\delta^{13}C$ and $\delta^{18}O$ signature of (-2.9;+17.9 ‰) which is depleted relative to it's host rock, Vsc358 (-0.5;+21.3 ‰). Of additional interest regarding this particular location is that the pure calcite extension of this vein (Vsc357b) has a $\delta^{13}C$ and $\delta^{18}O$ signature that is somewhat enriched in ^{13}C (-1.0 ‰) and slightly depleted in ^{18}O relative to Vsc357 (+15.6 ‰). This complex variability in $\delta^{13}C$ and $\delta^{18}O$ further supports the argument that these calcite-quartz pairs are not suitable for geothermometry. and are expressing some form of disequilibrium.

Ohmoto and Rye (1979) summarized data of Hoefs (1973) and Ronov and Yaroshevsky (1969) and calculated that approximately 93% of crustal carbon is fixed in sedimentary and metamorphic rocks with the remaining 7% being fixed in igneous rocks and less than 0.01% contained by the atmosphere,biosphere and hydrosphere combined. In addition to these estimates, they conclude that approximately 22% of the carbon in the sedimentary-metamorphic rock reservoir is in a reduced state whereas 78% is fixed in the oxidized state of carbonates. Hydrothermally oxidized carbon species may originate from three principal sources. The first reservoirs are the magmatic sources, where the $\delta^{13}C$ value is consistently near -5.0 ‰. The second source is the oxidization of reduced carbon species; organic compounds in sedimentary rocks and graphite in metamorphic rocks. Reduced carbon species are generally considered to have $\delta^{13}C$ values near -25 ‰ and typically range from -10 to -35 ‰. If this reduced carbon is oxidized ($C + O_2 \Rightarrow CO_2$) or undergoes hydrolysis ($2C + 2H_2O \Rightarrow CH_4 + CO_2$) it can become the source of carbon in the hydrothermal fluids. Fractionation of the carbon species is presumed to be minimal under conditions of oxidation and the $\delta^{13}C_{CO_2}$ would have a similar $\delta^{13}C$ range (-10 to -35‰) as the reduced form whereas hydrolysis would result in $\delta^{13}C$ enrichment by 3 to 12‰. Ohmoto and Rye (1979) further suggest that the combination of these reactions can result in considerable variability in $\delta^{13}C_{CO_2}$ values that are generally less than -10.0 ‰. The third, and probably most likely candidate for carbon source for the Sheep Creek carbonate system is the leaching of carbon from sedimentary carbonates. In contrast to the first two possible sources, marine carbonates have nearly constant $\delta^{13}C$ values of 0.0 ± 4.0 ‰ and these values are recorded from the wall rocks (host rock) carbonates of the camp. Dissolution and decarbonation reactions involving these rocks will result in oxidized carbon species that are isotopically similar to the original carbonates ($\delta^{13}C_{CO_2} \cong 0.0$ ‰) or possibly slightly enriched (Shieh and Taylor,1969). Carbonate bound carbon species are for the most part the most $\delta^{13}C$ enriched species and this is observed to be the case with the available data in this study. Preliminary $\delta^{13}C_{CO_2}$ values recovered from fluid inclusions in quartz have a very wide range in $\delta^{13}C$ values (-25.0 to+0.9 ‰; mean of -8.1 ± 8.6 ‰) which are relatively depleted compared to both carbonate suites. What these numbers represent is not fully understood and the data set is not large enough to either confirm or deny the observed range in values. Nesbitt and Muehlenbachs,(in prep.) have presented a few explanations for similar depletion phenomena observed elsewhere and argue that if a small component of reduced carbon was incorporated into the fluid system, the fluid would in fact exhibit $\delta^{13}C$ depletion but a much greater diversity of $\delta^{13}C$ values would be observed in the vein carbonates. Also worth considering is that fluids which equilibrate with the calcareous units at temperatures around 350° C could produce the observed depletion at precipitation temperatures of 200-250° C, however the oxidized carbon species (HCO_3^-) in this situation would result in a relatively alkaline fluid (ph>7) (Rye and Bradbury, 1988) which is not compatible with these types of systems. Liberation of CO_2, phase separation or degassing of CO_2 from the hydrothermal fluids would also result in $\delta^{13}C$ depletion. The $\delta^{13}C$ depletion observed in these veins is possibly not a result of any one process and any final statement regarding these observed values is not presently possible.

The recorded ^{18}O depletion can however be explained on the bases of the origin of the hydrothermal fluids that have interacted with the carbonate units and that these low ^{18}O, evolved meteoric fluids ($\delta^{18}O \cong 7.5$ ‰) are responsible for the minor $\delta^{18}O$ depletion. Nesbitt and Muehlenbachs further argue that the depletion could not be a product of decreasing temperatures of deposition as this would increase the $\delta^{18}O$ values of the vein carbonates (Rye and Bradbury, 1988)

$\delta^{13}C_{CH_4}$ values from fluid inclusions are much more tightly constrained with values that range form -23.7 to -28.5 ‰ and these values are typical for reduced carbon from sedimentary rocks. These values may represent essentially unaltered reduced-sediment bound methane that has been incorporated into the hydrothermal system and ultimately entrapped in the mineralized veins.

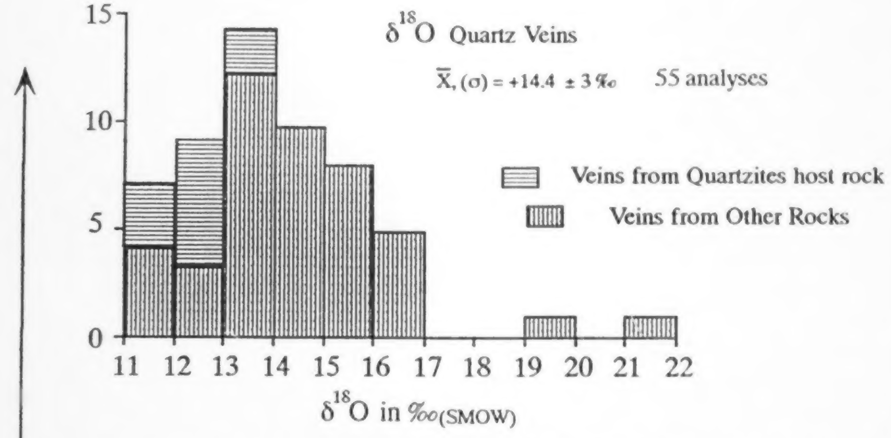

Figure 4.1a. Oxygen isotope ratios in per mil (‰ SMOW) values from quartz veins of the Sheep Creek Camp and district.

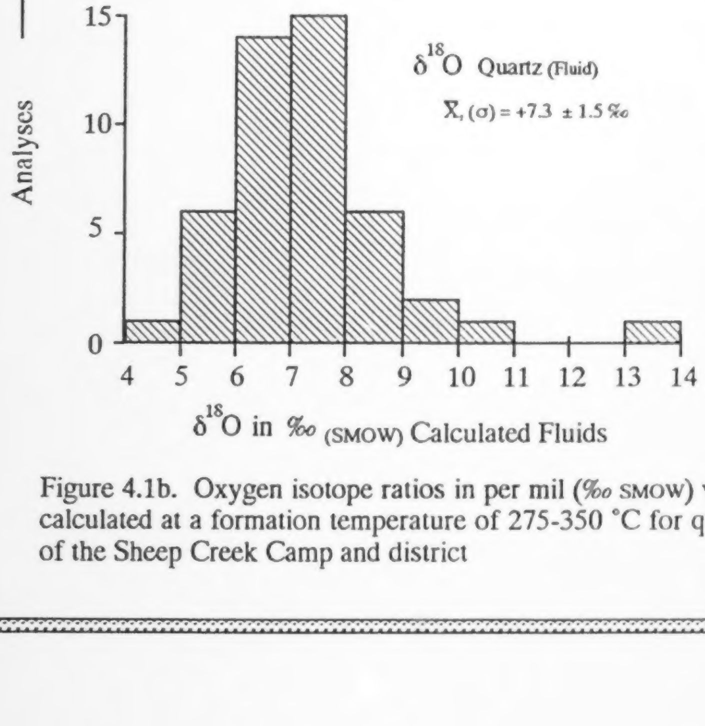

Figure 4.1b. Oxygen isotope ratios in per mil (‰ SMOW) values for fluids calculated at a formation temperature of 275-350 °C for quartz veins of the Sheep Creek Camp and district

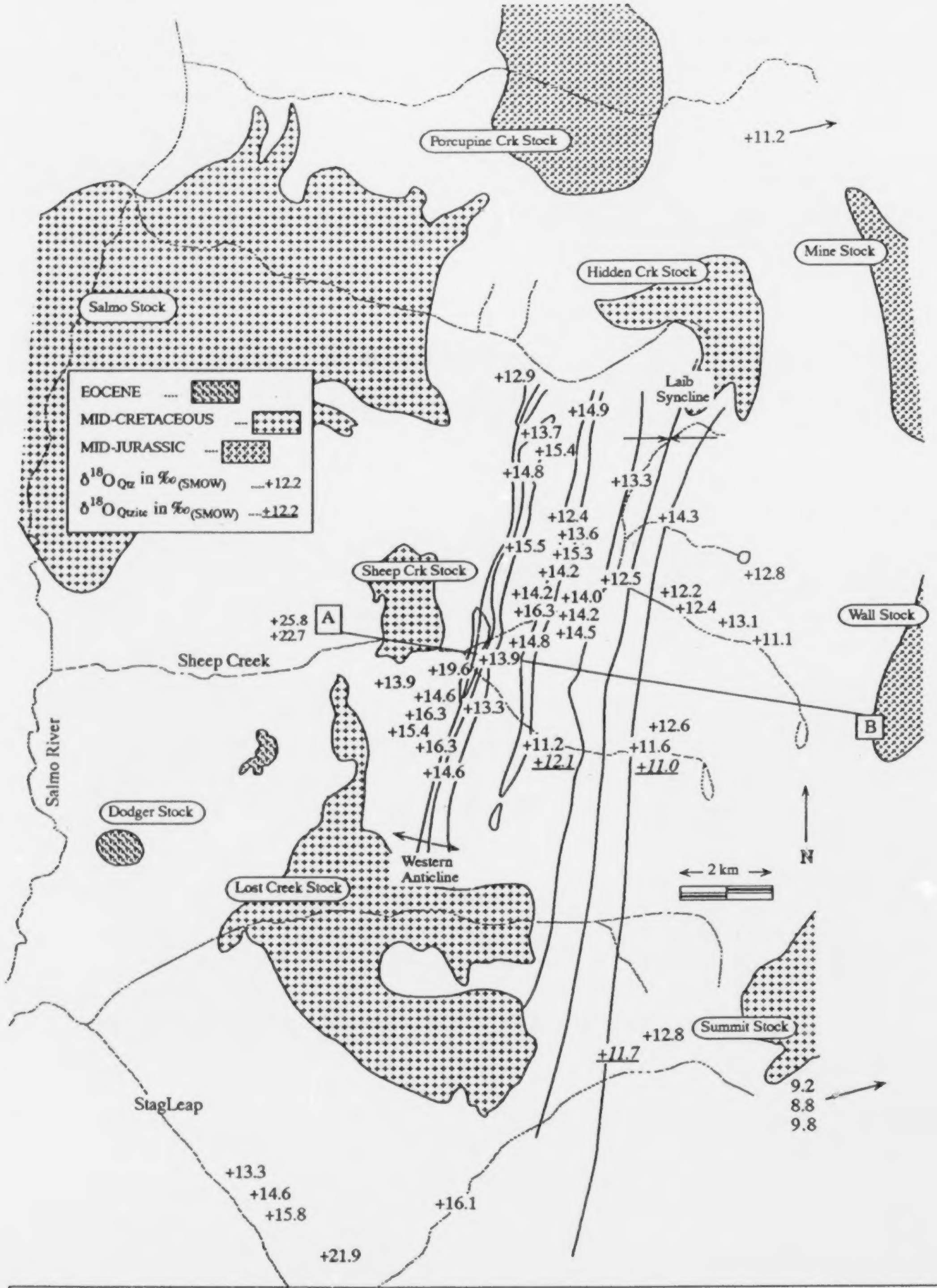
Porcupine Crk Stock
+11.2
Mine Stock
Hidden Crk Stock
Salmo Stock
EOCENE
MID-CRETACEOUS
MID-JURASSIC
δ18O Qtz in ‰(SMOW) +12.2
δ18O Qtzite in ‰(SMOW) +12.2
+12.9
+14.9
Laib Syncline
+13.7
+15.4
+14.8
+13.3
+12.4
+13.6
+14.3
+15.5
+15.3
+14.2
+12.8
Sheep Crk Stock
+12.5
+14.2
+14.0
+12.2
+16.3
+14.2
+12.4
+13.1
Wall Stock
+25.8
+22.7
A
+14.8
+14.5
+11.1
Sheep Creek
+13.9
+19.6
+13.9
+14.6
+16.3
+13.3
+15.4
+16.3
+12.6
B
+11.2
+11.6
+12.1
+11.0
+14.6
Salmo River
Dodger Stock
N
Western Anticline
2 km
Lost Creek Stock
+12.8
Summit Stock
+11.7
9.2
8.8
9.8
StagLeap
+13.3
+14.6
+15.8
+16.1
+21.9

Figure 4.2. Oxygen isotope ratios in per mil (‰ SMOW) values from vein quartz and associated quartzite whole rock. Statistics are given in Figure 4.1a. Values show a moderate trend towards higher $\delta^{18}O_{Quartz}$ from east of the Laib Syncline to the central, mineralized region. This trend is depicted in Figure 4.3.

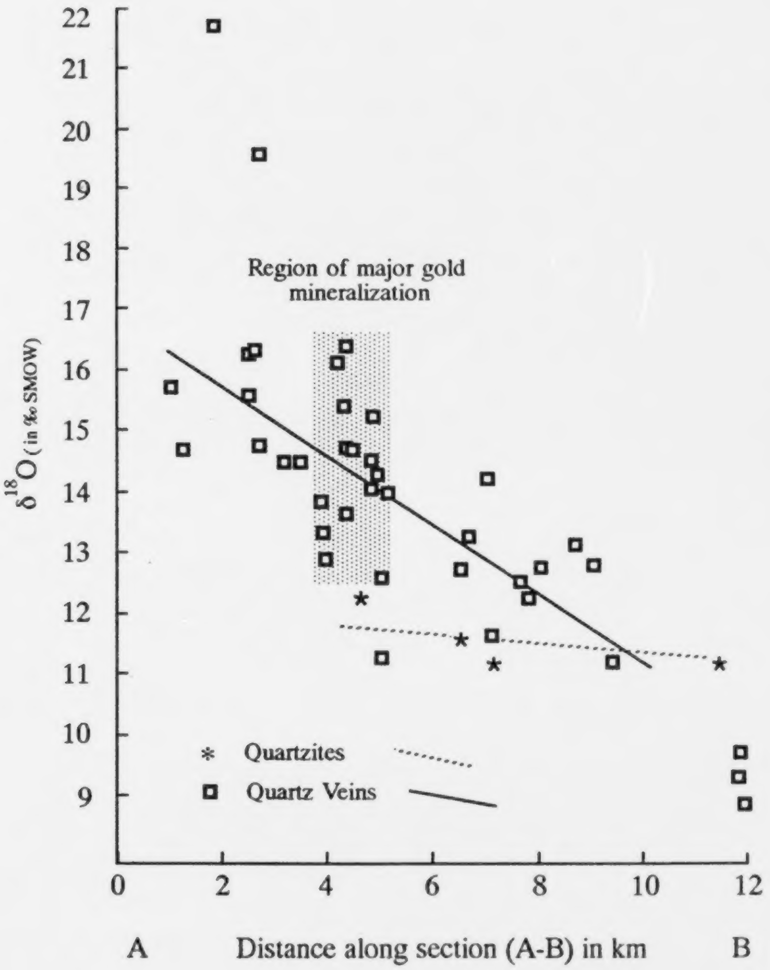

Figure 4.3. Plot of $\delta^{18}O$ quartz veins and $\delta^{18}O$ quartzites along projected section A-B as drawn on Figure 4.2. Solid line is best fit regression indicating a general trend of decreasing values from west to east across the Sheep Creek camp and outlying district.

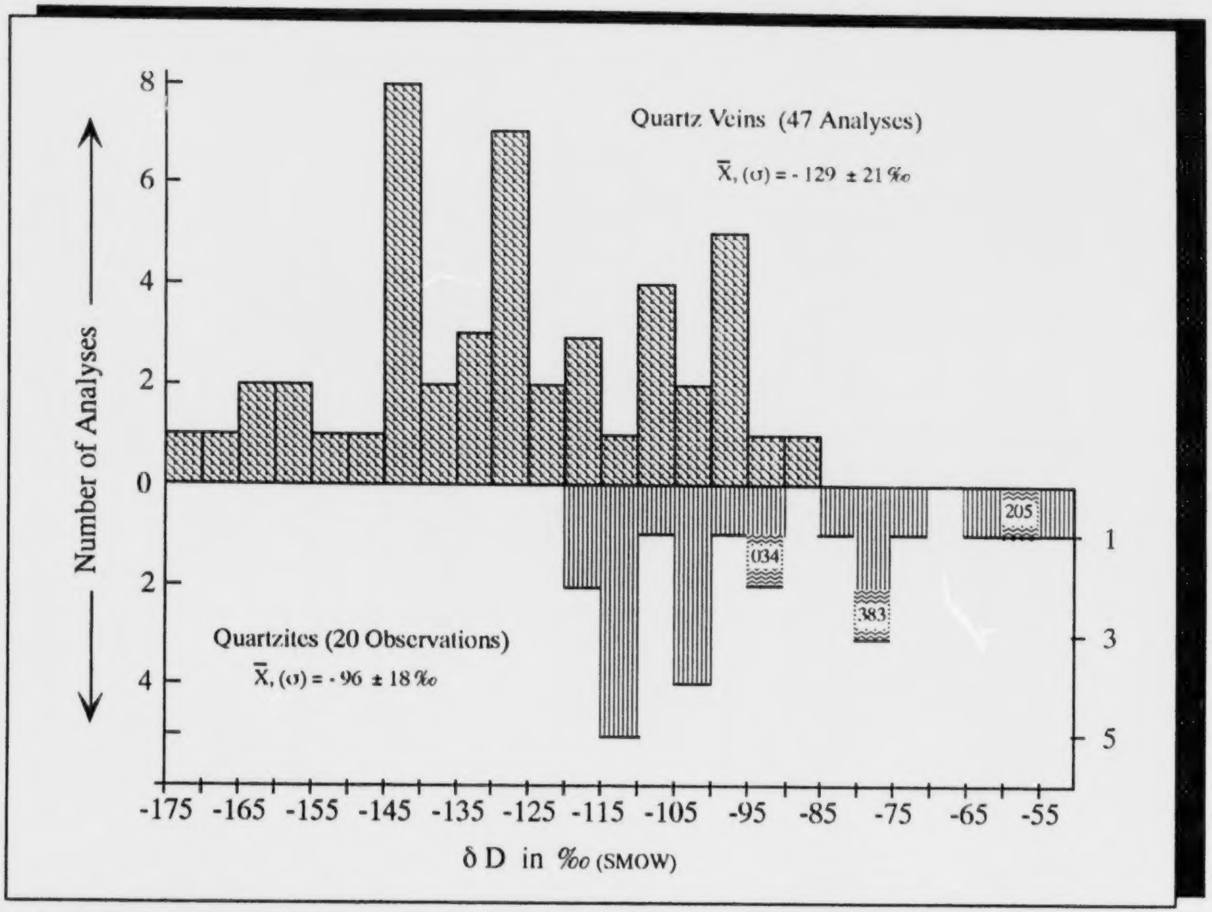

Figure 4.4. Histograms for deuterium from H_2O liberated from quartz veins and quartzites of the Sheep Creek Camp. Values are from thermally decrepitated primary and secondary inclusions from coarse crushed samples.

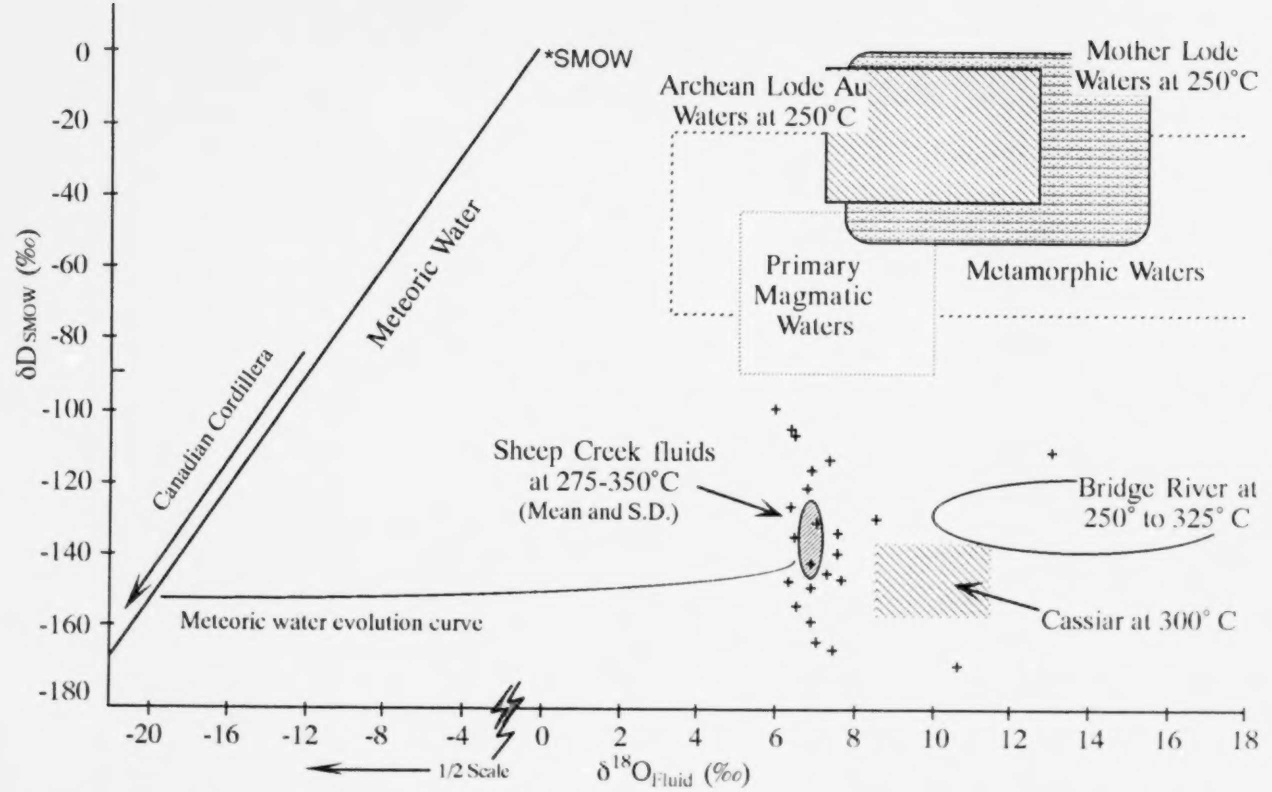

Figure 4.5. Plot of Deuterium (inclusion fluids) vs. $\delta^{18}O_{Fluid}$ for waters from vein quartz, from selected gold bearing deposits calculated at the temperatures indicated. Sheep Creek data is presented as '+' points, and standard deviation (from total data set) is presented as a cross-hachured oval. Isotopic composition of natural fluid reservoirs after Taylor (1974): MotherLode; Böhlke and Kistler (1986), Marshall and Taylor (1981), Weir and Kerrich (1987): Bridge River; Maheux (1989): Cassiar; Nesbitt et al. (1986).

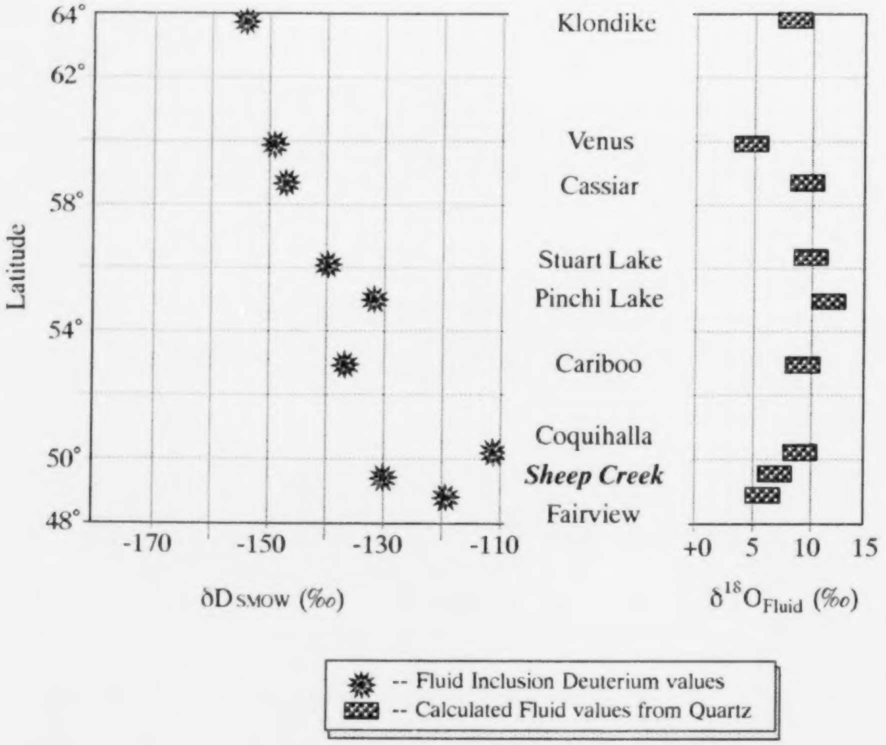

Figure 4.6. Latitudinal variations in deuterium ratios of fluids extracted from fluid inclusions plotted with calculated $\delta^{18}O$ values for ore forming fluids from quartz at 300° C using the fractionation equation of Matsuhisa et al. (1979). Figure is redrawn from Nesbitt et al.(1989), Klondike data from Rushton (1991).

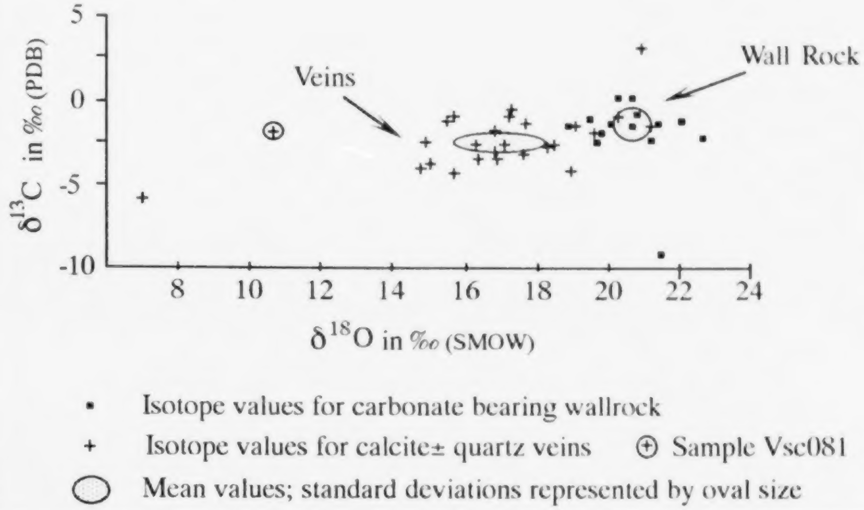

Statistics: Vein carbonates (Observations = 24)

$\delta^{13}C_{V.Carb}$ Range = (-5.8 <> -0.4 ‰) Mean = (-2.5 +/- 1.3 ‰)

$\delta^{18}O_{V.Carb}$ Range = (+7.0 <> 21.4 ‰) Mean = (+16.8 +/- 2.7 ‰)

Statistics: Wall rock carbonates (Observations = 13)

$\delta^{13}C_{Lst}$ Range = (-9.3 <> +0.34 ‰) Mean = (-1.9 +/- 2.4 ‰)

$\delta^{18}O_{Lst}$ Range = (+18.9 <> +22.7 ‰) Mean = (+20.6 +/- 1.1 ‰)

Figure 4.7. Carbon vs. oxygen isotope plot for vein (calcites) and wall rock carbonates (limestones and argillaceous limestones) from the Sheep Creek Camp and district.

SHEEP CREEK OXYGEN ISOTOPE PAIRS

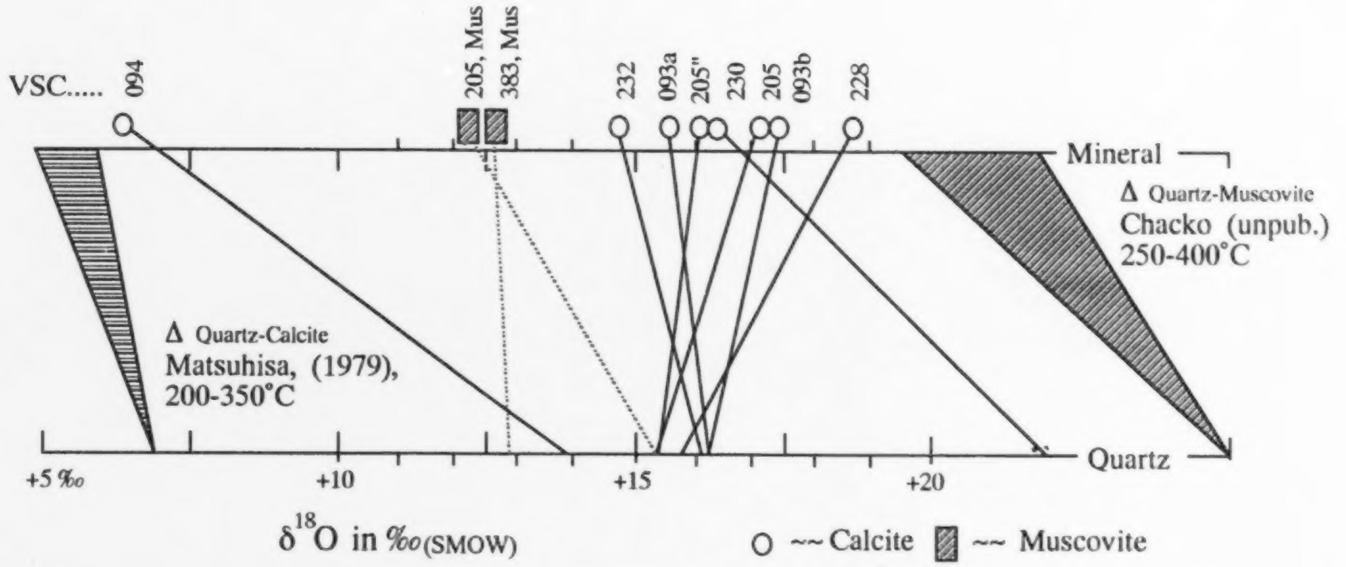

Figure 4.8. Exchange equilibrium diagram for vein quartz-calcite pairs and quartz-muscovite assemblage, illustrating isotopic equilibrium-disequilibrium relationships. Data indicates that some pairs may be in equilibrium whereas disequilibrium pairs are probably due to: 1) different stages of mineral deposition (late calcite or muscovite) or; 2) re-equilibration of mineral phases with post-depositional metamorphic or hydrothermal events.

TABLE 4.1
OXYGEN, DEUTERIUM & CARBON LIGHT STABLE ISOTOPE DATA SHEEP CREEK GOLD CAMP AND DISTRICT

Sample	T(h) °C	Rock Type	$\delta^{18}O_{Qtz}$ Vein	$\delta^{18}O$ Quartzite	δD_{Fline}	δD_{Wr} ($\delta D_{(Methane)}$)	$\delta^{13}C_{Carb}$ Vein	$\delta^{18}O_{Carb}$ Vein	$\delta^{13}C_{Lst}$	$\delta^{18}O_{Lst}$	$\delta^{13}C_{Fline}$ (CO_2:CH_4)
Vsc001		Qtz vein in qtzite	12.8		-95.0						
Vsc001b		Qtzite		11.7							
Vsc002		Qtz vein in qtzite	13.1								
Vsc006		Qtz vein in qtzite	11.1		-156.0						
Vsc007		Qtz vein in qtzite/Gal	12.4								
Vsc008b		Qtz vein in qtzite/Chl	12.2								
Vsc009		Qtz vein in Reno argil	15.5		-143.0						
Vsc010		"/ Limonite & mus	15.4								
Vsc012		Qtz vein in Reno argil	15.7								
Vsc012		"	16.4								
Vsc013		Qtz vein/py	14.6		-145.0						
Vsc014		Qtz vein/py,sph	13.8		-127.0						
Vsc015		Qtz vein/py	13.9								
Vsc017		Qtz vein/py,sph	15.3								
Vsc019		Qtz vein/py,sph,	13.8								
Vsc021		Quartzite				-116.0					
Vsc022	310	Qtz vein in qtzite	13.6		-138.0						
Vsc023		Qtz vein/ sph	12.4								
Vsc028		Qtz vein/py	13.3		-150.0						
Vsc031		Qtz vein			-145.0						
Vsc039		Quartzite				-112.0					
Vsc042	330	Qtz Vein: Minor Gl	11.6		-143.0;-125.0	(-243.0)					
Vsc042b		Quartzite									
Vsc043		Qtz vein		12.6	-101.0						
Vsc043b		Quartzite		11.0		-77.0					
Vsc045		Qtz vein/py, gal, sph			-134.0						
Vsc051		Qtz vein			-127.0						
Vsc061		Qtz vein/py, gal			-136.0						
Vsc066		Barren Qtz Vein			-111.0						
Vsc073		Qtz vein/ py			-171.0						
Vsc 081		Cc,Palygorskite vein					-2.2	11.1			

Sample	T(h) °C	Rock Type	$\delta^{18}O_{Qtz}$ Vein	$\delta^{18}O$ Quartzite	δD_{Fline}	δD_{Wr} ($\delta D_{(Methane)}$)	$\delta^{13}C_{Carb}$ Vein	$\delta^{18}O_{Carb}$ Vein	$\delta^{13}C_{Lst}$	$\delta^{18}O_{Lst}$	$\delta^{13}C_{Fline}$ (CO_2:CH_4)
Vsc083		Cc vein/ gal					-3.4	16.9			
Vsc093a		Qtz Vein /py,sph,gal	16.3		-126.0		-4.2	15.7			(+0.9: ?)
Vsc093a		discordant to	16.3								
Vsc093b		Limestone wall rock					-0.9	17.2			
Vsc093b							-0.4	17.3			
Vsc094	300	Quartz Vein/ py	13.9		-130.0		-5.8	7.0			
Vsc094		in Carbonate bearing	14.6								
Vsc094		Quartzite	15.4								
Vsc096		Quartz-(Calcite) vein					-2.5	14.9			
Vsc097		Qtz vein /py, cpy	19.6		-167.0						
Vsc102	314	Qtz vein in quartzite	14.3		-162.0	-52.0					
Vsc107		Qtz vein in quartzite	12.8								
Vsc118		Vein-Wlr, Breccia				-110.0					
Vsc128	295	Qtz vein/ ser,chl				-82.0					
Vsc130		Qtz Vein/ gal, py, limonite			-104.0	(-176)					(-16.3: -24.6)
Vsc141		Massive-Quartz Vein			-111.0						
Vsc148		Massive-Quartz Vein			-143.0						
Vsc150	265	Massive-Quartz Vein	13.3		-102.0	-94.0					
Vsc163		Quartz Vein	13.2		-122.0						
Vsc172		Recrystallized qtz?/qtzite				-99.0					
Vsc180		Quartz vein in Lst.					-1.3	17.7			
Vsc188	270	Quartz Vein/ mus,tour	14.9		-141.0						
Vsc192		Calcite in felsic dyke					-1.8	16.8			
Vsc193		Vuggy grey QuartzVein	13.7		-117.0						
Vsc193		"	24.0								
Vsc205	260	Qtz vein/ ser,bio	15.3		-130.0		-2.6	17.0			
Vsc205'	260	cc,siderite, Gold	15.4		-135.0	(-145)	-3.2	16.1			(-8.6: -23.7)
Vsc212		Quartz Vein/ Hematite			-164.0						
Vsc214		Quartzite/ ser		11.2		-53.0					
Vsc214		"				-59.0					
Vsc224	244	Quartz vein/Stag Leap	13.3		-131.0						
Vsc225		Quartzite/ Stag Leap				-79.0					
Vsc228	280	Qtz-Cc /py,chl Stag Leap	15.8		-216.0	-51.0	-2.6	18.5			
Vsc230		Quartz vein /cc	21.9		-104.0	-104.0	-3.0	16.8			
Vsc230					-116.0						

Table 4.1: Cont. PAGE 2

Sample	T(h) °C	Rock Type	$\delta^{18}O_{Qtz}$ Vein	$\delta^{18}O$ Quartzite	δD_{Flinc}	δD_{Wr} ($\delta D_{(Methane)}$)	$\delta^{13}C_{Carb}$ Vein	$\delta^{18}O_{Carb}$ Vein	$\delta^{13}C_{Lst}$	$\delta^{18}O_{Lst}$	$\delta^{13}C_{Flinc}$ (CO_2:CH_4)
Vsc232		Quartz vein/Cc	16.1				-4.0	14.8			
Vsc232b		Spotted Schist/Cc					-3.4	16.5			
Vsc234	242	Qtz vein/ bio,chl			-105.0	(-138)					(?: -28.5)
Vsc238		Quartzite				-65.0					
Vsc248		Quartz vein			-144.0						
Vsc254		Blue Qtz vein/py	13.9		-160.0	-111.0					(-7.6: ?)
Vsc254	270	from Yellowstone Mine	14.4		-143.0						
Vsc254		FeO, (Gold?)	13.4								
Vsc258		Qtz vein/ py,chl,ser			-128.0						
Vsc265	320	Qtz vein/FeO in	25.8		-125.0						
Vsc265'		Active Frm, slates	22.7								
Vsc288		Qtz vein in qtzite			-127.0						
Vsc355		Qtz/ cc vein					-2.6	16.3			
Vsc356	-32.6	Qtz vein in Laib Argill.			-151.0	-121					(-25: -26.1)
Vsc357	250	Qtz/cc vein in Lst					-3.2	17.6			
Vsc357a		Qtz/cc vein in Lst					-2.7	18.3			
Vsc357b		Cc extension of #357					-1.1	15.5			
Vsc357b		Cc extension of #357					-0.9	15.7			
Vsc364	312	Vuggy Qtz vein			-121.0						(-2.0: ?)
Vsc372		Qtz vein in qtzite			-86.0;-77.0	(-160)(-228)					(-5.9: -25.9)
Vsc383	310	Qtz,ser,tour vein	12.9		-109.0						
Vsc400		Druzzy Qtz on Bull Qtz			-130.0						
Vsc417		Qtz vein in Lst	11.2			-91.0					
Vsc420		Quartzite/ sericite		11.6		-74.0					
Vsc420		Quartzite/sericite		12.8							
VscGB01	290	Qtz vein/ py, Gold	13.7		-112.0						
VscGB01		"	14.8								
VscHe02		Marblized-vein					-3.7	14.9			
RB 120		Qtz vein/ Windermere	9.2		-107.0						
RB121		" in Amphibolite and	8.8								
RB122		Schists	9.8		-114.0						
RB123		Qtz vein/ Stag Leap	14.6		-116.0						
SC-2		Massive Qtz vein/ser	14.0								
SC-6		Coarse Qtz vein/py	14.2								
SC-8		Qtz vein/py	14.5								
SC-11		Qtz vein/py	12.5								

Table 4.1: cont. PAGE 3

Sample	T(h) °C	Rock Type	$\delta^{18}O_{Qtz}$ Vein	$\delta^{18}O$ Quartzite	δD_{Fline}	δD_{Wr} ($\delta D_{(Methane)}$)	$\delta^{13}C_{Carb}$ Vein	$\delta^{18}O_{Carb}$ Vein	$\delta^{13}C_{Lst}$	$\delta^{18}O_{Lst}$	$\delta^{13}C_{Fline}$ (CO_2:CH_4)
SC-12		Vitreous Qtz vein/py	16.3								
Vsc097		Qtz vein in Vsc098/py					-1.8	19.8			
Vsc097							-1.7	19.0			
Vsc98		Argil,Lst intercalation							-1.7	19.7	
Vsc218		Qtz vein in Argil/Lst.					3.4	20.9			
Vsc218b									-9.3	21.5	
Vsc220		Cc vein in Lst,					-1.3	21.4			
Vsc352	329	Qtz,cc Vein in Argil Lst					-1.0	20.3			
Vsc353		Argil. Lst.							-1.3	20.1	
Vsc358		Laib Lst.							-1.2	22.1	
Vsc358b		Laib Lst.							0.3	20.7	
Vsc358b									0.3	20.3	
Vsc371		Lst.							-2.2	22.7	
Vsc416		Lst,Qtz intercalated Wlr							-2.4	19.7	
Vsc421		Lst							-1.5	20.7	
Vsc421b		Limestone							-1.4	21.2	
VscHc01		Hidden Crk Marble							-2.2	21.2	
VscHc02		Marble					-3.7	14.9			
Vsc315		H.B. Pb-Zn							-1.0	19.5	
Vsc315		Replacement Lst.							-1.4	18.9	

Sample	Rock Type	$\delta^{18}O_{Mu}$	δD_{Mu}
Vsc034	Sericite	10.2	-94.0
Vsc205'	Muscovite	12.3	-58.0
Vsc383	Muscovite	12.7	-75.0

Table 4.1. Compilation of light stable isotope values from Quartz veins and quartzites: ($\delta^{18}O_{Qt}$; $\delta^{18}O_{Qtzite}$). Volatile phases as recovered from decrepitation of fluid inclusions: δD_{Fline}, δD_{Wr}, $\delta D_{(Methane)}$, $\delta^{13}C_{Fline}(CO_2:CH_4)$ and oxygen and carbon values from carbonate bearing veins: $\delta^{13}C_{Carb}$,$\delta^{18}O_{Carb}$ and limestones or calcareous argillites: $\delta^{13}C_{Lst}$,$\delta^{18}O_{Lst}$. T(h) °C is temperature of homogenization from the fluid inclusion study (see Chapter 3). Abbreviations used in table include: Wr=whole rock; Wlr=wall rock; Qtz=quartz; Qtzite=quartzite; Py=pyrite; Cpy=chalcopyrite; Gal=galena; Sph=sphalerite; Chl=chlorite; Ser=sericite; Mus=muscovite; Bio=biotite; Cc=calcite; Lst=limestone; Argil=argillite; Tour=tourmaline

Table 4.1: cont. PAGE 4

CHAPTER V

COMPARISONS AND DISCUSSION

"Mesothermal gold deposits of all ages, from Archean to Cenozoic have similar structural, mineralogical and geochemical characteristics (Hodgson et al., 1982; Kerrich, 1989a), implying a singular, rather than multiple genetic process" (Kerrich, 1991). With this rather unifying statement in mind, the geological and geochemical characteristics of the Sheep Creek gold camp are discussed in relationship to the well established parameters that define a mesothermal lode gold deposit.

Genetic hypotheses are numerous, vary broadly from those that suggest syngenetic processes to those that argue epigenetic to those that incorporate portions of more than one hypothesis. The genetic hypotheses are important regarding exploration, as it is the models that define certain depositional parameters from which explorationists imagine and test for the presence of new ore. The persistent and perennial controversy that surrounds the origins of these deposit types will probably not be resolved within the near future and the importance of these ongoing debates lies in the fact that the research will thus continue. A short discussion of the more prominent genetic models will follow the mesothermal gold deposits character comparisons section below.

Comparisons of Parameters;

Fourteen parameters regarding the overall character of Phanerozoic mesothermal lode gold deposits are presented and discussed in Nesbitt's (1991) contribution (Cpt. 4 "Phanerozoic gold deposits in tectonically active continental margins") to "Gold Metallogeny and Exploration" edited by R.P. Foster. It is around this synthesis of characteristics that the comparisons of the Sheep Creek gold camp are made. From this it will be made apparent that the Sheep Creek Camp is indeed a mesothermal gold system and should not be considered as an epithermal, Carlin-type, magmatic or an auriferous massive sulphide deposit, although some of it's characteristics do overlap with some of these classes of gold deposits. Note that following each of the fourteen parameters is the description quoted from Table 4.1 of Nesbitt (1991) and these quotes will be referenced only once.

TECTONICS "Typically in accreted, deformed and metamorphosed continental margin or island arc terranes" (Nesbitt, 1991).

In chapter two it has been shown that not only is the Sheep Creek Camp multiply deformed and poly-metamorphosed but the geological setting of the camp has been documented as an ancient continental margin. The camp is located about 10 km east of the accreted terrane suture zone which juxtaposes the western 'exotic' Quesnellia terrane from the thick and extensive sequence of miogeoclinal metasediments located to the east of the suture and onlapping the western flank of the Purcell Anticlinorium. Deformation and metamorphism are reviewed in some detail below.

SIZE AND GRADE "Generally several hundred thousand to a few million tonnes, typically 5-25 g/t"

The Sheep Creek Camp has supplied numerous mills with approximately 1.7 million tonnes of ore from which more than 750,00 ounces of gold have been recovered. The recovery rate at the time of the major workings was generally less than 70 % and from this, an average ore grade (assuming 100% recovery) would be approximately 17 g/t.

HOST LITHOLOGY "Widely variable; graywackes-pelites, chemical sedimentary units, volcanics, plutons, ultramafics"

The association of these types of deposits with any one rock type does not occur. The mineralization in the Sheep Creek veins does however have an affinity for the quartzites of the Nugget and Navada Members of the Quartzite Range Formation as well as for the argillaceous quartzites of the Reno Formation in the vicinity of the Reno mine. The physical association of these host rocks and the gold mineralization is difficult to determine because of the compounded influences of rock competencies, faulting and variabilities in primary and or secondary permeabilities. The chemical influences at the sites of precipitation are equally interesting in that, in those veins that occur in quartzites the recovered metal is primarily Au, and in those vein fractures which intersect carbonate bearing host rocks, the increase in galena, sphalerite, and Ag, As, Sb bearing minerals is significant and has resulted in a modest recovery of Pb, Zn and Ag, (eg. Ore Hill, Sumit mines).

METAMORPHISM "Typically sub-to upper greenschist; occasionally host terranes were metamorphosed to higher grade prior to mineralization."

As has been discussed, the host rocks exhibit upper greenschist grade metamorphism with indications that amphibolite grade rocks underlie and/or contain significant portions of the high grade vein system. The key phrase here though is: "...higher grade prior to mineralization." Other than the recognition that this vein system post-dates all or (most ?) deformation and metamorphism it is not at this time possible to constrain the temporal relationships of the regional or contact metamorphism to the main vein event.

RELATIONS TO PLUTONS "Variable; some areas close spatial and probable genetic link; other districts no evidence of plutonic activity."

The Sheep Creek Camp is not only surrounded by a plethora of intrusive bodies ranging in compositions from granites to diorites and spanning approximately 80 Ma, (if not more, ie. Eocene,Coryell intrusive bodies in the region) it is partly underlain by granitoids and is cross cut by aplitic and lamprophyric sills and dikes. The possible genetic relationships of these bodies to the gold veins is difficult to surmise. That a genetic relationship exists is highly possible but whether the relationship entails fluid sources, metal sources and/or sources of heat cannot be unequivocally stated. Fluid inclusion and stable isotope research suggest that the plutonic bodies were not significant factors regarding fluid sources. Similar vein structures found crosscutting many of the plutonic bodies in the region indicates that these local mineralization events occurred late relative to the specific pluton, however other bodies (eg. Salmo Stock) show no signs of hydrothermal alteration and/or mineralized veining which suggests that the pluton was emplaced during or after the Sheep Creek mineralization event.

The lamprophyre dikes, which both pre-date and post-date the vein system are the most temporally constrained of all the intrusive bodies and if these rocks were dated the timing of the mineralization would be better understood. The aplitic sills and dikes are for the most part considered as post-dating the mineralization and could also assist in constraining the period of mineralization if geochronological work was undertaken.

The probability that these plutonic bodies influenced and/or produced significant thermal gradients within the camp and district and did so over extended periods of time, is very high. The thermal complexities caused by these plutonic bodies in concert with the regional metamorphic processes (geothermal gradients) and the regional faulting systems is rather staggering and therefore cannot at this time be resolved into any type of simple thermal or hydrothermal circulatory model.

STRUCTURE "Varies from fold to fault control: where fault controlled, mineralization is generally confined to second-order faults related to major structures."

The mineralization is confined to the east-trending vein fracture system, which could be considered as a second-order structure with respect to the regionally significant shear (?) thrust faults located along the western margin of the camp (ie. Black Bluff, Argillite, Tillicum and Waneta faults). East of the camp, regional scale fault structures could include the Blazed Creek and Purcell Trench faults. Although the relationship between these regional structures and the vein fractures has not been studied directly, the probability of tectonic or crustal relationships does exist and may have direct bearings upon the origins of the Sheep Creek veins. Alternatively, or additionally, the complex folding that characterizes the region could have had a compounding (in association with the fault systems) influence upon vein formation. The majority of the mineralization has been mined from the upper limbs and axial regions of the Western and Eastern Anticlines but even more interesting is the observation that the major producers, the Reno and the Queen mines, occur at, or near to, the crest (?) of a third-order flexure (hinge region of the cross folds) and the trough of a similar structure to the south, respectively. This observation could be considered further and applied to other veins if more detailed structural research was available, however the precise locations and attitudes of the third-order folds is not well understood. Whether the Ore Hill-Sumit mine group of veins and the Motherlode, Nugget group of mines exist in these flexural regions, cannot at this time be argued.

TIMING "Late in orogenic sequence; subsequent to principal deformation and metamorphism."

Crosscutting relationships have shown that the mineralization post-dates principal deformation and similarly post-dates regional metamorphic structures as well as local contact metamorphism (ie. hornfels of the Reno Formation, within which is the Reno mine). Geochronological studies of the neighbouring granitoids indicate that at least locally, (ie. the Sheep Creek Stock) the plutonism pre-dated veining (Archibald, 1983) however, further constraints on these relationships cannot be made. The aplites and lamprophyres, as discussed above, could prove to be important temporal indicators.

One point of interest is the observation of metamorphic minerals in some of the non-mineralized veins and within portions of some of the deeper sections of the vein fractures. This late metamorphism is possibly coeval with the Eocene extensional tectonism that occurred in the region (Parrish et al., 1988), though the lack of geochronological support (in the immediate vicinity) for this event suggests that the latest moderate temperature (>250 to <500°C) event in the Sheep Creek Camp occurred in the mid-Cretaceous, about 98 Ma ago.

ORE MORPHOLOGY AND TEXTURES "Thick quartz veins, typically banded, occasionally vuggy with high grade ore shoots; vertically continuous mineralized zones; occasional stockwork and disseminated mineralization."

The discontinuous, high-grade (>5 oz/t to ≈ <10 oz/t) ore shoot nature of the Sheep Creek Camp has been documented since the first ore was mined. These shoot structures occur within the milky-white, massive to laminated, vertically and areally extensive quartz veins. Occasionally the vein structure is a zone of interlayering of en-échelon veins and wall rock. Other veining textures that have been recognized are characteristically crack-seal brecciations, located in zones surrounded by relative pristine massive or laminated veining (Mathews,1953). Though much of the veining is massive, a significant proportion of the system is banded (sulphides (pyrite) and quartz) parallel to the trend of the vein-wall rock margins.

That the ore seems to diminish in grade at depth is arguably atypical for these types of deposits. There is no confirmation of this actually occurring and it has been repetitively proven to be a false claim as new workings, at depth in old mines, have proven to be very successful, such as within the Queen, Black and Reno mines. The complex overall morphology and variable attitudes of these generally steeply-dipping structures indicates the possibility of late or coeval movement of the entire lithological package and this is further substantiated by the protracted and interrupted paragenetic sequence.

MINERALOGY AND PARAGENESIS " Early phases: quartz, Ca-Mg-Fe carbonates, arsenopyrite, pyrite, albite, sericite, chlorite, scheelite, stibnite, pyrrhotite, tetrahedrite, chalcopyrite, tourmaline. Late phases: gold, galena, sphalerite, tellurides"

The relatively simple mineralogy and paragenesis of the camp corresponds well to the parameter summarized above (see paragenesis in chapter II) , except for the lack of stibnite (at least, it has not been documented) and plagioclase and/or potassium feldspars have only rarely been observed in the veins. A general paucity of carbonates in the main structures is noted although zones with considerable carbonate do occur as the veins approach carbonate bearing host rocks.

The relationship of the base-metal sulphides and the carbonate bearing rocks has been discussed and leads to the question regarding the causes of mineral assemblage precipitation. There are at least four different and independent possible physicochemical realms which could result in precipitation and in any given solution several effects may be operating simultaneously. The issue of mineral precipitation will be 'lightly' addressed later within this chapter.

HYDROTHERMAL ALTERATION

"Carbonatization, albitization, sericitization, silicification, sulphidation, chloritization; listwanite development"

Minimal hydrothermal alteration of the host rock has been observed in the camp with silicification being the most prominent type of alteration. Minor sericitization and some sulphidation has also occurred. The general presence of relatively pure silici-clastic host rocks, extremely low primary permeabilities in the quartzites and the simple chemical compositions of the hosts are probably the most significant factors controlling the observed simple hydrothermal alteration. Some carbonatization and chloritization has been observe in those host rocks that exhibit more complex primary chemistry (argillites, calcareous argillites, lamprophyres and granites). This type of alteration (host rock dependent) is one of the most significant geological-geochemical characteristics of the mesothermal gold deposits and argues for the single process alluded to by Kerrich (1991).

ZONING AND ELEMENTAL GEOCHEMISTRY

"Au:Ag typically >1; associated elements: Ag, Sb, As, W, Hg, Bi, Mo, Pb, Zn, Cu, Ba. Zoned from high-temperature Au±Ag, As, Mo,W, to Sb±Au, Hg, W, to Hg±Sb"

For the most part Au is the primary metal produced from these veins except for those veins that are associated with carbonaceous/ calcareous wall rocks. Au:Ag ratios in the main Sheep Creek vein system (from production records) are consistently greater than 1, whereas the increased presence of Ag has been observed in all veins that have increased base metal contents. Hg and Mo are the only asociated elements that have not been documented to occur in these deposits (Robinson,1949) although Mo has been recovered from the mines located to the southwest. The tectonic, geochemical, structural and mineralogical relationships of the mines of the Salmo lead-zinc Belt (figure 2.2, including Jackpot, Aspen, H.B., Feeney, Emerald, Jersey, Tungsten King, and Trueman) and the Sheep Creek Camp have not been adequately researched and much controversy presently exists regarding their relationships and genesis so the observed presence of Mo, from less than 5 km to the southwest of the camp, should not be considered as part of the elemental geochemistry of the camp (?). Sb, As, W, Bi, Cu and Ba are relatively minor constituents of the ore and occur predominantly as elemental replacements in the more common sulphides and /or rare occurrences as minerals such as tetrahedrite, pyrargyrite-proustite, scheelite and chalcopyrite.

FLUID INCLUSIONS "H20-CO2 inclusions, typical X_{CO_2}= 0.05 to 0.2; < 5 equiv wt.% NaCl; T (homogenization) 250-350°C, p>1000 bars"

Quartz hosted fluid inclusions from mineralized and unmineralized veins display a broad range of compositions from low salinity aqueous inclusions to high density CO_2-CH_4 inclusions. The study showed that the salinity of the H_2O-NaCl±(CO_2-CH_4) was generally relatively low averaging approximately 5 equiv wt.% NaCl, however a number of higher salinity inclusions were observed. The origin of the complex chloride and /or high salinity inclusions could be a function of phase separation of the H_2O-NaCl±(CO_2-CH_4) fluids resulting in the concentration of chlorides in the high salinity aqueous inclusions. Local lithological heterogeneities (eg.. west of sample Vsc 042) where the vein fluids possibly transgressed carbonaceous-calcareous argillites or argillaceous quartzites could have incorporated higher concentrations of dissolved chlorides prior to deposition. Another possible explanation for the sporadic high salinities could include the infiltration of local magmatic devolitalizations (fluids) into portions of the otherwise low salinity hydrothermal system.

The probability that portions of the hydrothermal system underwent phase separation has been argued and accounts for the extreme variability in inclusion compositions (see figure 3.8). Phase separation is also one of the most probable mechanisms for ore precipitation and that this is observed in regions of major mineralization (eg. Reno mine) and not observed in barren locales, further substantiates the argument.

One of the most interesting observations to come out of the fluid inclusion study is the possibility of a CH_4 'front', where CH_4 is observed in the inclusions to the west of the 'front' and zero to very low X_{CH_4} is observed in inclusions to the east (see. figure 3.2). One explanation for this observation is that the vein forming fluids evolved compositionally in response to local lithological heterogeneities which is why CH_4 bearing inclusions are invariably intimately or proximally associated with carbonaceous ± calcareous argillaceous units and all the veins from the eastern regions, where the host rocks are invariably pure siliciclastics, are CH_4 free. That methane is observed in some of the mine veins could suggest that some of the fluids associated with mineralization had interacted with the carbonaceous ± calcareous argillaceous units of the Active Formation, (Laib Formation (?)), located immediately to the west of the camp.

Pressure fluctuations are considered to be one of the mechanisms for vein precipitation (Sibson et al., 1988) and the observed (estimated) ranges in inclusion densities probably reflects these pressure fluctuations. A general estimation of high pressures of formation (>1.0 to <2.0 kbars) has been documented from the inclusion study and this is consistent with those pressures observed in the majority of these types of deposits.

Temperatures of homogenization range from a low of 160°C to a high of near 400°C however the bulk of the inclusions studied either homogenized or decrepitated around 280±50°C which is a reasonable homogenization temperature for these types of systems. Temperatures of trapping (Tt) were very near to this value (280°C; theoretically equal to Th values) for those systems that were undergoing phase separation and Tt values for single phase fluids could be moderately (+50-80°C) higher depending upon the pressures at the time of trapping (pressure corrected Th values, see diagrams 3.09 and 3.10).

STABLE ISOTOPES "Typical values: $\delta^{18}O$ (Qz)=+11 to +18‰; $\delta^{13}C$ (Cb)=-25 to -3‰;
δD (fluid inclusions) = -160 to -30‰, $\delta^{34}S$ = -10 to+10‰ "

A stable isotope study of the vein quartz, the fluid inclusion fluids, vein carbonates, host rock carbonates and fluid inclusion 'gases' has shown that in all likelihood, the significantly most important fluid source for these veins was evolved meteoric ($\delta^{18}O_{Fluid}$= +7.8‰; δD=-129‰; see figure 4.5). Local lithological heterogeneities and/or homogeneities of host rocks were possibly responsible for not only the variability in $\delta^{13}C_{CO_2}$ values but could also be responsible for the observed ranges in $\delta^{13}C_{CH_4}$ (-23.7 to-28.5‰) and the significant variability in δD_{CH_4} values which range from -243 to -138 ‰. At this time the data set is much to small to make any type of formal statement on the observations and the above comment is obviously only a possibility. Interpretation of the carbon isotopes is interestingly enough often times more a function of the particular genetic model the researches invoke rather than the opposite, which suggests that the interpretation of the isotope data should invoke a genetic hypothesis.

By the same notion, vein carbonate isotope values possible reflect local host rock carbonates suggesting that these carbonates were carbon sources for the vein bound carbonates. Carbonate isotopes are also considered here to have been reset as a result of post-depositional re-equilibration reactions and are consequently not considered as viable for geothermometry. No mineral pairs from the isotope study were considered to be candidates for geothermometry because of inconclusive temporal relationships of the pairs and the general presence of post-depositional alteration. A $\delta^{34}S$ value reported by Nesbitt (1988) for pyrite from ore-grade vein material from the Sheep Creek is +12.7 ‰, and a value of +11.5‰ for H2S was calculated from the sulphur isotope fractionation equation of Ohmoto and Rye (1979).

RADIOGENIC ISOTOPES "Indicate heterogeneous crustal sources for Sr, Pb and Nd"

Although it is beyond the scope of this study the Pb-Pb data from lamprophyres indicate that they were influenced by significant crustal interaction. Without a complete radiogenic isotope study, any type of comment on the observed Pb-Pb data is merely conjecture and should not be considered as anything but conjecture.

Preliminary Sr-Sr analyses of vein carbonates reflect the high values (Sr^{87}/Sr^{86} = 0.711-0.723 (five analyses); Koffyberg, unpub..data.) that have been observed in this portion of the Kootenay Arc in other studies (Armstrong,1988) who has interpreted these high Sr^{87}/Sr^{86} ratios as being a result of underlying Precambrian crustal influences which have been incorporated into the younger magmas. The values recorded from the calcites in the Sheep Creek are also strongly suggestive of a crustal origin suggesting provinciality for the sources of fluids and the mineral constituents.

A summary of some of the significant characteristics of this type of deposit is depicted in figure 5.1. From a consideration of estimated pressures of trapping ranging from 1-1.5 kbars, and assuming a slightly suprahydrostatic pressure gradient of approximately 0.11 kbar/km (pressure fluctuations have been documented) an estimated depth range (9.0 to 13.5 km) for formation is established. The characteristics depicted along the 11 km depth line in figure 5.1 corresponds to many of those observations presented in the preceding discussion.

THE SHEEP CREEK CAMP and THE PAMOUR #1 MINE,Ontario;

A General Comparison of a Proterozoic and an Archean Mesothermal Lode Gold Deposit:

The intent of the following discussion is not to belabour the issue of common characteristics in these deposits but to present a couple of salient points regarding fluid compositions and a probable mechanism for gold deposition.

The Porcupine Camp is known to have produce in access of 69 million ounces of gold (Bertoni,1983) and many of the mines are characteristically wall rock-hosted gold bearing disseminated pyrite mineralization. (Wood et al., 1986). Spooner et al. (1985) suggests however, that the similarities in chemical and isotopic compositions of the veins and the surrounding mineralized wall rock are a result of the same fluids. In contrast to the disseminated gold deposits observed in these mines, Walsh et al., (1988) have completed detailed fluid inclusion work on the quartz-carbonate, vein hosted Pamour #1 gold deposit and this work held in comparison with inclusion characteristics of the Sheep Creek Camp reveals some interesting similarities.

The Pamour #1 mine is located within a few kilometres of the Destor-Porcupine Fault Zone and is part of a 5-km-long zone of mineralization including the Broulan Reef, Hallnor and Hoyle mines. The Pamour mine is found near the unconformable contact between the Tisdale Group (predominantly ultramafic to felsic volcanics with intrusive equivalents) and the Porcupine Group (metasediments, dominantly turbidites, graywackes and conglomerates). The Pamour #1 is hosted by overturned bedding (on the north limb of an overturned syncline) with ore being found in basalts, pervasively altered mafic and ultramafic flows, graywackes and conglomerates. Pre-ore faults and shear zones host the majority of the mineralization and "Styles of mineralization vary in the different lithologies, however, apparently reflecting differences in the competence of rock units" (Walsh et al.,1988). Gold in the veins occurs as erratic distributions (ore shoots) and has been observed to increase in grade at higher levels within the vertically extensive vein structures.

Hydrothermal alteration at the Pamour is quite complex as compared to the alteration observed at the Sheep Creek and can up to 100m of mineralogical assemblages including chlorite+carbonate±albite, carbonate+sericite±chlorite and combinations of these. Alteration of the graywacke hosted TN vein is somewhat less complex and includes arsenopyrite-sericite-dolomite-magnetite grading outwards into sericite-dolomite-pyrrhotite. Walsh et al.(1988) suggest that, "Both alteration patterns indicate addition of K, CO_2, As, S and Ca to the wall rocks and depletion of Na.

Fluid inclusion analyses of the Pamour quartz and sphalerite, resulted in the delineation of three types of inclusions. Type I inclusions are CO_2-CH_4 rich inclusions with no aqueous phase discernable. These inclusions would compare to the Type Cx inclusions described in this study. Type II inclusions are composed of 'carbonaceous' fluids (this study's carbonic phase) and an H_2O±NaCl phase. These inclusions are compared to those described in this study as Type Ch and Type C. Their third inclusion type, Type III, are two phase (vapor and liquid) at room temperature and are composed of H_2O±NaCl eq. This type is synonymous with Type A and Type As of this study. Analyses of leachates and decrepitation residues of these inclusions identified Na and K and minor amounts of Ca and Mg as the principal cations and chloride as the dominant anion.

The critical comparison of these inclusions is the presence of the Type I (Cx) non-aqueous, carbonic inclusions and the complex, Type II (Ch and C) inclusions which exhibit variable salinities ranging from 2-9 eq.wt.% NaCl. The Type III (A and As,?) inclusions in the Pamour study had relatively low homogenization temperatures and may not be directly comparable to the aqueous inclusions in the Sheep Creek study

Walsh et al. (1988) have interpreted the assemblage of Type I and Type II inclusions as representing immiscible fluids that were trapped at pressures of 1 to 2 kbars at temperature of 325±25°C along the H_2O-CO_2-CH_4±NaCl solvus and suggest that the separation of the fluid would increase the fO_2 and increase the pH of the residual fluid as

CO_2, CH_4, and H_2S would partition into the carbonaceous phase. The CO_2 immiscibility would decrease the solubility of the bisulfide-complexed gold (the assumed significant gold complex in these types of systems) and this would result in gold deposition They further suggest that decreasing temperature was not the physicochemical mechanism responsible for phase separation and refer to the fault -valve mechanism (Sibson,1988) which causes fluid pressures to cycle between pre-failure lithostatic (suprahydrostatic) and post-failure hydrostatic pressures.

This mechanism is ascribed to the vein fracture system of the Sheep Creek Camp on the grounds that the veins of the Sheep can be interpreted as being formed near the brittle-ductile (frictional-quasi plastic) transition zone as discussed by Sibson, (1991) and Nesbitt et al. (1989). The fractured, sheared and multiphased veining (protracted) process observed in the veins of the Sheep Creek Camp which overlie a region of upper greenschist, amphibolite facies rocks and the estimated temperature of formation near 300°C support this proposition.

GENETIC HYPOTHESES:

The evolution of thought regarding the origins of mesothermal gold deposits has expanded considerably in breadth and in depth and as a result of this significant expansion of knowledge as well as the complexities of their geological settings, a multitude of genetic models or hypotheses have been developed in an attempt to understand the genetic processes involved and to account for their characteristic spatial and temporal geological associations.

Mesothermal Au systems have been variously ascribed to : lateral secretion, exhalative processes, multistage exhalative remobilization, tonalite-trondhjemite-granodiorite (TTG) magma suites, oxidized felsic magmas, lamprophyres, mantle CO_2-granulitization, evolved meteoric water circulation, metamorphic replacement, devolatilization or metamorphism at collisional boundaries (Kerrich,1991).

Most of the models can account for some of the parameters discussed above and some of the models can account for most of the parameters (eg. metamorphic devolatilization, Fyfe and Kerrich, 1984; Goldfarb et al., 1988 and evolved meteoric convection, Nesbitt et al., 1989)

The metamorphic devolatilization model is perhaps one of the most reasonable models as it, unlike most of the other hypotheses can account for the bulk of the variabilities observed in these systems. Two persistent complications however plague this model. Most, if not all of the mesothermal vein systems post-date peak metamorphism (Groves and Phillips, 1987) and this is rather inconsistent with maximum devolitalization, which is necessary to produce these veins, yet occurs during prograde metamorphism. Kerrich (1991) argues that in regions of crustal thickening (collisional belts), peak metamorphism at depth will post-date metamorphism at the brittle-ductile transitional zone by up to 40 Ma, and this can, he suggests, account "...for the apparent inconsistency of metamorphic fluids generated at depth overprinting peak metamorphic assemblages at shallow crustal levels". This process of metamorphic overprinting does not adequately address the question of the quantity of fluids necessary to produce these massive vein systems. Another point worth considering here is that the associated metamorphic assemblage is invariable composed in part by hydrous silicates suggesting that complete devolitalization of the ductile lithologies has not occurred, further supporting the notion that the metamorphic process would produce inadequate quantities of fluids.

A further refinement of the metamorphic devolatilization model involves the generation of fluids by dehydration during a second metamorphic event during subcretion of material at a destructive collisional boundary (Wyman and Kerrich, 1988).

The second inconsistency of the metamorphic model is that it does not account for the δD values recorded from isotopic studies of the ore-forming fluids contained in gangue hosted (quartz) fluid inclusions. The latitudinal dependency of the δD values of the vein and ore-forming fluids are significantly depleted from fluids considered to be of metamorphic origin (see figure 4.5 and 4.6). These depleted δD values can be explained by invoking the evolved-meteoric-water convection hypotheses. "The advantage of the meteoric water convection model is that it is consistent with the data generally cited in support of the metamorphic devolatilization model as well as the δD data and the timing relationships between metamorphism and ore formation" (Nesbitt et al., 1989). The similarities of the metamorphic and meteoric hypotheses are well documented.

The meteoric model involves the penetration of meteoric waters through the upper brittle crust to the brittle-ductile transition where a decrease in overall permeability due to the ductile rheology act as a barrier to further penetration. In those regions where there are appropriate heat sources (magmatic bodies, compression, transpression or extension tectonic regimes) convective cell can develop and will circulate these fluids. As the fluids descend and/or circulate through these large masses of rock they will evolve by acquiring the chemical constituents necessary to produce mesothermal (and for that matter epithermal) deposits. These constituents will include CO_2, S, Si, W, As, Sb, and Hg (other metal; Pb, Zn, Ag and volatiles; CH_4) The fluids will also evolve isotopically. At low water/rock ratios the original $\delta^{18}O$ value of the meteoric (possible as low as -20‰) will be influenced by the $\delta^{18}O$ composition of the crustal rocks and as the water interacts with the rock it will evolve or "shift" towards the $\delta^{18}O$ value of the rock (Field and Fiferak, 1985). δD values will not be similarly "shifted" because of the extremely low hydrogen content of rock and as the evolutionary process is dependant upon exchange, the fluids will essentially retain their primary δD signature. At extremely low W/R ratios, deuterium evolution may occur assuming that there are hydrogen bearing rocks with which the waters can interact.

By the time these waters have reached the brittle-ductile transition, they will have evolved chemically, isotopically and thermally, achieving mid-crustal temperature of approximately 300-400°C (Sibson,1983; Nesbitt, 1989). Depending upon the associated geological configuration, simple to extremely complex thermal density gradients will occur and these density gradients can result in simple to extremely complex convective cells. These convective cells will also be intimately associated with permeability zones, such as deep crustal fractures, strike-slip faults and secondary associated fracture zones. Also, depending upon the general associated physicochemical (geological) configuration and ongoing processes; cooling, fault-valve behavior, gradual vertical pressure decreases or direct chemical interaction of the fluids with the wall rocks, deposition of the evolved hydrothermal fluids can occur. The fluids may undergo phase separation as a result of simple vertical cooling, or fault valve behavior and this phase separation will result in the deposition of gangue phases (quartz, carbonates, pyrite, other sulphides). As precipitation progresses the fluids can ultimately precipitate Au (generally observed to be late in the paragenetic sequence) as a result of conductive cooling; phase separation or boiling; solution mixing; and chemical interaction of the transporting solution and host rocks. (Romberger, 1991). A summation of the general characteristics of these types of systems is presented in Figure 5.1.

It is considered improbable that the fluids at depth would be significantly out of thermal equilibrium with the local wall rocks near the transitional zone and would therefore have to ascend to upper crustal levels before precipitation. As they ascend into crustal regions where they are out of equilibrium, both thermal and chemical, hydrothermal alteration of the wall rocks will result.

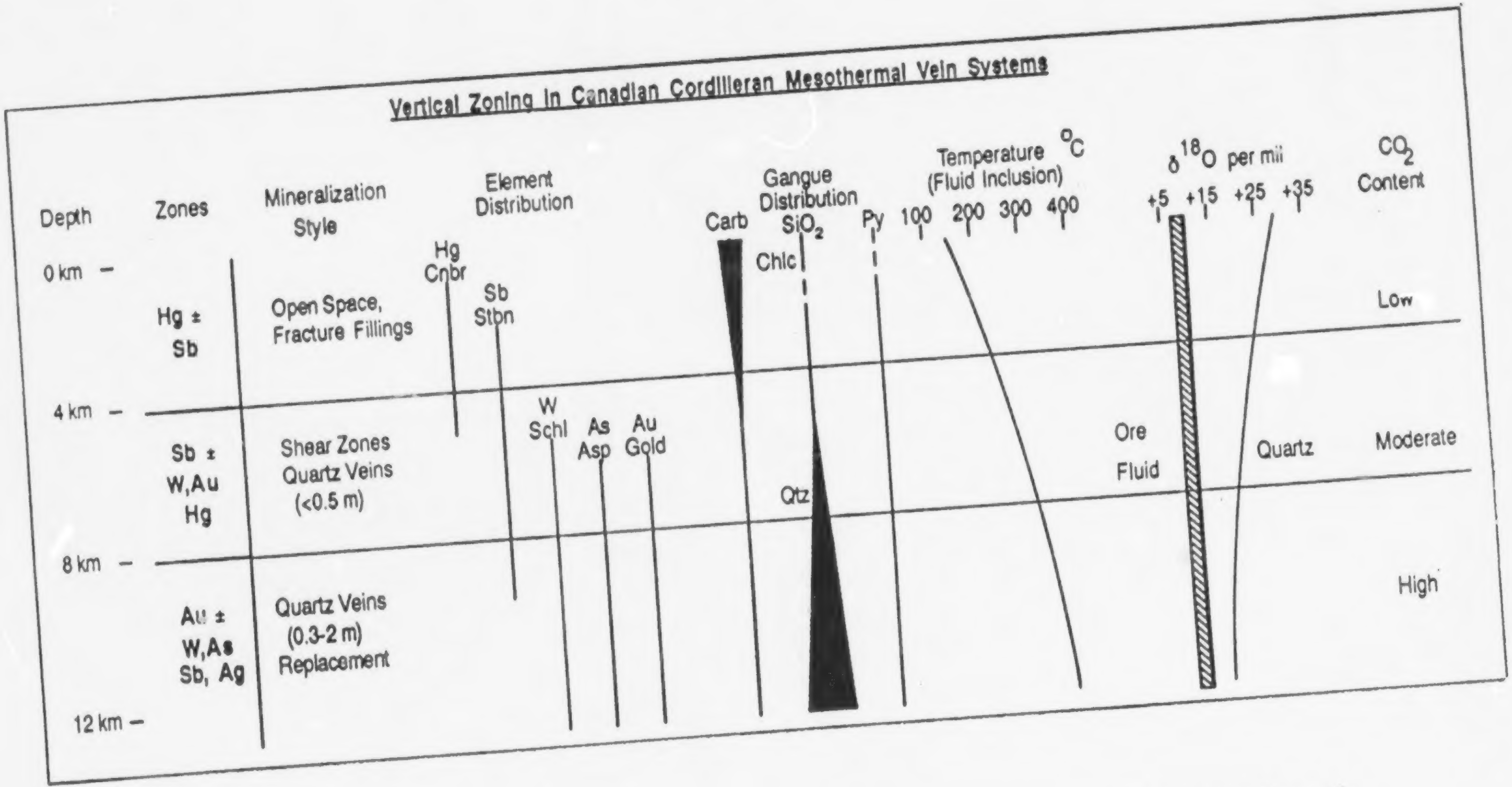
Vertical Zoning in Canadian Cordilleran Mesothermal Vein Systems
Depth
Zones
Mineralization Style
Element Distribution
Gangue Distribution
Temperature °C (Fluid Inclusion)
δ18O per mil
CO2 Content
0 km
4 km
8 km
12 km
Hg ± Sb
Sb ± W,Au Hg
Au ± W,As Sb, Ag
Open Space, Fracture Fillings
Shear Zones Quartz Veins (<0.5 m)
Quartz Veins (0.3-2 m) Replacement
Hg Cnbr
Sb Stbn
W Schl
As Asp
Au Gold
Carb
Chlc
SiO2
Qtz
Py
100
200
300
400
+5
+15
+25
+35
Ore Fluid
Quartz
Low
Moderate
High

Figure 5.1. Summation diagram of vertical transitions in mineralogy and geochemistry of the overall Au-Sb-Hg system. From fluid inclusion and stable isotope work documented in this study, a depth of 9-12 kms is suggested as the probable region of formation for the Sheep Creek vein system. Diagram from Nesbitt et al., 1989

REFERENCES

SHEEP CREEK GOLD CAMP

Andrew, K.P.E., Hoy, T., and Drobe, J., 1990a, Stratigraphy and tectonic setting of the Archibald and Elise Formations, Rossland Group , Beaver Creek area, southeastern British Columbia: B.C. Ministry of Energy, Mines and Petroleum Resouces, Geological Fieldwork 1989, Paper 1990-1, p.19-27.

Arai,Y., Kaminiski,G., and Saito., 1971, The experimental determination of the P-V-T-X relations for the carbon dioxide-nitrogen and carbon dioxide-methane system: Jour. Chem. Eng. Japan, v. 4, p.113-122.

Archibald, D.A., Glover,J.K., Price,R.A., Farrar, E., and Carmichael,D.M., 1983, Geochronology and tectonic implications of magmatism and metamorphism, southern Kootenay Arc and neighbouring regions, southeastern British Columbia. Part I: Jurassic to mid-Cretaceous: Can J. of Earth Sci., v. 20, p. 1891-1913.

Archibald, D.A., Krough, T.E., Armstrong, R.L., and Farrar, E., 1984, Geochronology and tectonic implications of magmatism and metamorphism, southern Kootenay Arc and neighbouring regions, southeastern British Columbia. Part II: Mid-Cretaceous to Eocene: Can J. of Earth Sci., v..21, p.567-583.

Armstrong, R.L., 1988, Mesozoic and early Cenozoic magmatic evolution of the Canadian Cordillera: *in* Clark, S.P., Burchfiel, B.C., and Suppe, J., Eds., Process in continental lithospheric deformation, G.S.of A., Spec. Paper 218, p.55-91.

Barton, P.B., Jr. and Toulmin. P.III, 1961, Some mechanisms for cooling hydrotherm al fluids: U.S. Geol. Surv., Prof. Paper 424-D, p.348-352.

Berger, G.W., and York, D., 1979, ^{40}Ar-^{39}Ar dating of multicomponent magnetizations in the Archean Shelley Lake granite, northwestern Ontario: Can. Jour. of Earth Sci., v. 16, p.1933-1941.

Bertoni, C.H., 1983, Gold production in the Superior province of the Canadian Shield: Canadian Inst. Mining Metall. Bull., v.76, p. 62-69.

Böhlke, J.K., and Kistler, R.W., 1986, Rb-Sr, K-Ar and stable isotopic evidence for the ages and sources of fluid components of gold bearing quartz veins in the northern Sierra Nevada foothills metamorphic belt, California: Econ Geol., v.81, p.296-322.

Bottinga, Y., and Javoy, M, 1975, Oxygen isotope partitioning among the minerals in igneous and metamorphic rocks: Rev. Geophys. Space Phys. 13, p.401-418.

Bowers,T.S., and Helgeson,H.C., 1983, Calculation of the thermodynamic and geochemical consequences of nonideal mixing in the system H_2O-CO_2-NaCl on phase relations in geologic systems: Equation of state for H_2O-CO_2-NaCl fluids at high pressures and temperatures: Geochim. et Cosmochim.Acta, v. 47,p.1247-1276.

Bowers,T.S., and Helgeson,H.C., 1983a, Calculation of the thermodynamic and geochemical consequences of nonideal mixing in the system H_2O-CO_2-NaCl on phase relations in geologic systems: metamorphic equilibria at high pressures and temperatures. Am. Mineral. v. 68, 1059-1075.

Bozzo, A.T., Chen, H.S., Kass, J.R., and Barduhn, A.J., 1975, The properties of the hydrates of chlorine and carbon dioxide: Desalinatin, v.16, p.303-320.

Brown, D.A., and Logan, J.M., 1988, Geology and mineral evaluation of Kokanee Glacier Provincial Park, southeastern British Columbia: in. Geologic Fieldwork, 1987, B.C. Ministry of E., M., and Petro. Res., Paper 1988-1, p.31-48.

Burnham, C.W., Holloway, J.R., and Davis, N.F., 1969, Thermodynamic properties of water to 1000°C and 10,000 bars: Geol. Soc. Amer. Spec. Paper #132, 96 pp.

Burruss, R.C., 1981, Analysis of phase equilibria in C-H-O-S fluid inclusions: Mineralog. Assoc. Canada. Short Course Handbook, v.6, p.39-44.

Burruss, R.C., 1981, Analysis of fluid inclusions: Phase equilibria at constant volume: Amer. Jour. of Sci., v.281, p.1104-1126.

Calderwood, A.D., Vander Heyden, P., and Armstrong, R.L., 1990, Geochronometry of the Thuya, Takomkane, Raft, and Baldy batholiths, south-central B.C.: G.S.C.,Prog.wth Abst. v. 15 , p.A19.

Carmichael, D.M., 1978, Metamorpnic bathozones and bathograds: a measure of the depth of post-metamorphic upliff and erosion on the regional scale: Amer. Jour. of Sci. v. 278, p.769-797.

Clayton, R.N., and Mayeda, T.K., 1963, The use of bromine pentafluoride in the extraction of oxygen from oxides and silicates for isotopic analyses: Geochim Cosmochim. Acta, v.27, p.43-52.

Collins, P.L.F., 1979, Gas hydrates in CO_2-bearing fluid inclusions and the use of freezing data estimation of salinity: Econ Geol., v.74, p.1435-1444.

Coney, P.S., Jones, D.L., and Monger, J.W.H., 1980, Cordilleran suspect terranes: Nature, v. 288, p.329-333.

Cook, F.A., Green,A.G., Simony, P.S., Price, R.A., Parrish, R.R., Milkereit, B., Gordy, P.L., Brown, R.L., Coflin, K.C., Patenaude, C., 1988, Lithoprobe seismic reflection structure of the southeastern Canadian Cordillera, initial results: Tectonics v. 7 no. 2, p.157-180.

Corbett, C.R., and Simony, P.S., 1984, The Champion Lake fault in the Trail-Castlegar area of southeastern B.C.: in Current research, Part A, G.S.C., Paper, 84-1A, p.103-104.

Craig, H., 1957, Isotopic standards for carbon and oxygen and correction factors for mass-spectrometric analysis of carbon dioxide: Gochim. Cosmochim. Acta, v.12, p. 133-149.

Crawford, M.L., and Hollister, L.S., 1986, Metamorphic fluids: The evidence from fluid inclusions: *in* Walther, J.V., and Wood, B.J., eds. Fluid-Rock interactions during metamorphism: Springer-Verlag, New York Berlin Heidelberg Tokyo, p. 1-35.

Crawford, M.L., 1981a, Phase equilibria in aqueous fluid inclusions, *in* L.S. Hollister and M.L. Crawford (eds.): Short course in Flluid Inclusions: Applications to Petrology, v.6, MAC, p. 75-100.

Crawford, M.L., 1981b, Fluid inclusions in metamorphic rocks-low and medium grade., In L.S. Hollister and M.L. Crawford (eds.): Short course in Flluid Inclusions: Applications to Petrology, v.6, MAC, p. 157-181.

Crosby, P., 1968, Tectonic, plutonic and metamorphic history of the central Kootenay Arc, Britixh Columbia, Canada: G.S.of A., Spec. Paper 99, 94pp.

Daly, R.A., 1912, Geology of the North American Cordillera at the Forty-ninth parallel: G.S.C., Mem.#38

Danniel,A., Todheide,K., and Frank, E.W., 1967, Verdamptung gleichgewichte and kritische Kurven in den systemen Athan/Wasser und n-Butan/Wasser bei hohen Drucken: Chemisch Ingenieurwesen Technik, p. 816-822

Devlin, W.J., 1989, Stratigraphy and sedimentology of the Hamill Group in the northern Selkirk mountains, British Columbia: evidence of lastest Proterozoic-Early Cambrian extensional tectonism: Can. Jour. of Earth Sci., v. 26, p.515-533.

Diamond, L.W., 1986, Hydrothermal geochemistry of late-metamorphic gold-quartz veins at Brusson, Val d'Ayas, Pennine Alps, N.W. Italy: Unpub. Ph.D. thesis, Swiss Federal Institute of Technology, Zurich, Switzerland, 256p.

Diamond, L.W., 1990, Fluid inclusion evidence for P-V-T-X evolution of hydrothermal solutions in late-alpine gold-quartz veins at Brusson, Val d'ayas, N.W. Italian Alps: Am. Jour. Sci. v. 290, p.912-958.

Donnelly, H.B., and Katz, D.L., 1954, Phase equilibria in the carbon dioxide-methane system: Indust. Eng. Chem., v.46, p.511-517.

Dowling, K., and Morrison, G., 1989, Application of quartz textures to the classification of gold deposits using North Queensland examples: Econ. Geol. Mon. #6, p. 342-355.

Drumond, S.E., and Ohmoto, H., 1985, Chemical evolution and mineral deposition in boiling hydrothermal systems: Econ Geol., v. 80, p.126-147.

Duncan,I.J., and Parrish, R., 1979, Geochronology and Sr isotope geochemistry of the Nelson batholith: a post-tectonic intrusive complex in southeast British Columbia (abstract): G.S.of A., Abst. wth Prog., v. 11, p.76.

Einarsen, J.M., 1991, Structural setting and geochemistry of granitic stocks in the Quesnellia-North American boundary of southeastern B.C.: G.S. of A., Prog. wth Abst., v. 22, no.3, p.20-21.

Einarson, J.M., 1991, Structural geology of the terrane accretion boundary in the southern Kootenay Arc: G.A.C.-M.A.C., Prog. with. Abst., p.A34.

Ellis, A.J., and Golding, R.M., 1963, The solubility of carbon dioxide above 100° C in water and in sodium chloride solutions: Am. Jour. Sci., v.. 261, p.47-60.

Field, C.W., and Fifarek, R.H., 1985, Light stable isotope systematics in the epithermal environment: Rev. Econ. Geology, v.2, p.99-128.

Friedman, I., and O'Neil, J.R., 1977, Compilation of stable isotope fractionation factors of geochemical interest; in Fleischer, M. (ed.), Data of Geochemistry, 6th edition: U.S.G.S. Prof Paper., 440-KK.

Fyfe, W.S., and Kerrich, R., 1984, Gold: Natural concentration processes:, *in* Foster, R.P., Gold '82: Rotterdam, A.A. Balkema Pub., P. 99-128

Fyles, J.T., and Hewlett, C.G., 1959, Stratigraphy and structure of the Slamo lead-zinc area: B.C. Dept. of Mines, Bull. #41. 162p.

Fyles, J.T., 1967, Geology of the Ainsworth-Kaslo area, British columbia: B.C. Dept. of Mines and Pet. Res., Bull. #53, 125p.

Gehrig, M., 1980, Phasengleichgewichte und PVT-Daten ternärer Mischungen aud Wasser, Kohlendiocid und Natriumchlorid bis 3 kbar und 550°C: University of Karlsruhe, doctorate dissertation, Hochschul Verlag, Freiburg.

Glover, J.K., 1978, Geology of the Summit Creek map-area, southern Kootenay Arc, B.C.: Ph.D. thesis, Queen's University, Kingston, Ont., 143 pp.

Goldfarb, T.J., Leach, D.L., Pickthorn, W.J., and Paterson, C.J., 1988, Origin of lode-gold deposits of the Juneau gold belt, southeastern Alaska: Geology, v. 16 p. 440-443.

Groves, D.I., and Phillips, G.N., 1987, The genesis and tectonic control on Archean gold deposits of the Western Australian Shield- a metamorphic replacement model: Ore Geology Review, v. 2,p.287-322.

Groves, D.I., and Foster, R.P., 1991, Archaean lode gold deposits: *in* Foster, R,P., ed., Gold metallogeny and exploration: Glasgow, Blackie and Sons Ltd., p.63-103.

Guha, J., Gauthier, A., v.allee, M., Descarreaux, J., and Lange-bard, F.,1982, Gold minealization at the Doyon Mine (Silverstack), Bousquet, Quebec: *in* Geology of Canadian Gold Deposits, Hodder, R.W., and Petruk, W. eds. CIM Spec v.24, p.50-66.

Hass, J.L., 1976, Physical properties of the co-existing phases and thermochemical properties of the H_2O component in boiling NaCl solutions. Preliminary steam tables for NaCl solutions: U.S. Geol. Surv. Bull. 1421-A.

Hedberg, H.D., 1974, Relation of methane generation to uncompacted shales, shale diapirs and mud volcanoes: Am. Assoc. Petroleum Geologists Bull., v. 58, p. 661-673.

Hedenquist, J.W., and Henley, R.W., 1985, The importance of CO_2 on freezing point measurements of fluid inclusions: Evidence from active geothermal systems and implications for epithermal ore deposition: Econ Geol., v. 80, p. 1379-1406.

Hedley, M.S., 1955, Lead-zinc deposits of the Kootenay Arc: Western Miner, v 28, no.7, p.31-35.

Heyen, G., Ramboz, C., and Dubessey, A., 1982, Simulation des equilibres de phases dans le systeme CO_2-CH_4 en dessous de 50° et de 100 bars. Application aux inclusions de fluides: Acad. Sci. (Paris) Comptes Rendus, v.. 294, ser.2, p.203-206.

Hodgson, C.J., Chapman, R.S.G., and MacGeehan, P.J., 1982, Application of exploration criteria for gold deposits in the Superior Province of the Canadian Shield to gold exploration in the Cordillera: *in* Levinson, A.A., ed., Precious etals in the Northern Cordillera: Assoc. of Expl. Geochem., p.173-206.

Hoefs, J., 1973, Stable isotope geochemistry: New York, Springer Verlag.

Holland, H.D., and Malinin, S.D., 1979, The solubility and occurrence of non-ore minerals: *in* Barnes, H.L., ed. Geochemistry of hydrothermal ore deposits: New York, Wiley Intersci., p. 461-508.

Hollister, L.S., and Burrus, R.C., 1976, Phase equilibria in fluid inclusions from the Khtada Lake metamorphic complex: Geochim. Cosmochim Acta, v..40, p.163-175.

Hollister, L.S., Crawford, M.L., Burruss, R.C., Spooner, E.T.C., and Touret, J., 1981, Practical aspects of microthermometry: Mineralog. Assoc. Canada, Short Course Handbook v.. #6, p. 278-301.

Hoy, T., 1980, Geology of the Riondel area, central Kootenay Arc, southeastern British Columbia: B.C. Ministry of Energy, Mines and Petroleum Resources, Bull. #73, 89p.

Hoy, T., and Andrew, K.P.E., 1988, Preliminary geology and geochemisty of the Elise Formation, Rossland Group between Nelson and Ymir, southeastern British Columbia: B.C. Ministry of Energy, Mines and Petroleum Resources, Geological fieldwork 1987, Paper 1988-1, p.19-30

Hoy, T., and Andrew, K.P.E., 1990, Structure and tectonic setting of the Rossland Group, Mount Kelly-Hellroaring Creek area, southeastern British Columbia: B.C. Ministry of Energy, Mines and Petroleum Resources, Geological fieldwork 1989, Paper 1990-1, p.11-17.

Hyndman, D.W., 1981, Controls on source and depth of emplacement of granitic magma: Geology v. 9, p244-249.

Juza, J., Kmonicek, V., and Sifner, O., 1965, Measurements of the specific volume of carbon dioxide in the range of 700 to 4000 b and 50 to 475°C: Physica #31, p. 1735-1744.

Kalyuzhnyi, V.A., and Kolltun,L.I., 1953, Some data on pressures and temperatures during formation of minerals in Nagol'nyy Kryazh, Donets Basin: Mineral. Sb. Lvov. Geol. Obshch., v. 7, p.67-74.

Keenan, J. H., Keyes, F.G., Hill, P.G., and Moore, J. G., 1969, Steam tables, thermodynamic properties of water including vapor, liquid and solid phases (International Edition-Metric Units): John Wiley and Sons Inc., New York, 162p.

Kennedy, G.C. and Holser, W.T., 1966, Pressure-volume-temperature and phase relations of water and carbon dioxide: *in* S.P. Clark,Jr., ed., Handbook of Physical Constants, Geol. Soc.Amer. Mem., #97, 371-384.

Kerrich, R.W., 1987, The stable isotope geochemistry of Au-Ag vein deposits in metamorphic rocks: Mineralogical Assoc. of Canada, Short Couse Handbook, v.13, p.287-336.

Kerrich, R., 1989a, Geodynamic setting and hydraulic regimes: Shear zone hosted mesothermal gold deposits: *in* Bursnall, J.T., ed., Mineralization and Shear Zones: G.A.C., Short Course, v. 6, p.89-128

Kerrich,R., 1991, Mesothermal gold deposits: A critique of genetic hypotheses: *in* Greenstone Gold and Crustal Evolution, NUNA conference volume, ed. F.Robert, P.A. Sheahan and S.B.Green, Geological Association of Canada, 252p.

Kesler,S.E., 1991, Nature and composition of mineralizing solutions: *in* Greenstone Gold and Crustal Evolution, NUNA conference volume, ed. F.Robert, P.A. Sheahan and S.B.Green, Geological Association of Canada, 252p.

Kyser, T.K., Janser, B.Q., Wilson, M.R. and Hattie, I., 1986, Stable isotope geochemistry related to gold mineralization and exploration in the Western Shield, Clark, L.A., ed., Can. Inst. Mining Metall., Special v.. 38, p.470-498.

Lambert, R.St. J., 1989, Tectonics and mineralization in southeastern B.C.: Tectonics of the Kootenay Arc: *in* Joseph, N.L., et al., eds. Geological guidebook for Washington and adjacent areas: Washington Div. of Geol. and Earth Resources Information Circular 86.

Little, H.W., 1950, Salmo map-area, British Columbia: G.S.C., Paper 50-19.

Little, H.W., 1960, Nelson map area, West half, British Columbia, (82F W1/2): Geol. Surv. of Can. Memior #308, 205p.

Lynch, J.V.G., 1989, Hydrothermal zoning in the Keno Hill Ag-Pb-Zn vein system: A study in structural geology, mineralogy, fluid inclusions and stable isotope geochemistry: Unpub. PhD. thesis, University of Alberta, 217p.

Magaritz, M. and Taylor, H.P. Jr., 1986, $^{18}O/^{16}O$ and D/H studies of plutonic granitic and metamorphic rocks across the Cordilleran batholiths of southern British Columbia: Jour. Geophys. Res., v.. 92, p. 2193-2217.

Maheux, P.J., 1989, A fluid inclusion and light stable isotope study of antimony-associated gold mineralization in the Bridge River District, British Columbia, Canada., Un.Pub Master Thesis, University of Alberta, 159pp.

Marshall, B. and Taylor, B.E., 1981, Origin of hydrothermal fluids responsible for gold deposition, Alleghany District, Sierra County, California: in Silberman, M.L. and Field, C.W., eds., Proceedings of the symposium of mineral deposits of the Pacific Horthwest, U.S.G.S., Open-File Report 81-355, p.281-291.

Mason, R., 1978, Petrology of the metamorphic rocks: George Allen & Unwin Ltd., Lon., 254 pp.

Mathews, W.H., 1953m Geology of the Sheep Creek camp: B.C. Dept. Mines, Bull. #31, 94 pp.

Matsuhisa, Y., Goldsmith, J.R., and Clayton, R.T., 1979, Oxygen isotopic fractionations in the system quartz-albite-anorthite-water: Geochim. Cosmochim. Acta., v.43, p. 1131-1140.

McCrea, J,M., 1950, On the isotopic chemistry of carbonates and a paleotemperature scale: J. Chem. Physics, v.18, p,849-857.

Monger, J.W., 1984, Cordilleran tectonics: a Canadian perspective: Bull. Soc. Géol. France, v. no.2, p.255-278.

Monger, J.W., and Price, R.A., Templeman-Kluit, D.L., 1982, Tectonic accretion and the origin of the two major metamorphic and plutonic welts in the Canadian Cordillera: Geology v.10, no.2, p.70-75

Moorehouse, W.W., 1959, The study of rocks in thin section: Harper and Row, New York.

Nelson, J. L., 1991, Carbonate-hosted lead-zinc (± silver, gold) deposits of British Columbia: *in* McMillan W.J. et al., Ore deposits, tectonics and metallogeny in the Canadian Cordillera: *in,* B.C. Ministry of E., M. and Petro. Resour., Paper 1991-4, p.71-88.

Nesbitt, B.E., Murowchick, J.B., and Muehlenbachs. K., 1987,. Repy to a comment on "Dual origins of lode gold deposits in the Canadian Cordillera": Geology, v..15, p.472-473.

Nesbitt, B.E., 1988, Reconnaissance study of δ^{34}S values of sulphides from mesothermal gold deposits of the eastern Canadian Cordillera: *in,* B.C. Ministry of E., M. and Petro. Resour., Paper 1988-1, p.543-545.

Nesbitt, B.E., Murowchick, J.B., and Muehlenbachs. K., 1986, Dual origins of lode gold deposits in the Canadian Cordillera: Geology, v..14, p. 506-509.

Nesbitt, B.E., and Muehlenbachs, K., 1989, Origins and movement of fluids during deformation and metamorphism in the Canadian Cordillera: Science, v. 245, p. 733-736.

Nesbitt, B.E., and Muehlenbachs, K., 1992, Isotope systematics of vein carbonate in the southern Canadian Cordillera as a key to interpreting crustal fluid regimes: (in prep.).

Nesbitt, B.E., Muehlenbachs, K. and Murowchick, J.B., 1989, Genetic implications of stable isotope characteristics of mesothermal Au deposits and related Sb and Hg deposits in the Canadian Cordillera: Econ Geol., v. 84, p. 1489-1506.

O'Neil, J.R., and Taylor, H.P., Jr., 1969, Oxygen isotope equilibrium between muscovite and water: Jour. of Geophys. Research, v. 74, p.6012-6022.

O'Neil, J.R., Clayton, R.N., and Mayeda, T.K., 1969, Oxygen isotope fractionation in divalent metal carbonates: Jour, Chem. Phys., v.51, p.5547-5558.

Ohmoto, H., and Rye, R.O., 1970, The Bluebell mine, British Columbia. I. Mineralogy, paragenesis, fluid inclusion and the isotopes of hydrogen, oxygen and carbon: Econ Geol., v. 65., p.417-437.

Ohmoto, H., and Rye, R.O., 1979, Isotopes of sulfur and carbon: *in* Barnes, H.L., ed., Geochemistry of hydrothermal ore deposits, 2nd Ed., John Wiley and Sons, New York, p.509-567.

Park, C.F., and Cannon, R.S., 1943, Geology and ore deposits of the Metaline quadrangle, Washington: U.S.G.S., Prof. Paper, # 202.

Parrish, W.R., and Prausnitz, J.M., 1972, Dissociation pressures of gas hydrates formed by gas mixtures: Ind. Eng. Chem. Process. Des. Develop. v.11, p.26-35.

Parrish, R., 1984, Slocan Lake fault: a low angle fault zone bounding the v.alhalla gneiss complex, Nelson map-area, Southern B.C.: *in* Current research, part A, G,S.C. Paper 84-1A, p.323-330.

Parrish, R., Carr,S., and Parkinson, D., 1988, Eocene extensional tectonics and geochronology of the southern Omineca Belt, B.C. and Washington: Tectonics, v. 7, p.181-212.

Parry, W.T., 1986, Estimation of XCO_2, P, and fluid inclusion volume from fluid inclusion temperature measurements in the system NaCl -CO_2-H_2O: Econ. Geol. v..81, p.1009-1013.

Pichavant, M., Ramboz,C., and Weisbrod, A., 1982, Fluid immiscibility in natural processes: Use and misuse of fluid inclusion data. I. Phase equilibria analysis. A theoretical and geometrical approach: Chem. Geology, v. 37, p. 1-27.

Pickthorn, W.T., Goldfarb, R.J., and Leach, D.l.,1987, Comment on Dual origins of lode gold deposits in the Canadian Cordillera: Geology, v..15, p.471-472.

Potter,C.J., Sanford, W.E., Yoos, T.R., Prussen, E.I., Keach, R.W.,II, Oliver, J.E., Kaufman S., Brown, L.D., 1986, COCORP deep seismic reflection traverse of the interior of the North American Cordillera, Washington and Idaho: Tectonics v. 5, no. 7, p.1007-1027.

Potter, R.W. II, Clynne, M.A., and Brown, D.L., 1978, Freezing point depression of aqueous sodium chloride solutions: Econ. Geol., v.73, p.284-285.

Potter, R.W.II, and Brown, D.L., 1977, The volumetric properties of aqueous sodium chloride solutions from 0°C to 500°C at pressures up to 2000 bar based on a regression of available data in the literature: U.S. Geol. Surv. Bull.1421-c, 36p.

Price, R.A., 1981, The Cordilleran foreland thrust and fold belt in the southern Canadian Rocky mountains: *in* Price, N.J., and MacClay, K., eds. Thrust and nappe tectonics, Geol. Soc. of Lon., Spec. Pub.,9, p.427-448.

Ramboz, C., Pichavant, M., and Weisbrod, A., 1982, Fluid immiscibility in natural processes: Use and misuse of fluid inclusion data.II. Interpretation of fluid inclusion data in terms of immiscibility: Chem Geology, v.37, p.29-48.

Ramboz, C., and Charef, A., 1988, Temperature, pressure, burial history and paleohydrology of the Les Malines Pb-Zn deposits: Reconstruction from aqueous inclusions in barite: Econ. Geol., v..83, p. 784-800.

Rice, H.M.A., 1941, Nelson map-area, East half, British Columbia: G.S.C., Mem #228.

Roedder, E., 1979a, Fluid inclusions as samples of ore fluids: *in* Barnes, H.L., ed., Geochemistry of hydrothermal ore deposits: 2nd edn: Wiley-Intersci., New York., p.684-737.

Roedder, E., 1981, Origin of fluid inclusions and changes that occur after trapping: *in*, Mineralogic Assoc. Canada. Short Course Handbook, v..6, p.101-137.

Roedder, E., 1984, Fluid inclusions: Reviews in Mineralogy, v.12, Min. Soc. Amer., 644p.

Roedder, E., and Bodnar, R.J., 1980, Geologic pressure determinations from fluid inclusion studies: Ann. Rev. Earth Planet Sci. v..8, p. 263-301.

Robinson, M.C., 1949, Geology and gold deposits of the Sheep Creek mining camp, B.C.: MSc. thesis, Queen's University, Kingston, Ont., 102pp.

Romberger, S.B., 1991, Transport and deposition of gold in hydrothermal systems: *in* Greenstone Gold and Crustal Evolution, NUNA conference volume, ed. F.Robert, P.A. Sheahan and S.B.Green, Geological Association of Canada, 252p.

Ronov, A.B., and Yaroshevsky, A.A., 1965, Chemical composition of the Earth's crust: in; The earth's crust and upper mantle: Hart, P.T., ed., Washington, D.C., Am.Geophys. Union, p.37-57.

Rushton, R.W., 1991, A fluid inclusion and stable isotope study of mesothermal Au-quartz veins in the Klondike schists, Yukon Territory: Unpub. Master thesis, University of Alberta, 192p.

Rye, D.M., and Bradbury, H.J., 1988, Fluid flow in the crust: An example from a Pyrenean thrust ramp: Am. Jour. Sci., v.288, p.197-235.

Schroeter, T.G., 1986, Gold in British Columbia: B.C. Ministry of Energy, Mines and Petroleum Resources, Preliminary map 64.

Schwarcz,H.P., 1969, The isotopes in nature, Handbook of geochemistry: v.1. Wedelpohl, K.H., ed., Berlin: Springer Verlag.

Seitz, J.C., Pasteris, J.D., and Wopenka, B., 1987, Characterization of CO_2-CH_4-H_2O fluid inclusions by microthermometry and laser raman microscope spectroscopy:

Inferences for clathrate and fluid equilibria: Geochim. et Cosmochim. Acta, v.51, p.1651-1664.

Shaw, R.P., Morton, R.D., Gray, J., and Krouse, H.R., 1991, Origins of metamorphic gold deposits: Implications of stable isotope data from the central Rocky MOuntains, Canada: Mineralogy and Petrology, v..43,p.193-209.

Shepherd,T.J., Rankin, A.H.,and Alderton, D.H.M., 1985, A practical guide to fluid inclusion studies: Glasgow, Blackie and Son Limited, 293 p.

Shieh, Y.N., and Taylor, H.P.Jr., 1969, Carbon and hydrogen isotope studies of contact metamorphism in the Santa Rosa Range, Nevada and other areas : Contrib. Mineral. Petrol., v..20 p.306-356.

Shelton, K.L., So, C.S., and Chang, J.S., 1988, Gold-rich mesothermal vein deposits of the Republic of Korea: Geochemical studies of the Jungwon gold area: Econ, Geol., v..83, p.1221-1237.

Sibson, R.H., 1983, Continental fault structure and the shallow earhtquake source: Jour. of the Geol. Soc. London, v.140, p. 741-767

Sibson, R.H., Robert,F., and Poulsen, K.H., 1988, High-angle reverse faults, fluid-pressure cycling and mesothermal gold-quartz deposits: Geology, v..16, p.551-555.

Sibson, R.H., 1990, Faulting and fluid flow: *ed.* B.E.Nesbitt, Mineralogic. Assoc. Canada Short Course Handbook, v.18, p.93-129.

Sibson, R.H., 1991, Fault structure and Mechanics in relation to greenstone gold deposits: *in* Greenstone Gold and Crustal Evolution, NUNA conference volume, ed. F.Robert, P.A. Sheahan and S.B.Green, Geological Association of Canada, 252p.

Smith, M.T., 1990, Stratigraphic, structural and U-Pb geochronologic investigation of lower Paleozoic eugeoglinal strata in the Kootenay Arc, NE. Washington and SE. British Columbia:Ph.D. dissertation, University of Arizona, Tucson,Az.

Smith, M.T., and Gehrels, G.E., 1991, Detrital zircon geochronology of Upper Proterozoic to lower Paleozoic continental margin strata of the Kootenay Arc: implications for the early Paleozoic tectonic development of the Eastern Canadian Cordillera: Can.J.Earth Sci. v..28, p.1271-1284.

Shmonov, V.M., and Shmulovich, K.I., 1974, Molar volumes and equation of state of CO_2 at temperatures from 100°C to 1000°C and pressures from 2000 to 10,000 bars: Dokl. Akad. Nauk. SSSR, Earth Sci.#217, p.206-209, (Eng. Trans.).

Sourirajan, S. and Kennedy, G.C., 1962, The system H_2O-NaCl at elevated temperatures and pressures: Am. Jour. Sci., v.260, p.115-141.

Spooner, E.T.C., Bray. C.J., Wood, P.C., Burrows, D.T., and Callan, N.J., 1987, Au-quartz vein and Cu-Au-Ag-Mo-anhydrite mineralization, Hollinger-McIntyre mines, Timmins, Ontario: ^{13}C values (McIntyre), fluid inclusion gas chemistry, pressure (depth) estimation and H_2O-CO_2 phase separation as a precipitation and dilation mechanism: Ontario Geol.Survey Misc, Paper 136, p.35-56.

Swanenberg, H.E.C., 1979, Phase equilibria in carbonic systems and their application to freezing studies of fluid inclusions: Contr. Mineralog. Petrol. v..68, 303-306.

Takenouchi, S., and Kennedy, G.C., 1965, The solubility of carbon dioxide in NaCl solutions at high temperatures and pressures: Am. Jour. Sci., v. 263, p. 445-454.

Taylor, H.P., Jr., 1974, the application of oxygen and hydrogen isotope studies to problems of hydrothermal alteration and ore deposition: Econ. Geol., v. 69, p. 843-883.

Taylor, H.P. Jr., 1977, Water-rock interactions and the origin of H_2O in granitic batholiths: Jour. Geol. Soc. Lon., v..133, p.509-558.

Taylor, H.P. Jr., 1979, Oxygen and hydrogen isotope relationships in hydrothermal mineral and Sons, New York, p.236-277.

Thompson, R.I., Mercier, E., and Roots, C., 1987, Extension and its influence on Canadian Cordilleran passive-margin evolution: *in*, Coward, M.P., Dewey, J.F., and Handcock, P.,L., eds., Continental extensional tectonics: G.S.of A., Spec. Publ. 28, p.409-417.

Tipper, H.W., 1984, The age of the Jurassic Rossland Group of southeastern B.C.: in Current research, Part A, G.S.C., Paper 84-1A, p.631-632.

Valakovich, M.P., and Altunin, U.V., 1968, Thermophysical properties of carbon dioxide: College of London.

Vogl, J.J., and Simony, P.S., 1992, The southern tail of the Nelson batholith, southeast B.C.: structure and emplacement: in. Current research, Part A, G.S.C., Paper 92-1A, p71-76.

Walsh, J.F., Kesler, S.E., Duff, D., Cloke,P.l., 1988, Fluid inclusion Geochemistry of high-grade, vein-hosted gold ore at the Pamour Mine, Porcupine Camp, Ontario: Econ. Geol. v..83, p.1347-1367.

Wanless, R.K., Stevens, R.D., Lachance, G.R., and Edmonds, C.M., 1968, Age determinations and geological studies, K-Ar isotope ages: report 8, G.S.C., Paper 67-2A, p. 1-53.

Weir, R.H., and Kerrich, D.M.,1987, Mineralogic, fluid inclusion, and stable isotope studies of several gold mines in the MotherLode, Tuolumne and Mariposa counties, California: Econ. Geol., v. 82, p.328-344.

Wood, P.C., Burrows, D.R., amd Spooner, E.T.C., 19896, Au-quartz vein and intrusion-hosted Cu-Au-Ag-Mo mineralization, Hollinger-McIntyre mines, Timmins, Ontario: Geological characteristics, structural examination, igneous hydrothermal alteration geochemistry and light stable isotope (hydrogen and oxygen) geochemistry: Ontario Geol. Survey Misc. Paper 130, p.23-46.

Wyman, D.A., and Kerrich, R., 1988, Archean lamprophyres, gold deposits and transcrustal structures: implications for greenstone belt gold metallogeny: Econ. Geol., v. 83, p.454-459.